4392

THE LOX AND LOXL2 AMINE OXIDASES

IN COLON AND ESOPHAGEAL CANCER

A DISSERTATION SUBMITTED TO THE GRADUATE DIVISION OF THE
UNIVERSITY OF HAWAI'I IN PARTIAL FULFILLMENT OF THE
REQUIREMENTS FOR THE DEGREE OF

DOCTOR OF PHILOSOPHY

IN

BIOMEDICAL SCIENCES (CELL AND MOLECULAR BIOLOGY)

DECEMBER 2003

By
Sheri F.T. Fong

Dissertation Committee:

Katalin Csiszar, Chairperson
Alan F. Lau
John Bertram
Randal K. Wada
Loic LeMarchand

ACKNOWLEDGEMENTS

ABSTRACT

Several members of the lysyl oxidase family of copper-dependent amine oxidases have been implicated in tumor development. The lysyl oxidase (LOX) and LOX-like 2 (LOXL2) genes have been mapped to chromosomal regions affected by loss of heterozygosity (LOH) in several cancers, including those of the colon and esophagus. Indeed, there have been numerous reports of reduced LOX and a few reports of reduced LOXL2 expression in various cancers. Identification of microsatellite markers within the LOX locus and the LOXL2 gene allowed for evaluation of the status of these gene alleles in colon and esophageal tumors. There was significant LOH of the LOX locus in colon tumors that was accompanied by reduced mRNA expression and a spectrum of alterations and mutations affecting the LOX gene. This study demonstrated, for the first time, that genetic events, namely LOH, deletions and mutations of the LOX gene, were responsible, at least partly, for the reduction of LOX gene expression. There was also significant LOH of the LOXL2 gene in both colon and esophageal tumors. However, instead of a reduction of LOXL2 expression, there was increased expression that correlated with less differentiated tumors and absent elastosis, both indicators of poor prognosis. Further studies indicated that both LOX and LOXL2 are absent in non-invasive tumor cell lines but re-expressed in invasive cell lines, likely as part of the epithelial-mesenchymal transition that occurs in the last steps of tumorigenesis to facilitate metastasis. The results presented and research strategy outlined in this dissertation will define the importance of LOXL2 amine oxidase activity and protein interactions in the critical but poorly understood process of tumor cell migration and invasion.

TABLE OF CONTENTS

vii

LIST OF TABLES

LIST OF FIGURES

LIST OF ABBREVIATIONS

aa	amino acid	cAMP	cyclic AMP
A, ala	alanine	CAO	copper amine oxidase
C, cys	cysteine	CCM	conditioned cell media
D, asp	aspartic acid	cDNA	complementary DNA
E, glu	glutamic acid	CL	cell layer
F, phe	phenylalanine	cm	centimeter, 10^{-2} meters
G, gly	glycine	cpm	counts per minute
H, his	histidine	CRL	cytokine receptor-like
I, ile	isoleucine	DAPI	4',6 deamidino-2-phenylindole
K, lys	lysine	ddNTP	dideoxynucleoside triphosphate
L, leu	leucine	DEPC	diethyl pyrocarbonate
N, asn	asparagine	DMSO	dimethyl sulfoxide
P, pro	proline	DNA	deoxy ribonucleic acid
Q, gln	glutamine	dNTP	deoxynucloside triphosphates
R, arg	arginine	DTT	dithiothreitol
S, ser	serine	ECM	extracellular matrix
T, thr	threonine	EDTA	ethylenediamine tetracetic acid
V, val	valine	EMT	epithelial-mesenchymal transition
W, trp	tryptophan	FBS	fetal bovine serum
X	any aa	fm	femtomoles, 10^{-15} moles
Y, tyr	tyrosine	g	grams
APC	adenomatous polyposis coli	GDP	guanosine diphosphate
AMP	adenosine monophosphate	GFP	green fluorescent protein
APS	ammonium persulfate	GTP	guanosine triphosphate
ATP	adenosine triphosphate	HRP	horseradish peroxidase
βAPN	beta-aminopropionitrile	IRF-1	interferon regulating factor-1
bFGF	basic fibroblast growth factor	kb	kilobase pair
BMP-1	bone morphogenic protein-1	kDa	kilo Dalton
bp	base pair	LB	Luria-Bertani

LOH	loss of heterozygosity	PEV	position effect variegation
LOX	lysyl oxidase	PVDF	polyvinylidene fluoride
LOXL	LOX-like	RER+	replication error+
LOXL2	LOX-like 2	RNA	ribonucleic acid
LOXL3	LOX-like 3	rpm	revolutions per minute
LOXL4	LOX-like 4	rrg	ras recision gene
LTQ	lysine tyrosylquinone	RT	room temperature
LTR	long terminal repeat	RT-PCR	reverse transcriptase-PCR
M	molar (moles/liter)	SAP	shrimp alkaline phosphatase
mA	millamps	SDS	sodium dodecyl sulfate
MCC	mutated in colon cancer	siRNA	small interfering RNA
μg	microgram; 10^{-6} gram	SRCR	scavenger receptor cysteine rich
mg	milligram; 10^{-3} gram	SSC	sodium chloride, sodium citrate
MIN	microsatellite instability	ssDNA	sheared salmon testis DNA
μL	microliter; 10^{-6} liter	TAE	Tris-Acetate-EDTA
mL	milliliter; 10^{-3} liter	TBE	Tris-Borate-EDTA
μm	micrometer; micron; 10^{-6} meter	TE	Tris-EDTA
mm	millimeters, 10^{-3} molar	TEMED	tetramethylethylenediamine
mM	millimolar, 10^{-3} molar	TGF-β	transforming growth factor-beta
mRNA	messenger RNA	TPQ	topaquinone
mTLD	mammalian tolloid	TSG	tumor suppressor gene
mTLL	mammalian tolloid-like	UTR	untranslated region
ng	nanograms	UV	ultraviolet
nm	nanometer; 10^{-9} meter	V	volts
nM	nanomolar; 10^{-9} molar	x g	times gravitational force
OD	optical density		
PAC	plasmid artificial chromosome		
PAGE	polyacrylamide gel electrophoresis		
PBS	phosphate buffered saline		
PCR	polymerase chain reaction		

CHAPTER I

INTRODUCTION

Lysyl oxidase (LOX) has been shown to be part of a tumor suppressor pathway
through progressive reduction of LOX mRNA and enzyme activity during tumor
development and metastasis. However, it is not known whether the lysyl oxidase gene is
a primary target for gene mutations, or if the loss of the transcript and protein is a
secondary effect in the cascade of mutations affecting other genes. In addition, the exact
mechanism of action of LOX as a tumor suppressor is not understood. It is well known
that LOX is an extracellular enzyme that catalyzes the cross-linking of elastin and
collagen in the extracellular matrix, and thus loss of the lysyl oxidase protein could result
in modulation of the extracellular matrix such that local invasion and tumor metastasis
could occur. In addition to this extracellular matrix cross-linking role, LOX has also been
demonstrated to have growth regulatory activity, and may play a role in modulating
tumor growth. This activity appears to occur intracellularly as lysyl oxidase has been
shown to inhibit the *ras* pathway downstream of activated Erk2, which translocates to the
nucleus to activate transcription. Indeed, LOX has been localized to the nucleus where it
has been linked to chromatin structure, and to the cytoskeleton as well. These
intracellular and intranuclear forms of LOX could exert a possible tumor suppressor
activity through cell growth control. The recent discovery that lysyl oxidase actually
belongs to a family of structurally related genes suggest that other members of the LOX
family may have similar but distinct roles in cancer pathogenesis.

1

The goal of this dissertation is to characterize two members of the lysyl oxidase

family, LOX and LOXL2, in cancer development. My hypothesis is that aberrant

expression of LOX and LOXL2 is a contributing factor in tumorigenesis through loss of

the normal function of these proteins.

A. THE LYSYL OXIDASE PROTEIN FAMILY

Amine oxidases that catalyze the oxidation of primary amines to their

corresponding aldehydes can be divided into two main classes based on the prosthetic

group co-factors required for their enzymatic activity. Flavine adenine dinucleotide is the

cofactor for the flavoproteins monoamine oxidase A and B and of an intracellular form of

polyamine oxidase (Binda et al, 2002). The second group is composed of enzymes whose

catalytic activity requires a quinone-containing prosthetic group. These quinoproteins are

also called copper amine oxidases (CAOs), and include diamine oxidase, semicarbazide-

sensitive amine oxidase and lysyl oxidase (Jalkanen and Salmi, 2001). Trihydroxyphenyl-

alanine quinone, or topaquinone (TPQ), a modified tyrosine side-chain utilized as a redox

co-factor, is the prosthetic group of copper-containing amine oxidases in bacteria, plants

and animals (Anthony, 1996). However, despite being a member of the CAO family,

lysyl oxidase was significantly smaller (monomer of 32 kDa) than other CAOs

(homodimers of 70-90 kDa each) and all LOX family members lacked the TPQ

consensus sequence found in all CAOs (Dove and Klinman, 2001). The quinone co-factor

of lysyl oxidase was identified in 1996 to be a lysine tyrosylquinone (LTQ), formed from

the autocatalytic hydroxylation and oxidation of Lys-314 and Tyr-349 (Wang et al,

1996), the only mammalian cofactor derived from the cross-linking of two amino acid side chains (Anthony, 1996). The LTQ is unique to lysyl oxidase and is one of two highly conserved sequences that define this family.

Crucial to the mechanism of LTQ is copper, and the copper-binding domain of the lysyl oxidase family is the other highly conserved motif that is unique to the LOX family. The presence of four histidines (H) in the amino acid sequence of the copper-binding domain, W_WH_CH_HYH, is unique to lysyl oxidase. The copper-binding domain of the other CAOs is composed of three conserved histidine residues that ligand the copper ion in a square pyramidal geometry (Dove and Klinman, 2001). In contrast, the four histidines of lysyl oxidase supply the nitrogen ligand for the copper coordination complex (Krebs and Krawetz, 1993) that holds the copper ion in a tetragonally distorted, octahedrally coordinated ligand field (Akagawa and Suyama, 2001). One atom of copper per molecule of lysyl oxidase is required for enzyme activity and cannot be replaced by other divalent metal ions such as zinc, cobalt, iron, mercury, magnesium and cadmium. In addition to one atom of tightly bound copper, preparations of purified lysyl oxidase are associated with 5-9 loosely bound copper atoms per LOX molecule (Gacheru et al, 1990).

Together, the LTQ and the copper-binding domain, sequences that define the LOX family, are responsible for the cross-linking activity of at least two members of this family, LOX and LOXL. In addition, there are two other conserved motifs, the cytokine receptor-like domain and the putative metal-binding sites, that share homology with

3

proteins unrelated to lysyl oxidase. The cytokine-receptor-like domain, the LTQ and the copper-binding domain are conserved in all LOX family members that have been described to date in mammals, including five members identified in *Homo sapiens* (human) and *Mus musculus* (mouse), two members identified in *Bos taurus* (bovine), and one member identified so far in *Rattus norvegicus* (rat) and *Gallus gallus* (chicken). They are also conserved in the LOX-like protein identified in *Perca flavescens* (fish), and in two LOX orthologues that are found in *Drosophila melanogaster* (fruit fly) (Figure 1.1).

There has been one report of a lysyl oxidase identified in *Pichia pastoris* (yeast) that preferentially oxidizes lysine and is able to use fibrillar collagen as a substrate (Tur and Lerch, 1988). However, the co-factor of this protein has been identified as TPQ, not LTQ (Dove et al, 1996), and thus is not a member of the LOX family. The fact that the yeast CAO and mammalian LOX have overlapping substrates indicates that LTQ is not involved in conferring substrate specificity. Rather, the other domains in the LOX proteins, the cytokine receptor-like (CRL) and the scavenger-receptor cysteine-rich (SRCR) domains are likely to confer this property.

The conserved CRL domain, which contains the catalytic site, has part of the consensus sequence of Class 1 cytokine receptors, with the sequence of C-X_{9-10}-C-X-W-X_{25-32}-C-X_{8-21}-C, where C is cysteine, W is tryptophan and X_n is a defined number of any amino acids (Bazan, 1990). Members of the Class 1 cytokine receptors include growth hormone, prolactin, granulocyte colony-stimulating factor and erythropoietin receptors,

4

                    Cu Binding   *lysine tyrosylquinone co-factor linkage*   *cytokine receptor-like domain*

HUMAN LOX   RYSWEWHSCHQHYHSMDEFSHYDLLDANTQRRVAEGHKASFCLEDTSCDYGYHRRFACT-AHTQGLSPGCYDTYGADIDCQWIDITDVKPG-NYILKVSVNPSYLVPESDYTNNVVRCDIRYTGHH--AYASGCTISP
HUMAN LOXL   RHTWEWHSCHQHYHSMDEFSHYDLLDAATGKKVAEGHKASFCLEDSTCDFGNLKRYACT-SHTQGLSPGCYDTYNADIDCQWIDITDVQPG-NYILKVHVNPKYIVLESDFTNNVVRCNIHYTGRY--VSATNCKIVQ
HUMAN LOXL2 RHAWIWHDCHRHYHSMEVFTHYDLLNLN-GTKVAEGHKASFCLEDTECGDIQKNYECANFGDQGITMGCWDMYRHDIDCQWVDITDVPPG-DYLFQVVINPNFEVAESDYSNNIMKCRSRYDGHR--IWMYNCHIGG
HUMAN LOXL3 RDSWVHECHGHYHSMDIFTHYDILTPN-GTKVAEGHKASFCLEDTECQEDVSKRYECANFGEQGITVGCWDLYRHDIDCQWIDITDVKPG-NYILQVVINPNFEVAESDFTNNAMKCNCKYDGHR--IWVHNCHIGD
HUMAN LOXL4 RDSWVHQCHQHYHSIEVFTHYDLLTLN-GSKVAEGHKASFCLEDTNCPTGLQRRYACANFGEQGVTVGCWDTYRHDIDCQWVDITDVGPG-NYIFQVIVNPHYEVAESDFSNNMLQCRCKYDGHR--VWLHNCHTGN
MOUSE LOX   RYSWEWHSCHQHYHSMDEFSHYDLLDANTQRRVAEGHKASFCLEDTSCDYGYHRRFACT-AHTQGLSPGCYDTYAADIDCQWIDITDVQPG-NYILKVSVNPSYLVPESDYTNNVVRCDIRYTGHH--AYASGCTISP
MOUSE LOXL   RHTWEWHSCHQHYHSMDEFSHYDLLDASTGKKVAEGHKASFCLEDSTCDFGNLKRYACT-SHTQGLSPGCYDTYNADIDCQWIDITDVQPG-NYILKVHVNPKYIVLESDFTNNVVRCNIHYTGRY--VSTTNCKIVQ
MOUSE LOXL2 RHAWIWHDCHRHYHSMEVFTYYDLLSLN-GTKVAEGHKASFCLEDTECGDIQKSYECANFGDQGITMGCWDMYRHDIDCQWIDITDVPPG-DYLFQVVINPNYEVPESDPSNNIMKCRSRYDGYR--IWMYNCHVGG
MOUSE LOXL3 RHSWVHECHGHYHSMDIFTHYDILTPN-GTKVAEGHKASFCLEDTECQEDVSKRYECANFGEQGITVGCWDLYRHDIDCQWIDITDVKPG-NYILQVVINPNFEVAESDFTNNAMKCNCKYDGHR--IWVHNCHIGD
MOUSE LOXL4 RHSWIWHQCHRHNHSIEVFTHYDLLTLN-GSKVAEGHKASFCLEDTNCPSGVQRRYACANFGEQGVAVGCWDTYRHDIDCQWVDITDVGPG-DYIFQVVVNPTNDVAESDFSNNMIRCRCKYDGQR--VWLHNCHTGD
BOVINE LOX   RYSWEWHSCHQHYHSMDEFSHYDLLDASTQRRVAEGHKASFCLEDTSCDYGYHRRFACT-AHTQGLSPGCYDTYAADIDCQWIDITDVKPG-NYILKVSVNPSYLVPESDYSNNVVRCEIRYTGHH--AYASGCTISP
BOVINE LOXL   RHQWIWHQCHRHYHSIEVFTHYDLLTLN-GSKVAEGHKASFCLEDTNCPTGMQRRYACANFGEQGVTVGCWDTYRHDIDCQWVDITDVGPG-DYIFQVVVNPKFEVAESDFSNNMMRCRCKYDGQR--VWLHNCHTGD
RAT   LOX   RYSWEWHSCHQHYHSMDEFSHYDLLDASTQRRVAEGHKASFCLEDTSCDYGYHRRFACT-AHTQGLSPGCYDTYAADIDCQWIDITDVQPG-NYILKVSVNPSYLVPESDYSNNVVRCEIRYTGHH--AYASGCTISP
CHICK LOX   RYSWEWHSCHQHYHSMDEFSHYDLLDASSHRKVAEGHKASFCLEDTSCDYGYYRRYACT-AHTQGLSPGCYDTYAADIDCQWIDITDVKPG-NYILKVSVNPSYLVPESDYSNNIVRCDIRYTGHH--AYASGCTISP
PERCH LOXL2 RESWTWHQCHRHYHSIEVFTHYDLLTLN-GTKVAEGHKASFCLEDTYCPEGIHKRYACYNMGQQGISVGCWDTYRHDIDCQWVDITDIRPG-EYIFQVEVNPTLDMAESDFQNNVMRCRCKYDGER--VYMFGCHAGD
DROSI LOXL-1 YKEWVWHQCHRHYHSMNVFATFDVYDLN-YRKVAQGHKASFCLMDSECRPGVRQKYTCGN-TTQGISVGCADTYTDVLDCQWVDVTRVPINRRYILRVALNPEYKLGEISFENNGAECLLDYTGVRQTTRIFNCRFKP
DROSI LOXL-2 KSQWEWHMCHMHFHSMEVFATFDIFNLR-GIKVAQGHKASFCLEDSNCLPGVAKKYNCANSGDQGISINCSDVYLYNLDCQWVDVTDLIPG-TYVLKIAINPEFKVAEMNYDNNAAICDLIYTAN--FARVQNCQIGR

Figure 1.1. Alignment of conserved domains of the LOX family of proteins. All known members of the LOX family of proteins across species are included. ClustalW, a multiple sequence alignment program, and a similarity index matrix was used. Identical, or commonly substituted amino acids, are shaded. There are two highly conserved sequences: the unique copper-binding domain that contains four histidines, and a cytokine receptor-like domain similar to type 1 cytokine receptors. The lysine and tyrosine residues highlighted in blue form the co-factor lysine tyrosylquinone (LTQ) which is unique to lysyl oxidase and responsible for catalytic activity.

as well as receptors for interleukin-2, 3, 4 and 6. The four spatially conserved cysteines are thought to be critical to the maintenance of the structural and functional integrity of these receptors (Figure 1.2A). The variable number of X is due to the variable length of linker regions between the β–strands (Figure 1.2b). Analysis of the predicted β-strands of this domain revealed that each member of the human lysyl oxidase protein family has a different pattern (Figure 1.2a). The β-strands of the Class 1 cytokine receptors fold in anti-parallel fashion to form two barrel shaped structures connected by a hinge, which has a pocket for cooperative binding of a cytokine with a second molecule (Figure 1.2c). The predicted β-strands of the CRL domain are similar in arrangement to the N-domain of the cytokine receptor. The CRL domain may form only one barrel and thus no pocket, but still may interact with other proteins. The differences in the β-strands, and thus the configuration of the barrel structure may define interacting proteins or substrates that are unique to each of these members (Csiszar et al, 2000).

Other than the cytokine receptor-like domain, additional domains that may interact with other proteins are the proline-rich region unique to LOXL (Williamson, 1994) and the scavenger-receptor cysteine-rich domains (SRCR) found on the amino-terminal end of LOXL2, LOXL3 and LOXL4 (Figure 1.3). The SRCR superfamily is an ancient and highly conserved family found in mammals, amphibians and invertebrates. Members of this family contain between one and eleven cysteine-rich protein domains, each about 100 amino acids in length. They are either secreted or transmembrane molecules, with the SRCR domains forming most of the extracellular portion of the

6

A

```
LOX    QGLSPGCYDTYGADIDCQWIDITDVKPGNYILKVSVNPSYLVPESDYTNNVVRCDIRYTGHHAYASGCTISP
LOXL   QGLSPGCYDTYNADIDCQWIDITDVQPGNYILKVHVNPKYIVLESDFTNNVVRCNIHYTGRYVSATNCKIVQ
LOXL2  QGITMGCWDMYRHDIDCQWVDITDVPPGDYLFQVVINPNFEVAESDYSNNIMKCRSRYDGHRIWMYNCHIGG
LOXL3  QGITVGCWDLYRHDIDCQWIDITDVKPGNYILQVVINPNFEVAESDFTNNAMKCNCKYDGHRIWVHNCHIGD
LOXL4  QGVTVGCWDTYRHDIDCQWVDITDVGPGNYIFVIVNPHYEVAESDFSNNMLQCRCKYDGHRVWLHNCHTGN
```


B

Adapted from Bazan, 1990

C

Figure 1.2. Amino acid alignment of the cytokine receptor-like domain in the human lysyl oxidase family. A: Conserved amino acids in each protein are shaded. Residues highlighted in blue are critical for secondary and tertiary structural folds of the Class 1 Cytokine Receptor Domain. The arrows below the sequence correspond to regions predicted to form β-strands in LOX (red), LOXL (orange), LOXL2 (green), LOXL3 (blue) and LOXL4 (purple) according to a consensus of protein secondary structure prediction programs from the Network Protein Sequence Analysis web site (http://npsa-pbil.ibep.fr/). B: Topology map with relative positions of conserved amino acids in mainly class 1 (circles) and class 2 (diamonds). Residues conserved in both classes are in squares. Residues conserved in LOX proteins are in blue (also seen highlighted in blue in A). C: Predicted configuration of cytokine binding. Linked β-strands form a barrel shaped structure. The C-terminal WSxWS motif, situated between the barrels and shown in A, creates a pocket for cooperative binding of a cytokine (red) and a secondary binding molecule (purple).

7
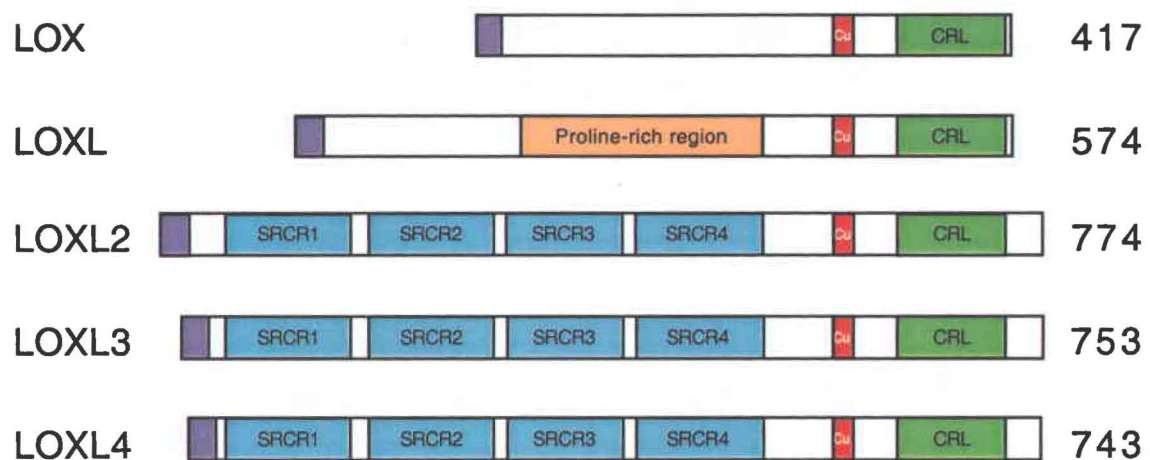
Figure 1.3. Domain organization of the human lysyl oxidase family of proteins. All members of the lysyl oxidase family of proteins share two highly conserved domains: a unique copper-binding domain containing four histidines, shaded in red, and a cytokine receptor-like domain similar to type I cytokine receptors, shaded in green. LOXL has a proline-rich region, shaded in orange. Unique to LOXL2, LOXL3 and LOXL4 are Scavenger Receptor Cysteine-Rich Domains (SRCR) domains, shaded in blue, that are commonly found in cell surface receptors and adhesion molecules. Predicted extracellular signal sequences are shaded in purple. The amino acid length is noted at the right margin.

molecule. The SRCR superfamily can be divided into two groups based on the SRCR domain structure: group A domains contain six cysteine residues while group B domains have six to eight cysteine residues, with the spacing pattern between the cysteine residues defining each group. The cysteines are important for the tertiary conformation of this motif (Resnick et al, 1994). All the SRCR domains in LOXL2, LOXL3 and LOXL4 are group A domains. Other proteins containing group A domains include the transmembrane proteins, scavenger receptor type I and speract receptor, and the secreted proteins, complement factor I and Mac-2 binding protein (M2BP). M2BP is a cell adhesive protein that can bind fibronectin, β1 integrin and certain collagens (Sasaki et al, 1998).

The crystal structure of the Group A SRCR domain of M2BP revealed a curved six-stranded β-sheet cradling an α-helix, and this has been suggested to be a valid template for the entire SRCR superfamily (Hohenester et al, 1999). Site directed mutagenesis of the third (of three) group B SRCR domain of CD6 revealed that this domain is important for binding to ALCAM (activated leukocyte cell adhesion molecule) (Aruffo et al, 1997), and that the three amino acid residues critical for interaction are located in the long loop connecting β-strands 5 and 6 (Hohenester et al, 1999). Alignment of various SRCR domains demonstrated that this loop region exhibits a high degree of variation compared to other regions of the domain, and makes this region a candidate site for ligand-binding while the remainder of the domain serves as a structural scaffold (Graversen et al, 2002). Alignment of the four SRCR domains of LOXL2, LOXL3 and LOXL4 reveal that the second SRCR has the most variability in terms of the α-helix, the

distance from β-strand 3 to the α-helix, β-strands 4 and 5, and the loop region between strands 5 and 6 (Figure 1.4), and is the most likely candidate SRCR domain for protein interaction.

Although there are currently five members of the human LOX family, this thesis focuses on the role of LOX and LOXL2 in colon and esophageal cancer. These two genes are described in greater detail.

1. Lysyl Oxidase (LOX)

The lysyl oxidase gene has been mapped to the long arm of chromosome 5 at 5q23.3-31.2 (Mariani et al, 1992; Hamalainen et al, 1991). The gene is composed of seven exons and six introns distributed through approximately 14.5 kb of genomic DNA (Boyd et al, 1995; Hamalainen et al, 1993). The first exon contains 273 bases of untranslated and 631 bases of translated sequence, nearly half of the protein coding sequence. The last exon codes for the last base of amino acid 416, the C-terminal amino acid Tyr-417, the termination codon and the 3' untranslated region (UTR). In contrast to these exons, exons 2-6 are smaller, between 96-157 bp long (Figure 1.5). The introns vary in size between 331 bp to 3.5 kb (Hamalainen et al, 1993).

Three transcripts of sizes 2.0 kb, 3.8 kb and 4.8 kb are produced (Mariani et al, 1992) as a consequence of differential use of several polyadenylation signals within the 3.8 kb long 3' UTR (Boyd et al, 1995). The transcript encodes for a 417-amino acid (aa)

SRCR 1
```
LOXL2  QLRLAGQKRKHSEGRVEVYYDGQWGTVCDDDFSIHAAHVVCRELGYVEAKSWTASSSYGKGEGPIWLDNLHCTGNEATLAACTSNGWGVTDCKHTEDVGVV  157
LOXL3  RFRLAGFPRKPYEGRVEIQRAGEWGTICDDDFTLQAAHILCRELGFTEATGWTHSAKYGPGTGRIWLDNLSCSGTEQSVTECASRGWGNSDCTHDEDAGVI  143
LOXL4  KLRLVGPESKPEEGRLEVLHQGQWGTVCDDNFAIQEATVACRQLGFEAALTWAHSAKYGQGEGPIWLDNVRCVGTESSLDQCGSNGWGVSDCSHSEDVGVI  131
```
HELIX

SRCR 2
```
LOXL2  CSDKRIPGFKFDNSLINQIENLNIQVEDIRIRAILSTYRKRTPVMEGYVEVKEGKTWKQICDKHWTAKNSRVVCGMFGFPGERTYNTKVY----------  247
LOXL3  CKDQRLPGFSDSN--VIEVEHH-LQVEEVRIRPAVGWGRRPLPVTEGLVEVRLPDGWSQVCDKGWSAHNSHVVCGMLGFPSEKRVNAAFY----------  230
LOXL4  CHPRRHRGYLSET-VSNALGPQGRRLEEVRLKPILASAKQHSPVTEGAVEVKYEGHWRQVCDQGWTMNNSRVVCGMLGFPSEVPVDSHYYRKVWDLKMRDP  231
```
HELIX

SRCR 3
```
LOXL2  --KMFASRRKQRYWPFSMDCTGTEAHISSCKLGPQVSLDPMKNVTCENGLPAVVSCVPGQVFSPDGPSRFRKAYKPE-QPLVRLRGGAYIGEGRVEVLKNG  345
LOXL3  --RLLAQRQQHSFGLHGVACVGTEAHLSLCSLEFYRANDTAR---CPGGGPAVVSCVPGPVYAASSGQKKQQQSKPQGEARVRLKGGAHPGEGRVEVLKAS  326
LOXL4  KSRLKSLTNKNSFWIHQVTCLGTEPHMANCQVQVAPARGKLR-PACPGGMHAVVSCVAGPHFRPPKTKPQRKGSWAE-EPRVRLRSGAQVGEGRVEVLMNR  330
```

SRCR 4
```
LOXL2  EWGTVCDDKWDLVSASVVCRELGFGSAKEAVTGSRLGQGIGPIHLNEIQCTGNEKSIIDCKFN-AESQGCNHEEDAGVRCNTPAMGLQKKLRLNGGRNPYE  445
LOXL3  TWGTVCDRKWDLHAASVVCRELGFGSAREALSGARMGQGMGAIHLSEVRCSGQELSLWKCPHKNITAEDCSHSQDAGVRCNLPYTGAETRIRLSGGRSQHE  427
LOXL4  QWGTVCDHRWNLISASVVCRQLGFGSAREALFGARLGQGLGPIHLSEVRCRGYERTLSDCPALEGSQNGCQHENDAAVRCNVPNMGFQNQVRLAGGRIPEE  431
```
HELIX

```
LOXL2  GRVEVLVERNGSLVWGMVCGQNWGIVEAMVVCRQLGLGFASNAFQETWYWHGDVNSNKVVMSGVKCSGTELSLAHCRHDGEDVACPQGGVQYGAGVACSET  546
LOXL3  GRVEVQIGGPGPLRWGLICGDDWGTLEAMVCRQLGLGYANHGLQETWYWD-SGNITEVVMSGVRCTGTELSLDQCAHHGTHITCKRTGTRFTAGVICSET  527
LOXL4  GLLEVQVEVNGVPRWGSVCSENWGLTEAMVACRQLGLGFAIHAYKETWFWSGTPRAQEVVMSGVRCSGTELALQQCQRHG-PVHCSHGGGRFLAGVSCMDS  531
```
HELIX

Figure 1.4. Alignment of the SRCR domains found in LOXL2, LOXL3 and LOXL4. ClustalW, a multiple sequence alignment program was used to align human LOXL2, LOXL3 and LOXL4. The four scavenger receptor cysteine-rich (SRCR) domains are shown. Identical or similar amino acids are shaded. The cysteines that are important for SRCR domain structure are shaded blue. A SRCR domain consists of a six-stranded β-sheet cradling a single α-helix, shown in green. The site responsible for interaction is thought to be the long loop between β-strands 5 and 6, while the rest serves as a structural scaffold. LOXL4 lacks β-strand 5 in third SRCR domain. The second SRCR domain is the most variable domain.
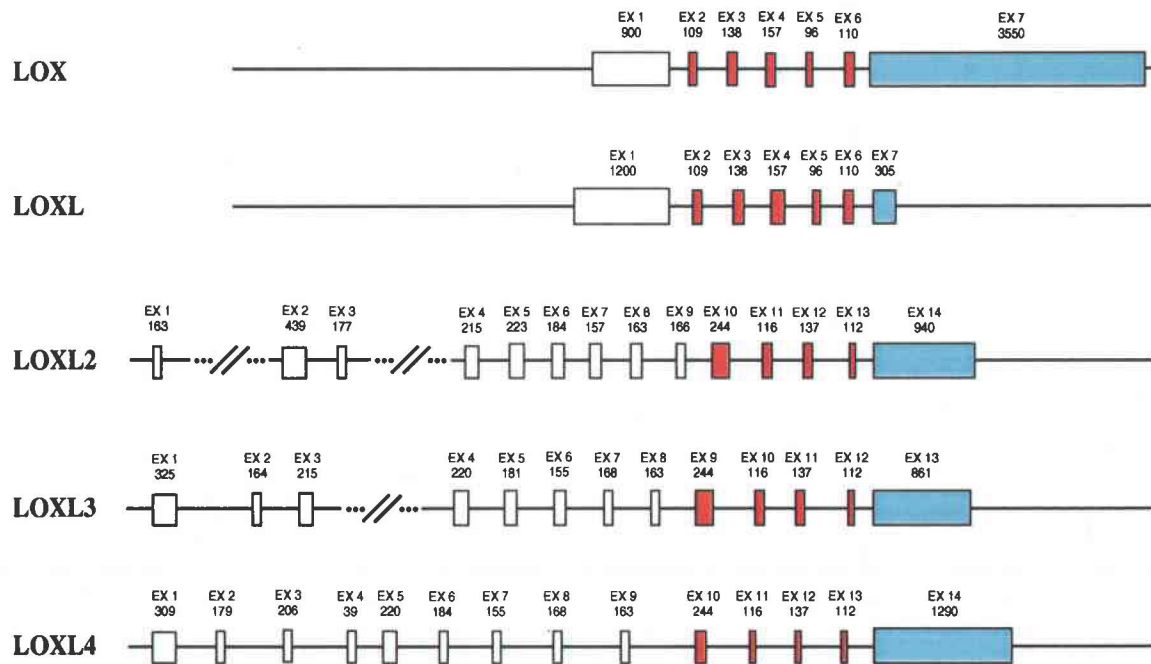
Figure 1.5. Gene structure of the members of the human lysyl oxidase family. Exons are depicted as boxes separated by intron sequences (solid lines). The size of each exon is shown in base pairs. The exons shaded in red encode amino acid sequences that are conserved in all lysyl oxidases. The sizes of these exons are conserved between LOX and LOXL, and between LOXL2, LOXL3 and LOXL4. The exons shaded in blue contain the 3' UTR sequences.

protein containing a signal peptide of 21 aa (Mariani et al, 1992; Hamalainen et al, 1991). Removal of the signal sequence from the 46 kDa prepro-protein and N-glycosylation at an Asn residue located in the propeptide region produces a 50 kDa proenzyme (Trackman et al, 1992). Incorporation of copper is thought to occur either in the endoplasmic reticulum or in the Golgi in advance and independently of glycosylation (Kosonen et al, 1997). After secretion into the extracellular space, the mature, non-glycosylated 32 kDa protein (Trackman et al, 1992) is produced by proteolytic cleavage of the propeptide region between Gly-168 and Asp-169 (Cronshaw et al, 1995).

The enzyme(s) that processes lysyl oxidase into the 32-kDa catalytically active protein is encoded by the *BMP1* gene, which produces bone morphogenic protein-1 (BMP-1) and mammalian tolloid (mTLD) through alternative splicing (Takahara et al, 1994). The *BMP1* gene belongs to a multigene family that includes the mTLD-related proteinases, mammalian tolloid-like-1 (mTLL-1) and mTLL-2, both of which have procollagen C-proteinase activity. These four enzymes are able to process the 50 kDa LOX precursor in mouse embryo fibroblasts at the correct physiologic site. However, BMP-1 was 3-, 15- and 20-fold more efficient than mTLL-1, mTLL-2 and mTLD, respectively (Uzel et al, 2001). Procollagen C-proteinase activity, along with pro-collagen N-proteinase, is also required to remove the C- and N-propeptides of fibrillar collagens, in order for the processed collagen molecules to form fibrillar aggregates (Prockop and Kivirriko, 1995). These fibrillar aggregates are the site of lysyl oxidase

13

activity (Siegel, 1974), thus the same enzyme efficiently produces the active LOX and its assembled collagen substrate.

The extracellular form of lysyl oxidase is crucial for the tensile strength and mechanical stability of collagen fibrils, the most abundant protein in mammals, and for the repetitive and reversible deformation of elastin, the major protein of elastic fibers that is essential for its characteristic resilience. Indeed, the LOX "knockout" mouse expires immediately after birth due to aortic aneurysm formation from incomplete cross-linking of elastin (Maki et al, 2002). Lysyl oxidase oxidizes peptidyl lysine and hydroxylysine residues in collagen and lysine residues in elastin to produce peptidyl α-aminoadipic-δ-semialdehydes. These aldehyde residues can spontaneously condense with vicinal peptidyl aldehydes or with ε-amino groups of peptidyl lysine to form the covalent cross-links that stabilize and insolubilize several fibrillar collagen types and elastin fibers. In elastic fibers, these cross-links are called desmosines and isodesmosines (Kagan and Li, 2003; Kagan, 1986). This catalytic reaction, shown in Figure 1.6, can be irreversibly inhibited by β-aminopropionitrile (βAPN), a specific inhibitor that binds to the active site of LOX (Tang et al, 1983).

As expected from its dependence on copper and its critical role in collagen and elastin crosslinking, lysyl oxidase is affected in a variety of human diseases. Menkes disease and occipital horn syndrome (also known as X-linked cutis laxa and Ehlers-Danlos syndrome type 9), which are X-linked, recessively inherited disorders of

14

NH₂
|
CH₂
|
CH₂   +O₂ + H₂O   **lysyl oxidase** →
|
CH₂
|
CH₂
|
NH—CH—CO
Lysine

O
‖
CH
|
CH₂   + H₂O₂ + NH₃
|
CH₂
|
CH₂
|
NH—CH—CO
AAS

O
‖
CH
|
CH₂
|
CH₂
|
CH₂
|
NH—CH—CO
AAS

1

2

**Spontaneous
Condensation**

NH—CH—CO
|
CH₂
|
CH₂
|
CH₂
|
CH
‖
N
|
CH₂
|
CH₂
|
CH₂
|
CH₂
|
NH—CH—CO

NH—CH—CO
|
CH₂
|
CH₂
|
C—CH
| ‖
HC   O
|
CH₂
|
CH₂
|
CH₂
|
NH—CH—CO
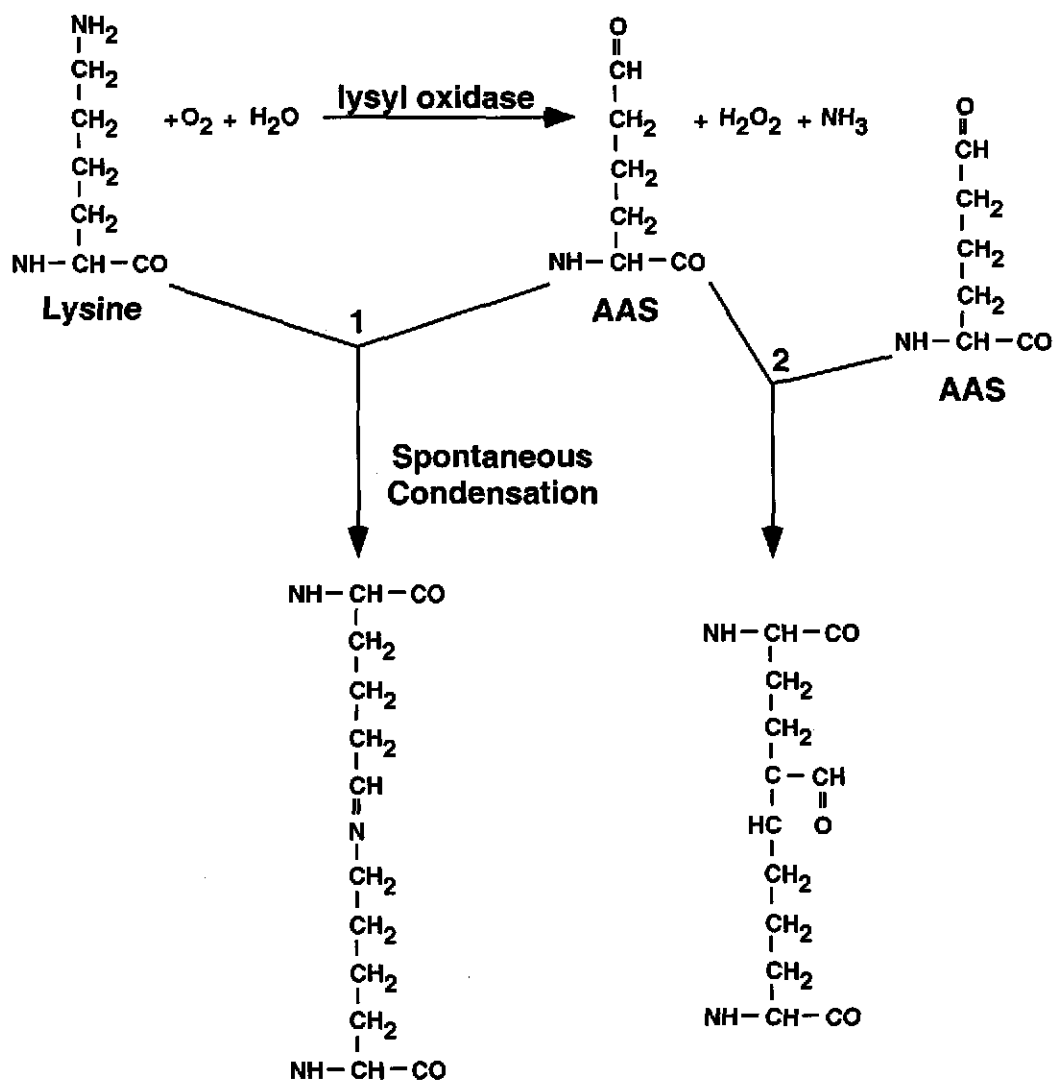
Adapted from Kagan and Trackman, 1991.

Figure 1.6. Enzymatic activity of lysyl oxidase. Lysyl oxidase oxidatively deaminates peptidyl lysine (or hydroxylysine) to generate the corresponding peptidyl α-aminoadipic-δ-semialdehyde (AAS). Spontaneous condensation of the aldehyde residue with the e-amino group of peptidyl lysine (1) or another peptidyl aldehyde (2) results in covalent cross-link formation.

abnormal copper transport and cellular copper sequestration, show connective tissue abnormalities due to defective cross-linking of collagen and elastin secondary to decreased levels of lysyl oxidase mRNA and enzyme activity (Kemppainen et al, 1996; Gacheru et al, 1993; Royce and Steinmann, 1990; Kuivaniemi et al, 1985; Byers et al, 1980; Royce et al, 1980). Increased lysyl oxidase activity has been observed in fibrotic disorders, including fibrosis of the lung (Streichenberger et al, 2001; Almassian et al, 1991; Counts et al, 1981), liver (Murawaki et al, 1991; Carter et al, 1982; Siegel et al, 1978) and skin (Chanoki et al, 1995).

Extracellular lysyl oxidase also plays a role in cell motility. Human blood monocytes, which are commonly found in inflammatory states associated with the accumulation of extracellular matrix, were demonstrated to have a chemo-attractant response to catalytically active lysyl oxidase. This chemo-attractant response was characterized by both chemokinetic (increased rate of movement) and chemotactic (directed migration due to concentration gradient of a diffusible chemical) components (Lazarus et al, 1995). In similar experiments, LOX was shown to have a predominantly chemotactic effect on rat vascular smooth muscle cells. The chemotactic response was eliminated by βAPN and by catalase, indicating that active lysyl oxidase is necessary and that the H_2O_2 by-product of LOX-catalyzed oxidation mediates the response (Li et al, 2000).

Lysyl oxidase has also been demonstrated to have a role in cell development, differentiation and growth. Six-fold increase in LOX activity was noted during sea urchin embryo development, and the treatment of the embryos with βAPN caused developmental arrest at the mesenchymal blastula stage (Butler et al, 1987). In *Xenopus laevis,* intracellular LOX is able to antagonize p21-Ha-Ras-induced and progesterone-dependent oocyte maturation (Di Donato et al, 1997b). Dexamethasone, which accelerates fetal lung development, was shown to enhance LOX expression in cultured murine fetal lungs (Chinoy et al, 2000) and LOX was identified as an early marker in adipocyte differentiation responsive to retinoic acid (Dimaculangan et al, 1994). Recently, a novel substrate for LOX, basic fibroblast growth factor (bFGF) was identified. The oxidation of lysine residues in bFGF caused covalent crosslinking of bFGF monomers to form dimers and higher order oligomers, leading to reduced mouse fibroblast proliferation (Li et al, 2003). Collectively, these effects are due to both extracellular and intracellular LOX.

Although the extracellular form of LOX has been well characterized, less is known about intracellular LOX. The LOX protein has been localized within the nuclei of rat vascular smooth muscle cells and mouse NIH 3T3 fibroblasts, and contains two possible nuclear localization signals, one in the preproenzyme and one in the mature protein. This nuclear protein has catalytic activity inhibited by βAPN and is thought have a novel functional activity (Li et al, 1997). Deamination of histones, which have been reported as *in vitro* substrates for lysyl oxidase (Kagan et al, 1983), would reduce the

17

positive charge, leading to histone dissociation from deoxyribonucleoprotein complexes, similar to action of histone deacetylase. Indeed, revertant *ras*-transformed NIH 3T3 cells transfected with a sense construct of LOX cDNA demonstrated less tightly packed chromatin than the same cells transfected with an anti-sense construct (Mello et al, 1995). The association of LOX with chromatin was confirmed by electron microscopy of bovine aorta that showed localization of lysyl oxidase in association with condensed chromatin in the nucleus (Kagan and Li, 2003). In addition to its nuclear localization, LOX has also been identified in the cytoplasm of cultured fibroblasts, chondrocytes, smooth muscle cells, endothelial and epithelial cells as a fine, filamentous structure, thought to be associated with the cytoskeleton (Wakasaki and Ooshima, 1990).

The regulation of LOX gene expression has been described in different tissues and cells from several species, and has revealed multiple complex mechanisms that coordinately regulate the expression and activity of LOX. These effectors, the observed effects in mRNA and enzyme activity, and the cell or tissue in which these effects were observed are listed in Table 1.1. The list includes transcription factors such as IRF-1 (Tan et al, 1996), metal ions such as cadmium (Li et al, 1995), cytokines and growth factors such as TGF-β (Bose et al, 2000; Hong et al, 1999; Shanley et al, 1997; Gacheru et al, 1997; Roy et al, 1996; Feres-Filho et al, 1995; Boak et al, 1994; Shibanuma et al, 1993), hormones such as testosterone (Bronson et al, 1987) and signaling molecules such as cAMP (Choung et al, 1998; Ravid et al, 1999). However, because of the differences in cell types and species used in these varied studies, it is impossible to determine which

Table 1.1. Transcriptional and post-transcriptional regulation of lysyl oxidase.

Effector	Cell or tissue	Effect
Adriamycin[1]	Rat kidney glomeruli, medula	Three-fold increase of mRNA
Bleomycin[2, 3]	Human dermal and pulmonary fibroblast	Decreased mRNA level
	Rat lung tissue	Increased enzyme activity
Cadmium[4-6]	Rat lung tissue	Increased enzyme activity
	Mouse fibroblast	Increased mRNA level
	Mouse cadmium-resistant fibroblast	Decreased mRNA level
cAMP[7]	Rat vascular smooth muscle cells	Upregulation of gene transcription
Dexamethasone[8,9]	Cultured fetal murine lungs	Upregulation of mRNA
	ras-transformed mouse fibroblast	Increased mRNA level
Fibroblast growth factor-2[10-12]	Rabbit retinal pigment epithelial cells	Decreased mRNA level
	Human gingival fibroblast	Decreased mRNA level; reduced enzyme activity
	Mouse osteoblastic cells	Decreased mRNA level (1-10 nM)
		Upregulation of mRNA (0.1-0.1 nM)
Fibroblast growth factor-2 + Insulin-like growth factor-1[13]	Rat inflamed oral tissues, rat fibroblastic mesenchymal cells	Two-fold increase of mRNA
Follicle stimulating hormone[14,15]	Rat granulosa cells	Decreased mRNA and enzyme activity
Hydralazine[2]	Human dermal fibroblast	Four-fold increase of mRNA
Interferon-gamma[16]	Rat aortic smooth muscle cells	Downregulation of mRNA
		Decreased mRNA half-life
Interferon regulatory factor-1[17]	mouse embryonic fibroblasts	Increased mRNA level
Interferon regulatory factor-2[17]	IRF-2 overepressing mouse fibroblast	Decreased mRNA level
Low density lipoprotein[18]	Porcine aortic endothelial cells	Five-fold reduced mRNA; reduced LOX activity
	Aorta from hypercholesteremic pigs	Three-fold reduction of mRNA levels
Minoxidil[2]	Human dermal fibroblast	Increased mRNA
Platelet-derived growth factor [10,19,20]	Rabbit retinal pigment epithelial cells	Increased mRNA level
	Rat vascular smooth muscle cells	Upregulation of mRNA
Prostaglandin E2[21,22]	Human embryonic lung fibroblasts	Downregulation of mRNA
	Rat lung fibroblasts	Unchanged steady-state mRNA level; reduced enzyme activity
ras[9, 23-26]	ras-transformed mouse fibroblast and human osteosarcoma cells	Reduced transcription, reduced mRNA levels
	Revertant ras-transformed rat & mouse fibroblasts	Upregulation of mRNA
Retinoic acid [10,27]	Rabbit retinal pigment epithelial cells	Decreased mRNA level
	Mouse adipocytes (early adipogenesis)	Prevents downregulation of mRNA and enzyme activity
Testosterone[14, 15, 28]	Rat granulosa cells	Increased LOX mRNA and enzyme activity
	Calf aortic smooth muscle cells	Increased activity
Transforming growth factor-beta-1[1,14,21,22,29-36]	Rat aortic smooth muscle cells, rat granulosa cells, mouse osteoblastic cells	Increased mRNA level and enzymatic activity
	Human gingiva, flexor reticulum cells, renal cell lines	Four-fold increase of mRNA

[1]Di Donato et al, 1997a; [2]Yeowell et al, 1994; [3]Counts et al, 1981; [4]Li et al, 1995; [5]Almassian et al, 1991; [6]Chichester et al, 1981; [7]Ravid et al, 1999; [8]Chinoy et al; 2000; [9]Contente et al, 1999; [10]Omori et al, 2002; [11]Hong and Trackman, 2002; [12]Feres-Filho et al, 1996; [13]Trackman et al, 1998; [14]Harlow et al, 2003; [15]Slee et al, 2001; [16]Song et al, 2000; [17]Tan et al, 1996; [18]Rodriguez et al, 2002; [19]Smith-Mungo and Kagan, 2002; [20]Green et al, 1995; [21]Roy et al, 1996; [22]Boak et al, 1994; [23]Csiszar et al, 1996; [24]Hajnal et al, 1993; [25]Krzyzosiak et al, 1992; [26]Contente et al, 1990; [27]Dimaculangan et al, 1994; [28]Bronson et al, 1987; [29]Bose et al, 2000; [30]Hong et al, 1999; [31]Shanley et al, 1997; [32]Choung et al, 1998; [34]Gacheru et al, 1997; [35]Feres-Filho et al, 1995; [36]Shibanuma et al, 1993.

factors may have a general effect across species and tissues. The particular factors that have relevance to the role of LOX in cancer will the described in Chapter II.

2. Lysyl Oxidase Like -2 (LOXL2)

The lysyl oxidase like-2 gene (LOXL2) is the third member of the lysyl oxidase family to be described. It was first characterized as a lysyl oxidase-related protein that was isolated as an overexpressed transcript from human senescent fibroblasts. The amino acid sequence demonstrated 48% homology to LOX and LOXL at the regions corresponding to the conserved exons 2-6 (Figure 1.5), but also contained four SRCR domains that distinguished it from LOX and LOXL. As with LOX, the mRNA level of LOXL2 was induced by TGF-β1 and inhibited by retinoic acid (Saito et al, 1997).

The LOXL2 gene has been mapped to chromosome 8p21.2-p21.3 (Jourdan-Le Saux et al, 1998). It is composed of fourteen exons varying in size from 112-940 bp, with exons 10-13 homologous to exons 2-6 of both LOX and LOXL (Figure 1.5). There are three major transcription termination sites within the 3' UTR at 690, 740 and 900 bp 3' of the termination codon, detected as a single transcript of 3.65 kb by Northern blot analysis. Higher steady state mRNA levels were detected in the reproductive tissues of placenta, prostate and uterus, as well as the pancreas. A much less abundant transcript of 4.9 kb was also detected in heart, liver and pancreas (Jourdan-Le Saux et al, 1999).

The 3.65 kb transcript of LOXL2 encodes a protein of 774 aa with predicted molecular weight of 87 kDa. The LOXL2 protein has a predicted signal peptide of 22 aa and three potential N-linked glycosylation sites (Saito et al, 1997). A search for a BMP-1 consensus site failed to reveal any potential processing site. Although the LOXL2 protein contains all the conserved amino acid sequences needed for catalytic activity, it is unknown whether LOXL2 is catalytically active, or if it has different or additional functions conferred by the SRCR domains.

Distinct patterns of expression of LOXL2 compared to LOX have been demonstrated. Northern analysis of a multiple human tissue blot, indicated higher expression of LOX in heart, lung and kidney (Kim et al, 1995), compared to higher expression of LOXL2 in placenta and pancreas (Jourdan-Le Saux et al, 1999). In full-term placenta, LOX is expressed predominantly in the amniotic epithelium, while LOXL2 is detected primarily in the syncytiotrophoblast and cytotrophoblast layer of the membranes with low expression in the amnion (Hein et al, 2001; Jourdan-Le Saux et al, 1999), indicating that these two family members may have distinct substrates and functions. One possible function that has been hypothesized for LOXL2 is a role in cell adhesion as LOXL2 mRNA expression was noted in various adherent tumor cell lines but absent in tumor cell lines that grew in suspension. This loss of adhesion was hypothesized to play a role in metastasis (Saito et al, 1997). Further evidence of the association between LOXL2 and cancer will be described in greater detail in Chapter III.

B. GENETICS OF MALIGNANT TRANSFORMATION

The pathogenesis of a normal cell to the production of a tumor *in vivo* requires the accumulation of several genetic lesions. It is generally believed that mutations in 5-10 genes are required for tumor development (Murphy and Levine, 2001), and indeed in the case of colon cancer, at least seven genetic alterations are required (Fearon and Vogelstein, 1990; Kinzler and Vogelstein, 1996). The time required for the accumulation of these mutations in a single cell explains the increase of cancer risk with age. The mutations accumulate affect three broad categories of genes: proto-oncogenes, tumor suppressor genes and mismatch repair genes.

The malfunction of mismatch repair genes, such as hMSH2, hMSH3, hMSH6 and hMLH1, are thought to accelerate the neoplastic transformation process (Chung and Rustgi, 1995). These deficiencies were first discovered in studies of hereditary non-polyposis coli (de la Chapelle and Peltomaki, 1995), and they have since been described in nearly every type of cancer, including breast (Contegiacomo et al, 1995), lung (Ryberg et al, 1995) and ovary (King et al, 1995). In a normal human cell, the spontaneous mutation rate is approximately 1.4×10^{-10} mutations per base pair per cell generation (Loeb, 1991). Tumors with mismatch repair deficiency have a 100-600 fold increase in the rate of spontaneous mutations at select loci such as the HPRT (hypoxanthine-guanine phosphoribosyltransferase) loci (Bhattacharyya et al, 1994), that consist mainly of base substitutions and frameshifts (Bhattacharyya et al, 1995). Tumors that are deficient in mismatch repair, noted as replication error or RER+ phenotype, can be identified by the

22

gain or loss of repeat units in microsatellites, or microsatellite instability (MIN) (Bhattacharyya et al, 1994; Shibata et al, 1994). Microsatellites are tandemly repeated nucleotide sequences often found in noncoding regions of the genome, and are thus not subject to selective pressure against sequence alterations. Because these repeat regions are inherently more difficult to replicate with high fidelity, they are generally variable in length among individuals in a population, but constant among the cells of an individual (Murphy and Levine, 2001). However, with mutations of mismatch repair genes, the number of repeats and therefore the length of the microsatellite is variable among affected cells, and this MIN can be used to identify RER+ individuals.

Oncogenes encode proteins that are able to cause cellular transformation, defined as morphological changes, loss of contact inhibition, anchorage-independent growth and the ability to form tumors when transplanted into nude mice (Kimmelman et al, 2001). Mutations of the normal proto-oncogenes either alter the protein product directly or are found in the regulatory portion of a gene, leading to the overproduction of a normal gene product. These activating mutations or protein overexpression cause a gain of function that is dominant to the wild-type allele, and is often involved in a continuous or abnormal signal for cell proliferation or growth (Murphy and Levine, 2001).

However, the definition that oncogenes are dominant, that activated oncogenes predispose the host cell to transformation despite the presence of a normal allele, has been challenged by recent studies on *ras*. Members of the Ras subfamily are small GTP-

23

binding proteins that act as intracellular molecular switches alternating from inactive GDP-bound state to an active GTP-bound state. They mediate a wide variety of cellular functions including proliferation, survival and differentiation, depending on the cell type and extracellular environment (Kimmelman et al, 2001). Thymic lymphomas induced in mice by the N-*ras* oncogene were more frequent on a background of null N-*ras* than on wild-type, and the overexpression of wildtype N-*ras* in the presence of *ras* oncogene resulted in decreased thymic lymphoma development (Diaz et al, 2002). Similar findings were reported for K*ras* and lung cancer development in mice (Zhang et al, 2001).

A tumor suppressor gene (TSG) is defined as a gene that normally prevents cancer or tumorous growth and that both copies of this gene must be lost or inactivated to initiate a cancer (Murphy and Levine, 2001). The loss of both alleles of a TSG is referred to as Knudson's two hit hypothesis, based on his observations with retinoblastomas. Normal individuals have two wild-type *RB* alleles and very rarely, two independent mutations occur in a single retinoblast, resulting in tumor formation. In the hereditary form, individuals inherit one mutant allele and with high frequency, mutations arise in the other allele due to chromosome loss, deletion, gene conversion or somatic mutation, resulting in cancer (Murphy and Levine, 2001; Knudson, 1971).

TSG encode proteins that are negative regulators of proliferation and cell cycle progression. As negative regulators, loss of one allele is expected to have no impact on the function of the other wild-type allele. TSG are recessive in behavior, and loss of

function leads to deregulated control of normal functions (Murphy and Levine, 2001).

Two TSG examples, APC and IRF-1, are discussed in the following section. A common way in which two TSG alleles are inactivated is by mutation in one allele and loss of the other allele. The loss of one allele is demonstrable by loss of heterozygosity (LOH) of a polymorphic marker, such as a microsatellite, linked to the TSG locus (Kinzler and Vogelstein, 1996; Lasko et al, 1991). In individuals heterozygous for a polymorphic microsatellite marker in close proximity or within a TSG, loss of one TSG allele is detected as loss of one microsatellite allele. This loss of heterozygosity, or reduction to homozygosity, in the genomic DNA of affected tumor tissue compared to normal tissue, indicates the loss of one parental copy of the tumor suppressor gene.

Previous studies on both colon and esophageal cancers demonstrate LOH, and thus possible tumor suppressor loci, in the same chromosomal regions as both LOX at chromosome 5q23 and LOXL2 at chromosome 8p21. Histologically, both the colon and esophagus are divided into the mucosa, submucosa, muscularis and adventia. The submucosa is quite dense and contains a network of collagen and elastic fibers (Kierszenbaum, 2002). Thus the expression of lysyl oxidase, and possibly other LOX gene family members, is expected to be important in the function of these tissues.

1. Colorectal Cancer Genetics and Epidemiology

Allelotype analysis identified the four chromosomal arms 5q, 8p, 17p and 18q as regions that were the most frequently affected in colon carcinoma (Vogelstein et al,

25

1989). At the most commonly affected loci, p53 has been identified at 17p (Baker et al, 1989), and DCC (deleted in colorectal carcinomas) and Smad4/DPC4 (deleted in pancreatic carcinoma, locus 4) have been identified at 18q (Fearon et al, 1990; Takagi et al, 1996). A chromosomal imbalance map based on over 300 cases of colon cancer narrowed the affected portion of chromosome 5 to the region 5q14 to 5q31, with slightly higher percentage loss for 5q21-31 (Mertens et al, 1997). This encompasses the IRF-1 gene at 5q31 (Itoh et al, 1991), and both the APC and MCC genes at 5q21 (Kinzler et al, 1991a).

APC was discovered as an early mutation in the hereditary disease, familial adenomatous polyposis coli (Bodmer et al, 1987; Leppert et al, 1987), and it was also found to be involved in the majority of sporadic colon cancers as well (Miyoshi et al, 1992; Powell, 1992). The C-terminus of the APC protein has microtubule binding regions and putative sites for indirect actin binding, and truncation of the APC protein causes altered cytoskeletal structure and microtubule dynamics, and reduced migration (Hughes et al, 2002). Most mutant APC proteins lack at least one of the two types of β-catenin binding repeats, resulting in increased levels of free β-catenin (Rubinfeld et al, 1996). Free β-catenin is able to translocate to the nucleus where it acts as an activator of T-cell factor (Tcf)-dependent transcription resulting in increased levels of c-Myc, cyclin D1, MMP-7 and ITF-2 (Kolligs et al, 2002). However, a mutation of APC is not a requirement for the pathogenesis of colon cancer, as 15% of colorectal cancers synthesize only full length APC protein (Smith et al, 1993).

The MCC gene is located approximately 180 kb from the APC gene (Joslyn et al, 1991; Kinzler et al, 1991b). Although there are MCC mutations in about 5% of colon cancers (Kinzler et al, 1991b), many of them are conservative amino acid changes, and they appear to occur only in those tumors that also have a mutation in APC (Curtis et al, 1994). Therefore, the LOH and mutations of MCC could be considered passenger mutations - alterations in genes, sometimes local residents of a targeted gene, that accumulate over time but do not contribute to the neoplastic phenotype (Kern, 2001). However, APC and MCC do share heptad repeat motifs that may mediate protein-protein interactions, possibly with each other (Fearon and Gruber, 2001), and MCC may have a role in regulating the G_1 to S phase of the cell cycle (Matsumine et al, 1996).

The IRF-1 gene encodes a DNA binding transcriptional activator (Tanaka and Taniguchi, 1992). IRF-1 null fibroblasts fail to undergo apoptosis and are readily transformed, indicating a role in tumor suppression. IRF-1 is induced by DNA damage through the ATM (ataxia telangiectasia mutated)-signaling pathway that also activates p53 (Pamment et al, 2002). IRF-1 cDNA can also suppress the transformed phenotype due to transfection with *ras* (Tanaka et al, 1994a), which is most likely due to the induction of the LOX gene through an IRF response element in the LOX gene promoter (Tan et al, 1996). IRF-1 is also able to suppress cell transformation by *c-myc* or *fos*B (Tanaka et al, 1994b).

Although a large area of chromosome 5q is affected by loss of heterozygosity in colon cancer, there are no documented tumor suppressor genes between APC at chromosome 5q21 and IRF-1 at chromosome 5q31. Deletions involving 5q21-31 would certainly affect the lysyl oxidase gene and based on evidence for its association with cancer, which will be reviewed in chapter II, lysyl oxidase is a possible candidate tumor suppressor gene.

The loss of chromosome 8p in colon cancer (Vogelstein et al, 1989) was narrowed to the 8p21 region (Lerebours et al, 1999; Arai et al, 1998; Cunningham et al, 1993). The introduction of normal chromosome 8p21-pter into colon carcinoma cells that show allelic loss of 8p21, resulted in suppressed tumorigenicity and invasiveness, indicating that indeed a tumor suppressor resides in this region (Tanaka et al, 1996). However, unlike in chromosome region 5q, there are no tumor suppressor genes that have been identified, and only one candidate. In twelve colorectal cancer cell lines, three were found to have amino acid substitutions in exon 3 of EXTL3, and only one cell line demonstrated loss of expression (Arai et al, 1999). The exact chromosomal location of this candidate is not known, and only LOXL2 maps within a 1 cM interval of common deletion in colorectal cancer (Lerebours et al, 1999). Although little is known about the function of LOXL2, based on the evidence for its family member, LOX, as a tumor suppressor, and as well as shared functional domains, LOXL2, is a promising candidate for a tumor suppressor gene in the 8p21 region.

Globally, colorectal cancer is the third most common cancer in incidence and the fourth most common cancer causing death for both men and women. An estimated 944,717 cases and 492,411 deaths occurred in 2000, representing 9.4% of all new cases of cancer and 7.9% of deaths due to cancer. High risk areas include North America, Europe and Australia, with the developed world accounting for 65% of the global incidence (International Agency for Research on Cancer, 2000). Similar to the rest of the world, colon cancer is the third most common cancer in the United States, with an estimated 147,500 new cases expected to occur in 2003. However, for males and females ages 40-79 years old, colon cancer is the second and third most common fatal cancer, respectively. The relative five-year survival rate for colon cancer was 62% from 1992-1998. When colon cancer is detected early, the five-year survival rate is 90%, but only 37% of cases are diagnosed at an early stage. If the cancer spreads to adjacent organs or lymph nodes, as in 37% of the cases of colon cancer, the 5-year survival drops to 65%, and when there is distant metastasis, it plummets to 9%. An estimated 57,100 deaths are expected to occur in 2003 (Jemal et al, 2003).

2. Esophageal Cancer Genetics and Epidemiology

Chromosome regions exhibiting LOH in esophageal cancer include 3p, 5q, 9p, 9q, 13q, 17p, 17q, and 18q (Montesano et al, 1996). The candidate genes for chromosome 5q were previously thought to be the APC and MCC genes. However, further studies revealed that mutations within these genes in esophageal tumors were very rare (Shibagaki et al, 1994; Aoki et al, 1994; Powell et al, 1994), thus indicating that these

29

genes are most likely not the principal targets of chromosomal rearrangements and mutations in the course of tumorigenesis. A more recent study of chromosome 5 in esophageal cancer showed the highest LOH of 5q to be between 5q23 and 31.1 (Peralta et al, 1998). This region is telomeric to the location of both APC and MCC genes, and encompasses both the lysyl oxidase (LOX) gene and the IRF-1 gene that is a transcriptional regulator of the LOX gene. No candidate tumor suppressors have been identified in this region.

An earlier report of allelotype analysis in esophageal squamous cell carcinoma identified both chromosome regions 5q and 8p as having frequent loss of heterozygosity (Shibagaki et al, 1994). In this study, Shibagaki and co-workers describe a lower but significant LOH of 33.3% for chromosome 8p compared to 52.6% for chromosome 5q. However, a more recent report using a Chinese cohort identified chromosome both 5q and 8p as having very high frequency (>75%) LOH in esophageal squamous cell carcinoma (Hu et al, 2000). One candidate tumor suppressor for esophageal cancer, FEZ1, has been identified at 8p22. Reduced mRNA expression was demonstrated in 2 of 3 esophageal cancer cell lines evaluated, and sequence analysis of 72 primary squamous cell carcinomas and 18 esophageal cell lines identified aberrations in four primary esophageal cancers. Two samples had truncated transcripts and two samples had different point mutations leading to amino acid substitutions (Ishii et al, 1999). Thus, FEZ1 is not a strong candidate, and for reasons mentioned previously, the LOXL2 gene is a promising candidate tumor suppressor gene.

30

Globally, esophageal cancer is the eighth most common cancer in incidence and the sixth most common cancer causing death. An estimated 412,327 cases and 337,501 deaths occurred in 2000, representing 4.1% of all new cases of cancer and 5.4% of deaths due to cancer. Among males, who account for 68% of the total cases, it is the sixth most common cancer. The incidence is also higher along the esophageal cancer belt that spans from north-central China through central Asia and northern Iran, and parts of South Africa and south-east Africa. Less developed countries account for 83% of the total cases (International Agency for Research on Cancer, 2000). In the United States, an estimated 13,900 new cases of esophageal cancer and 13,000 deaths are expected to occur in 2003. More than three-fold more cases are expected in males compared to females, and in African-Americans compared to Caucasians. The relative five-year survival rate was 15% in whites and 8% in African-Americans from 1992-1998. Even when detected early, the 5-year survival rate is only 27%. This drops to 13% if the cancer spreads to adjacent organs or lymph nodes, and is an abysmal 2% if distant metastasis occurs (Jemal et al, 2003).

C. SUMMARY AND DISSERTATION HYPOTHESIS

The LOX family of genes is currently composed of five members. The chromosomal loci of two of these members, 5q23 for LOX and 8p21 for LOXL2, demonstrate LOH in colon and esophageal cancer and thus indicate the presence of TSG at these loci that are involved in the pathogenesis of these two cancers which are responsible for significant morbidity and mortality both within the United States and

31

worldwide. Three functions ascribed to LOX, regulation of growth, maintenance of the integrity of the extracellular matrix and cell motility, indicate that LOX may be involved early in cancer development with the promotion of tumor growth, or in later stages with the breakdown of the extracellular matrix promoting local invasion, respectively. In addition, Chapter III will describe the association between LOXL2 and cancer, and the next chapter will describe the evidence involving LOX as part of a tumor suppressor pathway through its blockage of the *ras* pathway and the progressive reduction of lysyl oxidase mRNA and enzyme activity during tumor development and metastasis. However, there are no reports which demonstrated mutations within the gene itself and thus it could not be determined whether aberrations in LOX gene expression was a primary effect of a LOX gene mutation, or a secondary effect through pathways of cancer pathogenesis. The shared functional domains between LOX and LOXL2 indicate that it may have similar functions. The unique SRCR domains found in LOXL2 may have a function in cell adhesion, indicating that LOXL2 may also be involved in cancer metastasis or loss of growth inhibitory signaling.

The overall goal of this dissertation is to address if LOX and LOXL2 contribute to tumorigenesis and elucidate the possible role of these two amine oxidases in the development of cancer. Although LOX was initially described as a putative tumor suppressor, I believe that LOX and LOXL2 may not fit the simple tumor suppressor role, but rather, based on the multiple roles of this amine oxidase family, have a more complex role in tumor development. I intend to challenge the concept of LOX and LOXL2 as

32

tumor suppressors. My hypothesis consequently is that alteration or aberration in the expression of the LOX and LOXL2 genes are contributing factors in tumorigenesis.

I intend to address this hypothesis through the following two sets of specific aims. The first set focuses on the role of lysyl oxidase in colon and esophageal tumors. As the down-regulation of expression of the LOX gene in cancer has been reported by many investigators, my goal is to evaluate for mutations in the LOX gene which may be responsible for altered LOX gene expression. The specific aims are as follows:

1: **Characterize the deletional status of microsatellites (loss of heterozygosity (LOH)) surrounding the LOX gene in colon and esophageal tumors**

2: **Evaluate tumor samples with LOH for reduced gene expression**

3: **Identify LOX gene mutations in tumor samples with low LOX expression**

The second set of specific aims focuses on the role of the LOXL2 gene in colon and esophageal tumors. Because there is little known about the function of the LOXL2 protein in cancer development and in normal tissues, my goal is to evaluate expression patterns in normal and tumor cell lines and tissues. The specific aims are as follows:

1: **Identify normal tissue localization of the LOXL2 protein**

2: **Characterize the deletional status of the microsatellite within the LOXL2 gene in colon and esophageal tumors**

3: **Evaluate colon and esophageal tumors for aberrant LOXL2 expression**

33

CHAPTER II

LOSS OF HETEROZYGOSITY AND SOMATIC MUTATIONS OF THE LYSYL OXIDASE GENE IN COLORECTAL TUMORS

A. INTRODUCTION

The possibility of a role of lysyl oxidase in cancer was first realized with the isolation of a putative tumor suppressor gene named the *ras recision gene* (*rrg*) in mouse. The expression of this *rrg* gene was greatly reduced in NIH 3T3 mouse fibroblasts transformed by long terminal repeat activated c-H-*ras* (LTR-c-H-*ras*). Interferon treatment of these transformed NIH 3T3 cells resulted in revertant cells, characterized by contact inhibition, inability to proliferate in soft agar and rare tumor formation in nude mice. These revertants expressed pre-transformation levels of *rrg*, despite retaining high levels of *ras* expression. Persistently revertant *ras*-transformed NIH 3T3 cells transfected with an antisense construct of *rrg* cDNA demonstrated a transformed phenotype and were able to produce tumors in athymic mice. Conversely, cells transfected with a sense construct of *rrg* cDNA demonstrated a flat phenotype and were non-tumorigenic in athymic mice after 8 weeks (Contente et al, 1990).

Upon analysis of the mouse *rrg* cDNA sequence, it was found to be 92% identical to the sequence for rat lysyl oxidase (Kenyon et al, 1991) and 89% identical to the human LOX sequence (Mariani et al, 1992), indicating that *rrg* and lysyl oxidase were the same gene. In addition, the sizes of the human LOX mRNA (Mariani et al, 1992) correlated to

34

that of the *rrg* mRNA (Contente et al, 1990), and there was a direct correlation between

rrg mRNA expression and lysyl oxidase activity. Indeed, normal cells and revertants

exhibited approximately 10-fold higher LOX activity compared to transformed cells, and

the lower LOX activity of the transformed cells correlated with increased tumorigenicity

in nude mice (Kenyon et al, 1991). Normal rat kidney fibroblasts transfected with an

antisense construct of LOX demonstrated a transformed phenotype, 11- to 25-fold higher

levels of active $p21^{ras}$ and the ability to form fibrosarcomas in nude mice (Giampuzzi et

al, 2001). In malignant cell lines, including fibrosarcoma, rhabdomyosarcoma,

choriocarcinoma and melanoma, LOX activity was decreased (Kuivaniemi et al, 1986).

The decreased activity observed in these cell lines and in the *ras*-transformed NIH 3T3

cells were due to transcriptional down-regulation of the LOX gene, not from alterations

in message stability or RNA processing (Contente et al, 1999; Hamalainen et al, 1995).

Other investigators also confirmed the loss of LOX expression in transformed

cells. NIH 3T3 cells transformed either by *ras* or c-*erbB-2* lacked LOX expression that

was regained after reversion by treatment with azatyrosine or with interferon and retinoic

acid combined (Friedman et al, 1997; Krzyzosiak et al, 1992). Similarly, *ras*-transformed

rat fibroblasts, which spontaneously reverted or were reverted by interferon, had

increased LOX expression (Szpirer et al, 1996; Oberhuber et al, 1995; Hajnal et al, 1993).

The transcriptional down-regulation of LOX in *ras*-transformed osteosarcoma cells

compared to its non-transformed counterpart was also documented (Csiszar et al, 1996),

indicating that oncogenic *ras* expression could induce decreased LOX expression in both

normal fibroblasts cells and cancer cells. A recent genome wide survey of *ras* transformation targets in rat embryonic fibroblasts confirmed that lysyl oxidase is down-regulated more than 9-fold (Zuber et al, 2000), consistent with the 10-fold higher LOX activity observed in normal cells and revertants compared to transformed cells.

Decreased LOX expression was not only noted in transformed cells but also in the development of prostate and breast cancers. LOX was detected by differential display PCR in primary vs. metastatic prostate cancer cells following TGF-β1 stimulation, and reduced LOX mRNA levels appeared to be an acquired feature of the metastatic phenotype in cultured cells. In human and mouse tissues, progressive reduction of LOX expression was observed with the transition from normal prostate epithelium to malignant prostate epithelium to metastatic tumors (Ren et al, 1997). In a study on breast tumors, LOX could be detected at the invasion front of infiltrating tumors, but decreased in late stromal reactions and disappeared from the stroma of invading ductal carcinomas (Peyrol et al, 1997). The consistent finding of decreased lysyl oxidase expression in various transformed and cancer cell lines and in tumors was consistent with the loss of expression of a tumor suppressor gene in the development of cancer.

The ability of LOX to suppress the phenotype induced by the oncogene *ras* was demonstrated in a model system utilizing *Xenopus laevis* oocytes. The injection of activated p21-Ha-*ras* proteins in these oocytes induced their meiotic maturation similar to the induction of the transformed phenotype in *ras*-transformed cells. Purified,

36

catalytically active recombinant LOX protein injected into the oocytes was able to inhibit

ras-induced meiotic maturation in a dose-dependent manner. Interestingly, intracellular

LOX was also able to inhibit progesterone-induced maturation. The effect of lysyl

oxidase on both *ras*- and progesterone-induced maturation was blocked by βAPN, a

highly specific LOX inhibitor. The inhibition of protein synthesis by cyclohexamide also

inhibited the effect of LOX, indicating that LOX needs newly synthesized protein to

achieve its effect. The *ras* and progesterone pathways merge at Erk2, and indeed,

phosphorylation of Erk2 was not affected by LOX, indicating that LOX blocks the *ras*

pathway downstream of Erk2 (Di Donato et al, 1997b).

The anti-*ras* action of LOX was further characterized as preventing the activation

of NF-κB, a dimeric transcription factor activated by oncogenic *ras*. Ectopic expression

of lysyl oxidase by transfection of *ras*-transformed NIH 3T3 cells inhibited activation of

NF-κB, binding of NF-κB to DNA and expression of c-*myc*, a well-known target of NF-

κB. This effect of lysyl oxidase was demonstrated to be due to inhibited activation of the

kinases IKKα and IKKβ, causing IκBα, the NF-κB inhibitory protein, not be

phosphorylated, which prevents the translocation of NF-κB to the nucleus (Jeay et al,

2003). Activation of IKKα and IKKβ by the *ras* oncogene occurs through two distinct

pathways, phosphatidyl-inositol-3-kinase (PI3K) and Raf/MEK (Arsura et al, 2000), both

of which are inhibited by lysyl oxidase (Jeay et al, 2003). This blockage of the

downstream effects of *ras* by LOX explains the how the gain of pre-transformed levels of

LOX can lead to the loss of the *ras*-transformed phenotype in revertant cells that continue

to have high levels of ras. This effect would also explain the necessity of the down-regulation of LOX during *ras*-transformation.

Other cellular processes mediated by lysyl oxidase may also play a role in its tumor suppressor function. Extracellular LOX catalyzes the formation of covalent cross-links that stabilize and insolubilize several fibrillar collagen types and elastin (Kagan and Li, 2003; Kagan 1986). Loss of the lysyl oxidase protein could result in modulation of the extracellular matrix such tumor growth could occur. This is consistent with the observation of increased LOX expression in the stromal reaction at the invasion front of infiltrating oral squamous cell carcinoma and breast tumors (Trivedy et al, 1999; Peyrol et al, 1997).

Lysyl oxidase may also affect cell adhesion. Near complete down-regulation of LOX in H-*ras* transformed rat fibroblasts was associated with establishment of anchorage independence (Hajnal et al, 1993). An antisense construct of LOX transfected into immortalized rat kidney fibroblasts resulted in the growth of these cells in soft agar, a marker of anchorage independence, as well as the growth of classical fibrosarcomas that demonstrated high metastatic potential (Giampuzzi et al, 2001). Conversely, ectopic lysyl oxidase expression was able to reduce anchorage-independent growth of *ras*-transformed NIH 3T3 cells, an effect that was partially reversed by ectopic p65/p50 NF-κB subunit expression, indicating that inhibition of NF-κB by LOX is largely responsible for the decrease in anchorage-independence (Jeay et al, 2003). Decreased attachment of

endothelial cells lining the aorta of the LOX "knockout" mouse was also observed (Maki et al, 2002).

The decrease of lysyl oxidase associated with tumorigenesis may be due to several regulatory mechanisms. As indicated in Table 1.1, multiple factors involved in cancer, namely *ras*, IRF-1, TGF-β and bFGF, affect the transcription of LOX. There is a *ras*-regulatory element within the promoter of the lysyl oxidase gene that is responsible for the down-regulation of LOX in *ras*-transformed osteoblastic cells (Csiszar et al, 1996). The IRF-1 gene encodes a DNA binding transcriptional activator (Tanaka and Taniguchi, 1992), that has been described to have anti-oncogenic function due to the ability of IRF-1 cDNA to suppress the transformed phenotype induced by *ras, c-myc* or *fosB* transfection (Tanaka et al, 1994a; Tanaka et al, 1994b). The expression of LOX was dramatically reduced in IRF-1 null mouse embryonic fibroblasts, due to an IRF response element in the LOX gene promoter (Tan et al, 1996). In contrast, IRF-2, a transcriptional repressor that acts antagonistically to IRF-1 (Tanaka and Taniguchi, 1992), suppresses the expression of lysyl oxidase (Tan et al, 1996). Similar to Contente and co-workers (1990), transfection of *ras*-transformed IRF-1 null EF with a lysyl oxidase expression plasmid resulted in dramatic inhibition of colony formation (Tan et al, 1996).

The transforming growth factor (TGF)-β receptor complex is a tumor suppressor gene that is inactivated in multiple different human cancers. Binding of any of three closely related TGF-β isoforms, β1, β2 or β3, to the single heterodimeric TGF-β receptor

complex suppresses the growth of many different normal cell types through cell cycle

arrest in the late G1 phase, induction of apoptosis, and increased expression of a variety

of cell adhesion molecules, including fibronectin, collagen and integrins (Mendelson et

al, 2001). TGF-β1 also increases LOX expression in mouse osteoblasts, in rat vascular

smooth muscle cells (VSMC), granulosa cells and neonatal lung fibroblasts, and in

human flexor reticulum cells, renal cell lines and lung and gingival fibroblasts (Harlow et

al, 2003; Bose et al, 2000; Hong et al, 1999; Choung et al, 1998; Di Donato et al, 1997a;

Gacheru et al, 1997; Shanley et al, 1997; Roy et al, 1996; Feres-Filho et al, 1995; Boak et

al, 1994; Shibanuma et al, 1993). In rat VSMC, the effect of TGF-β1 on LOX expression

was shown to require protein synthesis and was mediated primarily through stabilization

of the half-life of LOX mRNA (Gacheru et al, 1997). Cancers are commonly TGF-β

resistant (Mendelson et al, 2001), and indeed, the response of LOX to TGF-β1 was lost in

prostate cancer, leading to a progressive decrease in LOX expression (Ren et al, 1998).

Basic fibroblast growth factor (bFGF), or FGF2, has been described to stimulate

the proliferation of multiple cell types, delay senescence, inhibit apoptosis, modulate

differentiated function and is involved in angiogenesis. Inappropriate expression of bFGF

is thought to result in tumor growth and development through stimulation of cell

proliferation and angiogenesis (Mendelsohn et al, 2001). bFGF decreases LOX

expression in mouse osteoblasts, rabbit retinal pigment epithelium cells and human

gingival fibroblasts in the concentration range of 1-10 nM (Hong and Trackman, 2002;

Omori et al, 2001; Feres-Filho et al, 1996). Changes in mRNA decay rates were

responsible for at least half of the LOX down-regulation, with the remainder likely transcriptional (Feres-Filho et al, 1996).

The lysyl oxidase gene has been mapped to chromosome 5q23.3-31.2 (Mariani et al, 1992; Hamalainen et al, 1991), and the evidence indicating that lysyl oxidase has tumor suppressive properties is abundant. Chromosome 5q21-31 and 5q23-31.1 are affected by loss of heterozygosity in colon and esophageal cancer, respectively, indicating the existence of a tumor suppressor gene in this area, although no candidates have been identified (Peralta et al, 1998; Mertens et al, 1997). Therefore, to investigate the possibility that the loss or reduced function of lysyl oxidase in the course of tumor development not only arises through regulatory mechanisms, but as a direct result of deletions and mutations affecting the LOX gene, the mutational status and expression level of the LOX gene was tested in a cohort of colorectal and esophageal tumors.

B. MATERIALS AND METHODS

1. Patient population

a. *Colon tumor panel*

The colon tumor panel consisted of sixty-six consenting patients who were undergoing surgery for colon cancer and who had no obvious family history of colon cancer. After standard histological assessment, tumor samples were removed from a representative area of the tumors, and along with matched blood samples, were stored at -80°C, until DNA and RNA isolation could be performed. The composition of the patient

panel was 54% female and 46% male, with an age range of 35-89 years of age and an

average age of 70.6 years of age with a standard deviation of 11.5 years. All tumors were

adenocarcinoma. Of these, 30% were removed from the proximal colon with the

remainder from the distal colon. The majority of the tumors were Stage B (73%),

followed by Stage C (14%), Stage A (9%) and Stage D (4%).

b. *Esophageal tumor panel*

The esophageal cancer panel consisted of sixty-two consenting patients. The

composition of the panel was 22.6% female and 77.4% male, in this male-predominant

disease. The age range was 38-85 years, with an average age of 60.4 years, standard

deviation of 11.3 years. All individuals were diagnosed with squamous cell carcinoma,

located at the middle third of the esophagus. The majority of the tumors were Stage 3

(83%), followed by stage 4 (9%), stage 2 (4%), stage 1 (2%) and stage 0 (2%). Biopsies

were taken of the tumor and of the normal part of the esophagus, frozen in liquid nitrogen

immediately after endoscopy and stored at -80°C. Lyophilized samples of DNA extracted

from these tissues were received from University of Cape Town, South Africa.

2. Culture of Human Smooth Muscle Cell Line

a. *Seeding from Frozen Cell Stocks*

All cell culture work was performed in the SterilGARD II biological safety

cabinet (The Baker Company, Sanford, ME). Immortalized human smooth muscle cell

line (myo) was cultured as a positive control of lysyl oxidase expression. The media

42

composition was Dulbecco's Modified Eagle Medium (DMEM) supplemented with 10%

fetal bovine serum (FBS) and 1% PSN (final concentration: 0.05 μg/mL penicillin G

(sodium salt); 0.05 μg/mL streptomycin sulfate; 0.10 μg/mL neomycin sulfate in 0.85%

saline) mixture (all from Invitrogen, Carlsbad, CA). One mL of frozen cell stock was

removed from liquid nitrogen storage, placed immediately in a 37°C water bath, and upon

thawing, was immediately added to 4 mL of prewarmed media in a vented T-25 culture

flask. This was incubated at 37°C under 5% CO_2 in a humidified chamber (3110

Incubator, ThermoForma, Marietta, OH) overnight, then the media was changed by

removal of cultured cell media and addition of 5 mL of prewarmed media to remove

residual DMSO (dimethyl sulfoxide) and any nonviable cells.

b. *Maintenance and Passage of Cells*

To maintain the cultured cells, media was changed every two days until 80-90%

confluent (considered "confluent"). Cells were monitored daily for growth and absence of

contamination. Confluent cultured cells were passaged into a larger T-75 flask to avoid

reduced mitotic index and cell death. The media was removed and the cells were rinsed

once with 2-3 mL of 1x PBS (phosphate buffered saline; 154 mM NaCl, 1.1 mM

KH_2PO_4, 3.0 mM $Na_2HPO_4\cdot7H_2O$; Invitrogen) to remove any Ca^{2+} and Mg^{2+} ions and

residual FBS that would cause cells to stick together and interfere with trypsin activity.

The PBS solution was free of Ca^{2+} and Mg^{2+} ions and the trypsin solution contained

EDTA (ethylenediamine tetraacetic acid) as a chelating agent to bind these ions.

One mL of trypsin-EDTA solution (0.25% trypsin/0.2% EDTA in Hanks'

Balanced Salt Solution; Sigma. St.Louis, MO) was added to the flask. The cells were

monitored under the microscope until they rounded up and detached from the surface.

The flask was tapped gently to completely suspend the cells, and prewarmed media was

immediately added to halt the digestion reaction of trypsin. The cell suspension was

pipetted up and down to dissociate cells and to dislodge any remaining adherent cells.

The resuspended cells were then centrifuged at 300 x g (1500 rpm in a CentraCL2;

ThermoIEC, Needham Heights, MA) for 5 minutes, and the trypsin-containing

supernatant was poured off. The pelleted cells were resuspended in 10 mL of media and

passaged into a T-75 flask. The cells were incubated as above, with media changes every

2 days until confluent. The confluent cells were then harvested for RNA.

3. Isolation of Nucleic Acids

a. *Extraction of Genomic DNA from Blood*

Genomic DNA from peripheral blood was isolated using the method of Madisen

et al (1987). Whole blood was mixed with 5 volumes of filter sterilized Tris:NH$_4$Cl (1:9)

(0.017 M Tris-HCl, pH 7.65, 0.1395 M NH$_4$Cl) prewarmed to 37°C, incubated at 37°C

for 5 minutes to lyse the erythrocytes, then centrifuged at 800 x g (2000 rpm in Sorvall

Super T21 with ST-H750 rotor; Kendro, Newton, CT) for 10 minutes. The pelleted

leukocytes were resuspended in a volume of 0.15 M NaCl equal to the original volume of

whole blood, followed by centrifugation at 2000 rpm for 10 minutes. The resuspension

and centrifugation was repeated, and then the pellet was resuspended in one-fifth volume

44

(of NaCl) of high TE buffer (100 mM Tris-Cl, pH 8.0; 40 mM EDTA, pH 8.0). The leukocytes were lysed with forceful injection of an equal volume (as high TE) of lysis buffer (100 mM Tris-Cl, pH 8.0; 40 mM EDTA, pH 8.0; 1 M NaCl; 0.2% SDS). At this stage, the lysate could be stored for up to 5-6 years before proceeding with the extraction.

An equal volume of TE-saturated phenol was added to the lysate and mixed by rotary mixer for 10 minutes to remove proteins. After centrifugation at 2000 rpm for 5 minutes, the upper aqueous phase was reserved. The white interphase was removed to a separate tube, mixed with high TE buffer, and reextracted with an equal volume of TE-saturated phenol to achieve best recovery of DNA. After centrifugation, the upper aqueous phase was pooled with what was previously reserved, reextracted with an equal volume of TE-saturated phenol and centrifuged. The upper aqueous phase was removed, extracted with an equal volume of chloroform to remove residual phenol, and then centrifuged again. The upper aqueous phase was reserved for isolation of DNA.

DNA was recovered by a modified ethanol precipitation. Ethanol depletes the hydration shell from nucleic acids and exposes negatively charged phosphate groups. Positively charged ions, such as Na^+ or NH_4^+ bind to the charged groups and reduce the repulsive charges between the polynucleotide chains such that a precipitate can form. Substitution of isopropanol for ethanol allows for minimization of volume, although it is more difficult to remove as it is less volatile and Na^+ cannot be used as it precipitates with the DNA. One-tenth volume of 4M ammonium acetate was added and mixed well.

45

An equal volume of isopropanol was added and the tube was mixed by inversion until the DNA strands could be visualized. These were fished out with a pipette tip to a separate tube, washed with 70% ethanol, air-dried to remove residual isopropanol, resuspended in 1 x TE (10 mM Tris-HCl, pH 7.6; 1 mM EDTA) buffer and stored at -20°C.

b. *Extraction of Genomic DNA from Tumor Tissue*

Genomic DNA from tumor was isolated using the QIAamp Tissue Kit (Qiagen Inc, Valencia, CA). The composition of the buffers in the kit was not provided by Qiagen. Approximately 25 mg of tumor tissue was cut into small pieces and 180 µL of Buffer ATL was added. To this, 20 µL of proteinase K stock solution was added and incubated at 55°C until the tissue was completely lysed. Proteinase K efficiently digests native proteins, remains active in detergents that are routinely used to lyse mammalian cells and can rapidly inactivate DNases and RNases in cell lysates to facilitate the isolation of high molecular weight DNA. After digestion, 20 µg of RNAase A, which is an endoribonuclease that specifically attacks single stranded RNA 3' to pyrimidine residues and cleaves the phosphate linkage to the adjacent nucleotide, was added to remove RNA. After incubation for 2 minutes at RT, 200 µL of Buffer AL was added and the mixture was incubated at 70°C for 10 minutes. After 210 µL of 100% ethanol was added, the entire mixture was placed in QIAamp spin column.

The spin columns utilize the method of silica chromatography for DNA isolation. DNA binds in a reversible manner to silica in the presence of high concentrations of salt,

thought to be due to the dehydration of the phosphodiester backbone by the chaotrophic

salts, which allows the exposed phosphate residues to adsorb to the silica. Once adsorbed,

the DNA cannot be eluted from the matrix by solvents (e.g. 50% ethanol) that displace

other biomolecules. However, when DNA is rehydrated by the addition of aqueous

buffers, it can be eluted from the silica. DNA was absorbed by the silica membrane in

the spin column by centrifugation at 6000 x g (8000 rpm in Eppendorf 5415C,

Brinkmann, Westbury, NY) for 1 minute. The spin column was rinsed twice with 500 μL

of Buffer AW with centrifugation at 8000 rpm for 1 minute for the first rinse, then at

18,000 x g (14,000) rpm for 3 minutes. The DNA was then eluted from the spin column

with preheated Buffer AE, and stored in -20°C.

c. *Extraction of Total RNA from Tumor Tissue and Cultured Cells*

All solutions to be used in RNA experimentation were DEPC (diethyl

pyrocarbonate)-treated. DEPC (Sigma, St. Louis, MO) is a highly reactive alkylating

reagent that destroys the enzymatic activity of RNases. DEPC was mixed with 0.5 x

volume of 100% ethanol to make it more soluble in water, then the solution of 0.1%

DEPC in ddH$_2$O was constantly stirred until homogenized, then autoclaved for 25

minutes to inactivate the DEPC.

Total RNA was isolated using RNA STAT-60 from Tel-Test, Inc (Friendswood,

Texas). Approximately 50-100 mg of tumor tissue was homogenized with 1 mL of RNA

STAT-60 solution, a monophasic reagent containing phenol, a phenol solubilizer and

47

guanidium thiocyanate, which is able to disrupt cells, solubilize their components and denature endogenous RNases simultaneously. For cultured cells, 7.5 mL of RNA STAT-60 (1 mL per 10 cm^2) was added directly to the cell culture flask after removal of media (the cells were not rinsed with 1x PBS to avoid degradation of RNA). The homogenate was incubated for 5 minutes at RT to allow for complete dissociation of nucleoprotein complexes. At this stage, the samples could be stored for at least 2 weeks at -80°C.

Upon addition of one-fifth volume of chloroform to the samples followed by vigorous shaking and incubation for 2-3 minutes at RT, the homogenate separated into two phases, the aqueous phase and organic phase. Centrifugation at 3800 x g (4300 rpm in Sorvall Super T21 with ST-H750 rotor) for 15 minutes at 4°C allowed for complete separation of the two phases. The upper aqueous phase, which retains the RNA, was transferred to another tube. The interphase and lower organic phase, which retains the DNA and proteins, was discarded. Total RNA was precipitated by addition of one-half volume of isopropanol, incubated for 5-10 minutes at RT, and centrifuged at 4300 rpm for 10 minutes at 4°C. The pellet was washed once with 75% ethanol (equal volume as RNA STAT-60) in DEPC-treated ddH$_2$0, recentrifuged for 5 minutes, allowed to air-dry for 10-15 minutes, resuspended in DEPC-treated ddH$_2$0, and stored at -70 °C.

d. *Isolation of Recombinant Plasmid DNA*

The human LOX cDNA clone (HLO-2) used was previously described (Mariani et al, 1992). The 1.2 kb cDNA fragment (411-1551 bp) had been cloned into an

ampicillin-resistant plasmid, transformed into *Escherichia coli* and stored as glycerol

stocks in -80°C. Using a flame-sterilized wire loop, the frozen glycerol stock was

streaked onto Bacto Agar plates (1.5 g per 100 mL) of Luria-Bertani (LB) media (1 g

tryptone, 0.5 g yeast extract, 1g NaCl per 100 mL, pH 7.0) with ampicillin (100 μg/mL)

and incubated overnight at 37°C. Individual colonies were inoculated into 3 mL of liquid

LB-ampicillin media in a loosely capped 15 mL culture tube (to ensure adequate

aeration) and placed in a 37°C incubator-shaker overnight to stationary phase.

The WIZARD mini-prep kit (Promega, Madison, WI) was used to isolate plasmid

DNA by alkaline lysis with SDS. The overnight culture was transferred to a microfuge

tube and centrifuged at maximum speed for 45 seconds to pellet the bacteria. The

supernatant was removed and the cells were completely suspended in 200 μL of cell

resuspension solution (50 mM Tris-HCl, pH 7.5, 10 mM EDTA, 100 μg/mL RNase A).

An equal volume of cell lysis solution (0.2 M NaOH, 1.0% SDS) was added and inverted

gently. The alkaline-detergent solution opens the bacterial cell wall, denatures

chromosomal DNA and proteins and releases plasmid DNA. The DNA strands of the

circular plasmid are topologically entwined and unable to separate. After incubation for 2

minutes at RT, 200 μL of neutralization solution (1.32 M KAc, pH 4.8) was added and

mixed by inversion. The return to neutral pH allows the plasmid DNA strands to

reanneal, and the addition of K+ ions causes the SDS-coated complexes of bacterial

proteins, ruptured cell walls and denatured chromosomal DNA to precipitate. After

centrifugation at maximum speed for 20 minutes, the supernatant containing the native

plasmid DNA was removed and centrifuged again for 10 minutes. Plasmid DNA was precipitated from 500 µL of the supernatant by the addition of 2 x volume of ice-cold 100% ethanol and incubation at RT for 10 minutes. After centrifugation for 10 minutes at maximum speed to pellet the plasmid DNA, the pellet was washed twice with 70% ethanol, air-dried to remove residual ethanol and resuspended in 30 µL of TE.

e. *Quantitation of Nucleic Acids*

The absorbance at several different wavelengths by spectrophotometry was measured to evaluate the purity and concentration of DNA samples. The absorbance at a wavelength of 260 nm (A_{260}) is quantitative for relatively pure microgram quantities of nucleic acids. Prior to measuring samples, the Beckman DU530 spectrophotometer (Beckman-Coulter, Fullerton, CA) was blanked using the solvent in which the DNA or RNA sample was dissolved. An aliquot of 50-100 µL of DNA or RNA solution was placed in a microcuvette and the optical density (OD) at 260 and 280 nm was measured. One OD unit at 260 nm is equivalent to 50 µg/ml of DNA and 40 µg/ml of RNA. The purity was calculated with the A_{260}/A_{280} ratio, as proteins have a peak absorption at 280 nm. Ratios of 1.8-2.0 indicated purified preparations. Other useful measurements include A_{230}, which is affected by organic contaminants such as phenol and urea, and A_{325}, which indicate contamination by particulate matter.

Spectrophotometry is only able to accurately measure microgram amounts of DNA. For smaller amounts, DNA of unknown concentration was electrophoresed, on an

agarose gel containing 0.5 µg/mL ethiduim bromide, with digests of known

concentration, such as φX174 digested with HaeIII, which are similar in size to the DNA

fragment to be quantitated. Digestion of HaeIII digested φX174 yields four clear bands: a

1353 bp fragment consisting of 25.1%, a 1078 bp fragment consisting of 20.0%, a 872 bp

fragment consisting of 16.1% and a 603 bp fragment consisting of 11.2% of the total

mass. The DNA of unknown concentration is run alongside serial dilutions of the digest

by agarose gel electrophoresis (II.B.5.b.) and the intensities of the bands are compared

after ethidium bromide staining.

Ethidium bromide intercalates between the stacked base pairs of DNA

independent of base composition. The fixed position of the ethidium bromide and its

close proximity to the bases cause the bound dye to have a 20-25 fold increase in

fluorescence compared to the dye in solution. UV radiation is absorbed by the dye and re-

emitted in the red-orange region of the visible spectrum. This fluorescence emitted by

ethidium bromide is proportional to the total mass of DNA and by finding a digest band

of similar intensity, DNA concentration as little as 1-5 ng can be estimated.

f. Concentration of Nucleic Acids

In certain cases, such as Southern blot analysis and first strand synthesis, it was

necessary to have nucleic acids at a specific concentration because volume was a limiting

factor. To concentrate nucleic acids, ethanol precipitation was used as described in

II.B.3.a. One-tenth volume of 3 M sodium acetate was added to the DNA solution then

3x volume of 100% ethanol was added. The DNA was allowed to precipitate at -20°C for

at least 30 minutes, and then was pelleted by centrifugation at maximum speed for 30

minutes. The supernatant was carefully removed and the pellet was rinsed once with

70% ethanol, and then recentrifuged for 10 minutes. The DNA was allowed to air dry for

10 minutes to allow most of residual ethanol to evaporate, before resuspension in the

desired amount of TE.

4. Characterizing Microsatellites for Loss of Heterozygosity Analysis

a. *Microsatellites at the Lysyl Oxidase Gene Locus*

Prior to this dissertation work, two overlapping PAC clones containing the lysyl

oxidase gene were used for Southern blot analysis to identify six CA-dinucleotide

repeats, three of which were further characterized. These three microsatellites were used

for genotyping and loss of heterozygosity analysis. Two microsatellites centromeric to

the LOX locus, D5S421 and D5S471, and two microsatellites telomeric to the LOX

locus, D5S490 and D5S642, were also amplified. In addition, D5S346, a microsatellite

between the APC and MCC genes at 5q21 was amplified. Oligonucleotide primers were

synthesized by Genosys Biotechnologies Inc.(The Woodlands, TX) and Invitrogen. The

sequences of these primers are shown in Table 2.1.

b. *End-labeling of Primers*

End-labeled oligonucleotide primers were used for detection of PCR amplified

microsatellites. One set of each primer pair was labeled with T4 polynucleotide kinase

Table 2.1. Sequences of Primers used for PCR and RT-PCR analysis

5' Primer	Sequence	3' Primer	Sequence
	PCR of microsatellites		**PCR of microsatellites**
D5S346a	5'-ACT CAC TCT AGT GAT AAA TCG GG-3'	D5S346m	5'-AGC AGA TAA GAC AGT ATT ACT AGTT-3'
D5S421a	5'-TGG AAA TAG AAT CCA GGC TT-3'	D5S421m	5'-TCT ATC GTT AAC TTT ATT GAT TCA G-3'
D5S471a	5'-TTT TCA CAC ATT TTC CCA GC-3'	D5S471m	5'-AAA ACT TCA TTT ACA AAA ACA GGAG-3'
Ims1a	5'-GCT CAT TAA TGA GAG AAA C-3'	Ims1m	5'-ACA CCA GCA ATC TCA ACA-3'
D5S467a	5'-CTA ACC AGA GGC TGC AAG-3'	D5S467m	5'-TGA TCT TAG TGT GCC TTA GT-3'
Ims15a	5'-TTG CAG GAC TTC TCA GCC-3'	Ims15m	5'-CAG CCT CCA ATC TGA TTG-3'
D5S490a	5'-GAA TCT GAA GGT GTT CTA AAA GTA-3'	D5S490m	5'-AAA GTG AGG AGT CAA GGA GG-3'
D5S642a	5'-AGC TCT TTA CTT CTG GAC TTA CAAA-3'	D5S642m	5'-CTA GAC CAT AGA TAA CCC TGT GAT-3'
	RT-PCR		**RT-PCR**
LOXf	5'-CCT GGC TGT TAT GAT AC-3'	LOXr	5'-GAG GCA TAC GCA TGA TG-3'
catf	5'-CAT AAC CTT TCC CAT CAT C-3'	catr	5'-AAT CAA TCC AAC AGT AGC C-3'
LOX1-4f	5'-CTG CTG ATC CGC GAC AA-3'	LOX1-4r	5'-CCT CTG GGT GTT GGC ATC-3'
	LOX gene PCR		**LOX gene PCR**
RFLPf	5'-TCA TCT GGA GTC ACC GCT GG-3'	RFLPr	5'-GGT TGT CGT CAG AGT AC-3'
Exon 1a	5'-TCA TCT GGA GTC ACC GCT GG-3'	Exon 1m	5'-AGC TGG GGA CCA GGT GCA C-3'
Exon 2a	5'-CCG GGT TGT TTC ACT CGT-3'	Exon 2m	5'-CCC CTG AAG GTA GAC CG-3'
Exon 3a	5'-ACT CTT GGA ACT GAT AG-3'	Exon 3m	5'-CTG AGA AAT GAA AAG CAA-3'
Exon 4a	5'-GCT TTC TCT GTA TGT AAC-3'	Exon 4m	5'-ACC CGA TTC TCT CTG AGG-3'
Exon 5a	5'-GAC AGC TCA CTC TGA AA-3'	Exon 5m	5'-TAA ATC AAG CAG GGA AGG G-3'

(PNK) enzyme (Amersham Pharmacia Biotech, Arlington Heights, IL) and γ-^{32}P-ATP

(ICN Pharmaceuticals Inc., Costa Mesa, CA). The PNK enzyme is a 5' phospho-

transferase that phosphorylates the 5'-hydroxyl termini of the synthetic double-stranded

oligonucleotide primer by the transfer of the γ-phosphate of γ-^{32}P-ATP. The labeling

reaction was performed in a final volume of 25 μL with 8 μM primer, 1 x T4 PNK buffer

(50 mM Tris-HCl, pH 7.6, 10 mM MgCl$_2$, 10 mM 2-mercaptoethanol), 100 μCi of γ-^{32}P-

ATP (3000 Ci/mmol) and 50 units of T4 PNK enzyme. The labeling reaction was

incubated at 37°C for 45 minutes, followed by enzyme inactivation at 65°C for 10

minutes. This provided enough end-labeled primer for 50 PCR samples of 25 μL each.

c. Polymerase Chain Reaction

Polymerase chain reaction (PCR) has seven essential components: template DNA,

a thermostable DNA polymerase, divalent cations, deoxynucleoside triphosphates

(dNTP), buffer to maintain pH, monovalent cations and a pair of synthetic oligo-

nucleotide primers. Divalent cations, usually Mg^{2+}, are necessary for DNA polymerase

activity. The phosphate groups of the dNTP and primers bind Mg^{2+} so the molar

concentration of Mg^{2+} must exceed the molar concentration of the phosphate groups.

Standard PCR buffers contain 50 mM KCl, 10 mM Tris-Cl, adjusted to a pH between 8.3

and 8.8 at RT that falls to pH 7.2 during incubation at 72°C. In addition, chemicals such

as DMSO and detergents can be added to reduce mispriming and increase efficiency of

amplification in G+C rich templates. The design of the primers is the most crucial

component. Primers should be 18-30 nucleotides long, free of secondary structures, have

a G+C content between 40-60% with no homopolymeric tracts, and should not be self-complementary nor have significant sequence homology to any sequence other than the target sequence. The primer pair should have similar melting temperatures (difference less than 5°C) and the sequences should not be complementary. PCR is composed of the cycling of three steps, denaturation of the template by heat, annealing of the oligonucleotide primer to the denatured single-stranded target sequence, and extension of the annealed primers by a thermostable DNA polymerase.

PCR reactions were performed in a final reaction volume of 25 µL with the following conditions: 50 mM KCl, 10 mM Tris-HCl pH 8.3, 1.5 mM $MgCl_2$, 20 ng genomic DNA (approximately $6x10^3$ copies of a single-copy autosomal gene), 0.16 µM of radiolabeled primer 1 and 0.6 µM of unlabeled primer 1, 1 µM of unlabeled primer 2, and 0.5 units AmpliTaq polymerase (PE Applied Biosystems, Foster City, CA). The final nucleotide concentration for primers D5S346, D5S421, D5S471, lms1 and lms15 was 31 µM; for primers D5S467 and D5S642, 124 µM; and for primers D5S490, 200 µM. In reactions with primers D5S421, D5S471, D5S490 and D5S642, 1% Triton X-100 was used, and with primers D5S421, D5S467, lms15, D5S490 and D5S642, 10% DMSO was used. The reactions were incubated in either the GeneAmp PCR system 9600 or 9700 from PE Applied Biosystems. All reactions were subjected to an initial denaturation step of 94°C for 3 minutes and a final extension of 72°C for 7 minutes. The thermocycle profile for the markers D5S346, lms1, D5S467 and lms15 was 94°C for 30 seconds, 58°C for 30 seconds and 72°C for 30 seconds, and for the remaining markers, the annealing

temperature was 55 °C. All reactions were amplified for 30 cycles, except for those PCR reactions containing DMSO, which required an additional 5 cycles. The completed reactions were stored at 4°C until ready for analysis.

d. Denaturing Polyacrylamide Gel Electrophoresis

Denaturing polyacrylamide gel electrophoresis, a method for the separation of single-stranded fragments of DNA, was used for genotyping and loss of heterozygosity analysis. A pair of 33.5 x 42 cm glass plates were meticulously cleaned, the front larger plate with the abrasive cerium oxide and the smaller back plate with a nonabrasive dishwashing detergent. These were thoroughly rinsed and dried with Kimwipes. The plates were then wiped with 70% ethanol and again dried with Kimwipes. The smaller back plate was then treated with Rain•X (Blue Coral-Slick 50, Cleveland, OH), a silanizing fluid, to facilitate pouring the gel and to ensure the gel would remain on the larger gel when the glass plates were separated. The gel plates were placed together with the clean sides facing inwards, with spacers measuring 0.4 mm thick, and the glass sandwich was placed in a silicone gasket to prevent leaks.

Polyacrylamide gels are composed of chains of acrylamide monomers cross-linked by N,N'-methylene-bis-acrylamide. The gel mixture was made of 6% polyacrylamide (19% acrylamide:1% bis-acrylamide), 1 x TBE buffer (45 mM Tris borate; 1 mM EDTA) and 7 M urea as the DNA denaturing agent, in a final volume of 60 mL. TBE buffer has a relatively high buffering capacity and is preferred when

56

electrophoresis is carried out for prolonged periods. To polymerize the reaction, 330 μL of 10% APS (ammonium persulfate) and 30 μl of TEMED (N,N,N',N'-tetramethyl-ethylenediamine) was added, and the gel mixture was poured immediately between the two glass plates. Monomers of acrylamide are polymerized into long chains in a reaction driven by free radicals that are generated by an oxido-reduction reaction in which APS is the catalyst and TEMED is the adjunct catalyst. In the presence of bis-acrylamide, the long chains of acrylamide become cross-linked to form a gel whose porosity is determined by the length of chains (percentage of polyacrylamide in gel) and degree of cross-linking (ratio of acrylamide to bis-acrylamide). The gel sandwich was placed such that there was 2.5 cm elevation of the top edge. The flat side of a 0.4 mm sharkstooth comb was placed into the gel solution to a depth of 6 mm, and the top of the gel was clamped so that no solidified gel would form between the combs. The gel was allowed to polymerize for at least 2 hours and was used within 24 hours of pouring.

After polymerization, the combs were carefully removed and the wells were rinsed with ddH₂O to remove any unpolymerized acrylamide. The combs were then reinserted with the teeth just into the flat surface of the gel such that the flat surface formed the bottom of the wells. The plates were then attached to the electrophoresis equipment (BRL S2 Sequencing Gel Equipment, Gibco BRL, Grand Island, NY) and the top and bottom chambers were filled with 1 x TBE buffer. The wells were rinsed with buffer and the gel was allowed to prerun at 1800 V for approximately one hour or until the temperature of the gel reached 50°C. The samples were then mixed with an equal

57

volume of denaturing loading dye (0.1% bromophenol blue, 0.1% xylene cyanol and 100 μM EDTA in formamide), denatured at 94°C for 5 minutes, placed immediately on ice to prevent reannealing and loaded onto the gel. The urea in the gel maintains the DNA in a denatured state that migrates through the gel completely independent of base composition and sequence. The samples were electrophoresed at 1800 V for 100 minutes to 5 hours, depending on the length of the DNA fragment.

e. *Autoradiography and Quantitation*

Following electrophoresis, the buffer was drained and the plates were removed from the electrophoresis equipment. The comb and spacers were removed, and using a thin spatula, the two glass plates were pried apart and the gel was allowed to adhere to one of the plates. Whatman 3MM chromatography paper was placed on the gel starting from one edge and gradually smoothed to the other edge, avoiding any bubbles. The paper was then lifted off gently, and the gel surface was covered with plastic wrap. The gel was dried for 2 hours under vacuum using a BioRad Model 583 Slab Gel Dryer (Hercules, CA). Although ^{32}P emits a β-particle with sufficient energy to penetrate water to a depth of 6 mm, drying the gels increases the sharpness of the radiographic image.

The plastic wrap was removed and the dried gel was placed in a metal film cassette with a BioMax HE Transcreen (Eastman Kodak, Rochester, NY) specific for ^{32}P and Fuji RX-U film (Fuji Medical Systems, Stanford, CA) to expose overnight at -80°C. The BioMax Transcreen enhances the signal by converting the β-particles to photons that

are then recorded by photographic emulsion. Autoradiographic film is composed of an emulsion of silver halide crystals in gelatin. Exposure to radiation causes ejection of electrons from the crystals and the capture of the ejected electrons by silver ions produces silver atoms. To prevent fading of the resultant latent image due to rapid loss of captured electrons by the silver atoms, the autoradiographic film is exposed at -80°C. The subsequent development of film converts the latent image to a true image.

In a dark room, the film was removed from the cassette, and placed in film developer until the expected bands were visible. During development, the activated nuclei of the silver atoms catalyze the conversion of the entire silver halide crystal to metallic silver. The film was rinsed in water, placed in film fixative until transparent, rinsed in ddH$_2$0, and allowed to completely dry. The film was both visually evaluated and quantified using an image acquisition and analysis system (Ambis Inc., San Diego, CA).

f. *Evaluation of Microsatellites*

Those PCR products that were homozygous for a microsatellite were labeled as uninformative. Loss of an allele or allele deletion (loss of heterozygosity) was determined if one of the two alleles present in blood was absent or diminished by at least 50%. Complete absence was not required as both normal and tumor cells may coexist in a tumor sample. Allelic imbalance was determined if one of the two alleles from tumor tissue was greater in intensity than the matching blood allele or if the two alleles from tumor DNA differed in the ratio of intensity when compared to the alleles in the blood

59

DNA. Although allelic imbalance can result from either loss of an allele, amplification or heterogeneity, loss of heterozygosity and allelic imbalance were grouped as they both indicate a contribution of this gene to tumor progression. New alleles were determined if additional alleles were found in tumor DNA that were not present in blood DNA.

5. cDNA Array Analysis

a. *Excision of LOX cDNA Insert from Plasmid Host*

Plasmid DNA was isolated as described in II.B.3.d. The concentration of the plasmid DNA was determined as described in II.B.3.e. The plasmid was subjected to restriction digestion to isolate the human LOX cDNA fragment from the plasmid host. Although the entire plasmid can be used for labeling, utilizing just the sequence encoding the target of interest creates a more specific probe with less background. Four µg of plasmid DNA was added to 1x Buffer H (90 mM Tris-HCl, pH 7.5, 10 mM $MgCl_2$, 50 NaCl) and 5 units of *Eco*RI (Promega) for a final volume of 20 µL. One unit of restriction enzyme is defined as the amount needed to digest 1 µg of DNA in 1 hour at the appropriate assay temperature in a 50 µL reaction volume. After incubation at 37°C for 1-2 hours, the digested DNA fragments were separated on a 1% agarose gel in order to isolate the human LOX cDNA fragment from the plasmid host. .

b. *Agarose Gel Electrophoresis*

Agarose gel electrophoresis is effective for the separation and identification of DNA fragments measuring 0.25 to 25 kilobases. Agarose gels were prepared in 1 x TAE

(40 mM Tris-acetate; 1 mM EDTA) buffer with an agarose concentration appropriate to the length of DNA. For DNA fragments less than 0.5 kb, agarose concentrations of 1.5-2.0% were used; for DNA fragments from 0.5 kb to 10 kb, agarose concentrations of 0.8-1.2% were used. TAE buffer has relatively low buffering capacity and will become exhausted if electrophoresis is carried out for prolonged periods, but it has superior resolving power for high molecular weight DNA compared to TBE.

The agarose and buffer were microwaved at high power until the agarose was completely dissolved, swirling to ensure even mixing. When cooled to approximately 55°C, ethidium bromide, which intercalates between the stacked bases of DNA and fluoresces with UV illumination, was added for a final concentration of 0.5 μg/mL and the agarose was poured into a sealed gel platform with gel comb. The agarose was allowed to sit for 1 hour, the gel comb was removed carefully, and the gels were placed in an electrophoresis tank with enough 1 x TAE buffer to cover the gel to a depth of 1 mm. The DNA samples were mixed with one-fourth volume of 4 x loading dye (0.25% SDS, 30% glycerol, 0.2% each of bromophenol blue and xylene cyanol) and loaded into the wells of the gel. The samples were electrophoresed at 50 volts until the loading dye had entered the agarose, and then increased to 100 volts for an appropriate amount of time. The lower voltage at the beginning of the run prevented streaking of the bands of DNA, producing sharper bands that could be more easily excised. The gel was removed from the electrophoresis tank, placed on an UV light source, and then photographed with Polaroid 667 film.

c. *Isolation of cDNA Insert from Agarose Gel*

The cDNA insert was purified by silica chromatography, as described in II.B.3.b., using the GeneClean Kit (BIO 101-qbiogene, Carlsbad, CA). The composition of the buffers provided with the kit was not supplied by BIO 101. The 1.2 kb human LOX cDNA fragment was excised from the agarose gel using a scalpel and placed in a microfuge tube. The gel slice was weighed and 2.5-3 volumes of NaI solution was added for a final concentration above 4M NaI. The tube was placed in a 45-55°C waterbath and mixed by inversion every 1-2 minutes until the agarose completely melted. To this, 5 μL of completely resuspended Glassmilk (silica suspension) was added and placed on ice for 5 minutes. The solution was mixed by inversion every 1-2 minutes to ensure that the Glassmilk was in suspension. After centrifugation at maximum speed for 5 seconds to pellet the DNA-silica matrix, the supernatant was removed and the pellet was completely resuspended in 500 μL of New Wash (51% ethanol with NaCl, Tris and EDTA). This step was repeated for a total of three washes with New Wash. After isolation of the pellet by centrifugation and removal of supernatant, the pellet was resuspended in 5 μL of TE buffer and incubated at 45-55 °C for 2-3 minutes. After centrifugation, the supernatant containing the DNA was removed to another tube for quantitation.

To quantitate the isolated cDNA fragment, it was electrophoresed on an agarose gel with φX174 digested with *Hae*III, which is similar in size to the 1.2 kb human LOX cDNA fragment, and evaluated as discussed in II.B.3.e.

d. *Random-Labeling of cDNA Fragment*

Random-labeled cDNA probes were synthesized using the Megaprime kit from Amersham (Piscataway, NJ). Template cDNA (25 ng) was added to 5 μL of random primer solution (kit) and 16 μL of DEPC-treated ddH$_2$O. The mixture was denatured for 5 minutes at 95-100°C and allowed to cool to RT to allow for annealing of primer to template cDNA. Random primers form hybrids at many positions, thus the complement of every nucleotide of the template, except those at the very 5' terminus, will be incorporated at equal frequency. The probe length is inversely proportional to the primer concentration, so longer cDNA fragments need more primer to yield a probe of optimal length 200-800 nucleotides. Four μL each of dATP, dGTP and dTTP (kit), 5 μL of 10x reaction buffer (kit), 5 μL of ^{32}P α-dCTP (3000 Ci/mmol, ICN) and 2 μL of Klenow enzyme were added. The Klenow fragment of DNA polymerase I lacks the 5' to 3' exonuclease activity so the probe is synthesized exclusively by primer extension and is not degraded by exonuclease activity. The reaction mixture was incubated for 1 hour at 37°C then terminated by the addition of 2 μL of 0.5 M EDTA.

Unincorporated ^{32}P α-dCTP was removed by spin column gel-filtration chromatography using a G-50 spin column (Amersham). The columns contain G-50 DNA Grade F Sephadex, a highly specialized gel filtration and chromatographic matrix composed of macroscopic beads synthetically derived from the polysaccharide, dextran, which is cross-linked to give a three-dimensional network. Spin column chromatography is used to separate DNA, which passes through the matrix, from lower-molecular weight

molecules retained in the pores of the gel. Sephadex G-50 retains DNA less than 80 nucleotides in length, thus is able to remove unincorporated radiolabeled ^{32}P α-dCTP.

The Sephadex matrix in the column was resuspended by gentle vortex, then the cap was loosened one-fourth turn and the bottom closure was snapped off. The column was placed in a microfuge tube for support and was centrifuged at 1000 x g (3000 rpm in a Eppendorf 5415C microcentrifuge) for 1 minute. The column was then placed in a new microfuge tube and the sample was applied to the center of the angled surface of the resin bed without touching the surface of the resin or the sides of the tube. The unincorporated nucleotides enter the Sephadex beads and upon centrifugation at 3000 rpm for 2 minutes, the labeled probe flows through the column and can be collected. One μL of this purified probe was placed in a scintillation vial with 5 mL of Bio-Safe II scintillation cocktail (RPI, Mount Prospect, IL) and quantified in a Beckman LS6500 scintillation counter to ensure an activity of at least 5 x 10^6 cpm per ml of hybridization solution.

e. *Hybridization of cDNA Probe to Array*

A Matched Normal/Tumor Expression Array from Clontech (Palo Alto, CA) was utilized according to the user manual. The array was placed in the hybridization chamber, wet briefly with ddH$_2$0 then allowed to prehybridize at least 30 minutes at 65°C in prehybridization solution (ExpressHyb (Clontech) with 100 μg/mL sheared salmon testis DNA (ssDNA)). In a total volume of 200 μL, 180 μg of ssDNA and 50 μL of 20 x SSC (3 M NaCl, 0.3 M Na$_3$citrate•2H$_2$O) was added to the purified probe. The mixture was

heated to 95°C to denature the probe, quickly iced to prevent reannealing, and then added

to fresh ExpressHyb with 100 μg/ml ssDNA to make the hybridization solution. The

prehybridization solution was removed, replaced with the hybridization solution, and

allowed to hybridize overnight at 65°C to the array.

After the hybridization solution was removed, the array was washed 4 times with

Wash Solution 1 (2 x SSC, 1% SDS) for 30 minutes each at 65°C, once with Wash

Solution 2 (0.1 x SSC, 0.5% SDS) for 30 minutes at 65°C, and a final wash with 2 x SSC

for 5 minutes at RT. The array was not allowed to become dry and decrease of the

background signal in successive washes was crudely monitored by Geiger counter. After

excess liquid was removed from the array, it was heat-sealed in a plastic seal-a-meal bag.

f. PhosphorImage Analysis

The sealed membrane was placed on a PhosphorImage tray and taped down flat.

Mylar was placed over the sealed membrane to protect the phosphor plate that was placed

over the mylar, locked into place, and exposed at RT for 7 days. The energy emitted by

the hybridized probe is stored in a europium-based coating on the phosphor plates by the

oxidation of Eu^{2+} to Eu^{3+}. The plates are scanned by a laser to release photons emitted

during the reversion of Eu^{3+} to Eu^{2+} and are collected to form an image. Although the

images have lower resolution, the densitometric analysis is more accurate as the linear

dynamic range is 5 orders of magnitude compared to 1.5 orders of magnitude for X-ray

film, and the exposure times are 10-250 times faster than X-ray film. Signal intensities

were quantified using the PhosphorImager:SI and the ImageQuant 5.0 Software program (Molecular Dynamics, Sunnyvale, CA). All measurements of signals and background were measured in triplicate and averaged. Graphs were produced using Microsoft Excel.

6. RT-PCR Analysis

Reverse transcriptase-PCR analysis consists of two steps: the enzymatic conversion of RNA to a single-stranded cDNA template followed by standard polymerase chain reaction. The production of cDNA from RNA requires a primer: either an oligo(dT), random hexamer or a gene-specific primer. If amplification of multiple genes are needed, oligo(dT), which binds to the endogenous poly(A)$^{+}$ tails of mammalian mRNA, or random hexamers, which bind to many points along the template, can be used.

a. *First Strand Synthesis*

First strand cDNA was synthesized using SuperScript Preamplification System (Invitrogen) and total RNA extracted from tumor tissue samples and cultured smooth muscle cells. Superscript is a modified reverse transcriptase. It lacks RNase H activity that can cleave the template near the 3'terminus of the growing DNA strand if the polymerase pauses during synthesis. Thus, Superscript is able to transcribe a greater proportion of template molecules and to synthesize longer cDNA molecules.

To denature any secondary structures that may have formed in the RNA, 5 μg of total RNA was mixed with 250 ng of random hexamer primers and DEPC-treated ddH$_2$0

to a volume of 12 μL, incubated for 10 minutes at 70°C, then immediately placed on ice. One sample was duplicated and served as a control. To the samples was added, in order and in noted in final concentration, reverse transcriptase buffer (20 mM Tris-HCl, pH 8.4, 50 mM KCl), 2.5 mM MgCl$_2$, 0.5 mM dNTP and 10 mM DTT (dithiothreitol). After incubation at RT for 5 minutes to anneal the primers, 200 units of Superscript II was added to all samples except for the control, followed by a 10 minute incubation at RT and a 50 minute incubation at 42°C to synthesize the cDNA. To terminate the reaction by inactivation of the enzyme, the samples were incubated for 15 minutes at 70°C, and then placed on ice.

The reverse transcriptase must be inactivated to avoid decreased efficiency of the subsequent amplification. To remove RNA, 2 units of RNase H was added to each sample and incubated for 20 minutes at 37°C. RNase H catalyzes the endonucleolytic degradation of the RNA moiety of DNA-RNA hybrids, leaving the single-stranded cDNA. The tubes containing the first strand cDNA synthesis reactions were stored at -20°C until ready for analysis.

b. *Polymerase Chain Reaction*

Three transcripts were amplified: a 152-bp fragment of LOX cDNA using primers LOXRTf and LOXRTr; a 452-bp fragment of G3PDH cDNA using G3PDH primer pairs from Clontech; and a 849-bp fragment of β-catenin using primers catf and catr (sequences in Table 2.1). These RT-PCR reactions were performed as described in

II.B.4.c, except with 1 µL of the first strand cDNA synthesis reaction as template, and 124 µM of dNTP for LOX, 200 µM for G3PDH and 1 mM for β-catenin. One µM of primers were used except for β-catenin that used 0.8 µM of primers and 2.5 units of AmpliTaq. The thermocycle profiles were an initial denaturation of 94°C for 3 minutes, followed by 25 cycles of 94°C for 30 seconds, annealing for 30 seconds at 50°C for LOX and β-catenin, and 57°C for G3PDH, 72°C for 30 seconds and a final extension of 72°C for 7 minutes. The amplified β-catenin product was evaluated by 2% agarose gel electrophoresis as described in II.B.5.b. LOX and G3PDH amplified products were evaluated by non-denaturing polyacrylamide gel electrophoresis.

c. Non-denaturing Polyacrylamide Gel Electrophoresis

Small double-stranded DNA fragments less than 1000 bp can be effectively separated with nondenaturing polyacrylamide gel electrophoresis. Two glass plates, sized 10.1 cm x 7.3 cm and 10.1 cm x 8.2 cm was cleaned with dishwashing soap, rinsed with ddH₂O and wiped with 70% ethanol. The gel plates were placed together with the clean sides facing inwards, with 1.5 mm thick spacers, mounted firmly into the gel casters, and placed on paper towels parallel to the bench. The gel mixture was made of 6% polyacrylamide (19% acrylamide:1% bis-acrylamide) and 1 x TBE buffer in a final volume of 12 ml. To catalyze the polymerization reaction, 120 µl of 10% APS and 12 µl of TEMED were added, respectively. Before polymerization could occur, the gel mixture was pipetted between the two plates and the gel comb was inserted. The gel was allowed

to polymerize for at least 30 minutes. Unlike in agarose gels, ethidium bromide cannot be added prior to casting because it inhibits the polymerization of the acrylamide.

After polymerization, the combs were carefully removed and the wells were rinsed with ddH$_2$O to remove any unpolymerized acrylamide. The plates were then attached to Biorad Mini-Protean II electrophoresis equipment and the top and bottom chambers were filled with 1 x TBE buffer. The DNA samples were mixed with one-fourth volume of 4 x loading dye and loaded into the wells of the gel. The samples were electrophoresed at 100 V for an appropriate length of time, stained with 0.5 µg/mL ethidium bromide solution and photographed under UV light using Polaroid 667 film.

7. Restriction Fragment Length Polymorphism Analysis

a. *Amplification of Exon 1 of the LOX Gene*

A previously published restriction fragment length polymorphism (RFLP) within exon 1 of the lysyl oxidase gene (Csiszar et al, 1993) was used to evaluate for loss of exon 1 in those individuals who showed LOH of the LOX region. Exon 1 of the matched blood and tumor pairs were PCR amplified with primers RFLPf and RFLPr (sequences in Table 2.1) that flank the polymorphism. PCR reactions were performed as described in II.B.4.c except with 5% DMSO and 31 µM dNTP. The thermocycle profile was an initial denaturation of 94°C for 3 minutes, followed by 35 cycles of 94°C for 30 seconds, 58°C for 30 seconds and 72°C for 30 seconds, and a final extension of 72°C for 7 minutes.

b. *Restriction Digestion Analysis*

After amplification, One-Phor-All Plus buffer was added (final concentration of

10 mM Tris-acetate, pH 7.5, 10 mM magnesium acetate, 50 mM potassium acetate), then

subject to digestion with 10 units *Pst*I restriction enzyme for 2 hours at 37°C. The

digestion products were separated by electrophoresis through a 10% non-denaturing

polyacrylamide gel as described in II.B.6.c and stained with ethidium bromide.

8. Mutation Analysis

a. *Polymerase Chain Reaction*

For genomic sequencing of the LOX gene, exons and flanking intronic sequences

were PCR amplified. The sequences of the intron derived primers for exons 1-5 are listed

in Table 2.1. PCR reactions were performed as described in II.B.4.c, except with 200 μM

dNTP. For intronic primers flanking exons 2 and 3, 10% DMSO was used in the PCR

reactions. The thermocycle profiles were initial denaturation at 94°C for 3 min, followed

by cycles of denaturation at 94°C for 30 sec; annealing for exon 1 primers was carried out

at 60°C, for exon 2 and exon 4 primers at 48°C, exon 3 primers at 50°C, exon 5 at 46°C

for 30 sec; followed by extension at 72°C for 30 sec. Final extensions were at 72°C for 7

min. Exon 1 was amplified for 40 cycles and all of the other exons for 35 cycles.

For sequencing of the LOX mRNA, exons 1-4 were RT-PCR amplified from first

strand cDNA, synthesized as described in II.B.6.a. The sequences of the primers, LOX1-

4f and LOX1-4r, are listed in Table 2.1. The PCR reaction was performed as described in

II.B.6.b, except with 200 μM dNTP. The thermocycle profile was an initial denaturation at 94°C for 3 min, followed by 35 cycles of denaturation at 94°C for 30 sec, annealing at 60°C for 30 sec, and extension at 72°C for 30 sec, and a final extension at 72°C for 7 min.

b. *Pre-sequencing Treatment of PCR Products*

Any unconsumed primers and dNTP remaining after completion of the PCR reaction must be removed to prevent interference in the subsequent sequencing reaction. The PCR Product Pre-Sequencing Kit (Amersham) was utilized for this purpose. Five microliters of PCR product was treated with 10 units of Exonuclease I and 2 units of Shrimp alkaline phosphatase (SAP). Exonuclease I degrades single stranded DNA processively in the 3' to 5' direction, and removes unincorporated primers and any extraneous single-stranded DNA produced by the PCR reaction. SAP removes residual unincorporated dNTP by rendering the dNTP unusable through removal of the 5' phosphates from nucleic acid templates. This was incubated for 37°C for 15 minutes, heat inactivated at 80°C for 15 minutes, then utilized as the template.

c. *Manual Sequence Analysis*

Thermal cycle sequencing is based on the Sanger method of dideoxy sequencing (Sanger et al, 1977). Dideoxynucleoside triphosphates (ddNTP) are nucleoside analogs that can be substituted for deoxynucleotides and terminate DNA synthesis due to absence of the 3' hydroxyl group preventing formation of a phosphodiester bond with the succeeding dNTP. Four populations are created that terminate at A, G, C and T residues,

71

respectively, randomly along the length of the template DNA. A small number of

template DNA molecules are repetitively utilized through repeated rounds of denaturing,

annealing and extension for linear amplification of sequencing products, creating nested

fragments whose lengths are determined by the template sequence.

Thermal cycle sequencing was done with the Thermo Sequenase radiolabeled

terminator cycle sequencing kit (Amersham). The termination mix consisted of four tubes

per reaction, with each tube containing 15 pmol of each dNTP and 0.5 μL of one of the

four radiolabeled ^{33}P-ddNTPs (1500Ci/mmol) in the order A, G, C and T. In a separate

tube, 20 μL of reaction mixture was prepared, consisting of 1 x reaction buffer (26 mM

Tris-HCl, pH 9.5 and 6.5 mM MgCl$_2$) with 3 μL of pretreated PCR product, 2 pmol of

primer and 8 units of Thermo Sequenase. Sequenase is a modified version of

bacteriophage T7 DNA polymerase that lacks 3' to 5' exonuclease activity and due to the

reduced preference of dNTP over ddNTP, is able to generate DNA ladders with bands of

similar intensity and readable sequence, up to 500 bases, over the full length of the gel.

To each of the four tubes labeled A, G, C and T, 4.5 μL of reaction mixture was added.

These underwent a thermal cycling profile similar to their PCR profile except for the

absence of an initial denaturation and final extension, and cycles ranging from 50-60

cycles. When the profile was completed, 4.0 μL of stop solution/loading dye (95%

formamide, 20 mM EDTA, 0.05% bromophenol blue, 0.05% xylene cyanol FF) was

added to each tube and stored at-20°C until electrophoresis.

d. *Sequencing Gel Electrophoresis*

The method for sequencing gel electrophoresis is similar to denaturing gel electrophoresis as described in II.B.4.d, except for the gel buffer, loading dye, denaturing conditions and run time. The gel buffer was glycerol tolerant since the enzyme mixture used in the sequencing reactions contained a high glycerol concentration and use of other buffers such as TBE could result in severe distortion of the sequencing bands. The glycerol tolerant buffer (89 mM Tris base, 29 mM taurine, 0.54 mM $Na^2EDTA \cdot 2H_2O$) was used for the polyacrylamide gel (6%) and the running buffer. The stop solution replaced the loading dye used in II.B.4.d, and after denaturation of the samples at 70°C for 2-10 minutes, the samples were placed immediately on ice to prevent reannealing and half the volume of the sample was loaded in the wells of the prewarmed gel. The samples were run in the order AGCT so that the two reactions (G and C) that suffer most from compression are located next to each other. For extended runs, the samples were electrophoresed at 1800 V until the xylene cyanol was one-fourth the distance from the bottom of the gel. The gel was then stopped and the remainder of the sample was loaded for the shorter run. This was electrophoresed until the bromophenol blue just exited the gel. The gel was then transferred to Whatman 3MM paper and dried as described in II.B.4.e. In the case of ^{33}P, the water in the gel dampens the signal, so the drying step was critical. The dried gel was exposed overnight at -80°C with a Biomax LE Transcreen specific for ^{33}P and Fuji RX-U film.

C. RESULTS

1. Characterization of Two Novel Microsatellite Markers in the LOX Gene Locus

Work previous to this dissertation had identified six CA-dinucleotide repeats within two overlapping PAC clones containing the lysyl oxidase gene. Three of these were further characterized. A comparison of these microsatellite sequences to the Genbank GCG database revealed that lms1 and lms15 were novel markers, and that the third microsatellite was identical to a previously identified marker, D5S467 (Gyapay et al, 1994). All three microsatellites were found to be polymorphic in our populations of interest. Five alleles for lms1were detected, with the number of CA-repeats varying from 13 to 17 (Figure 2.1a). Twelve alleles for lms15 were detected with the number of CA-repeats varying from 18 to 29 (Figure 2.1a). Mendelian segregation of different alleles was confirmed in a 15-member, three generation Venezuelan population (CEPH#107) for the novel markers lms1 and lms15. Figure 2.1c shows the pedigree for lms15.

2. Lysyl Oxidase Maps to Marker D5S467 at 5q23.1

Identification of the third microsatellite as D5S467 placed the LOX locus to chromosome 5q23.1. This was confirmed by a collaboration with Dr. Stephen A. Krawetz *(Department of Molecular Medicine and Genetics, Wayne State University)*. His Southern blot and sequence analysis of PAC clone gs8423 established the order of these markers relative to the LOX gene as follows: centromere - lms1 - D5S467 - LOX - lms15 - telomere. Microsatellite lms1 lies 20 kb, D5S467 5 kb centromeric to the LOX gene and
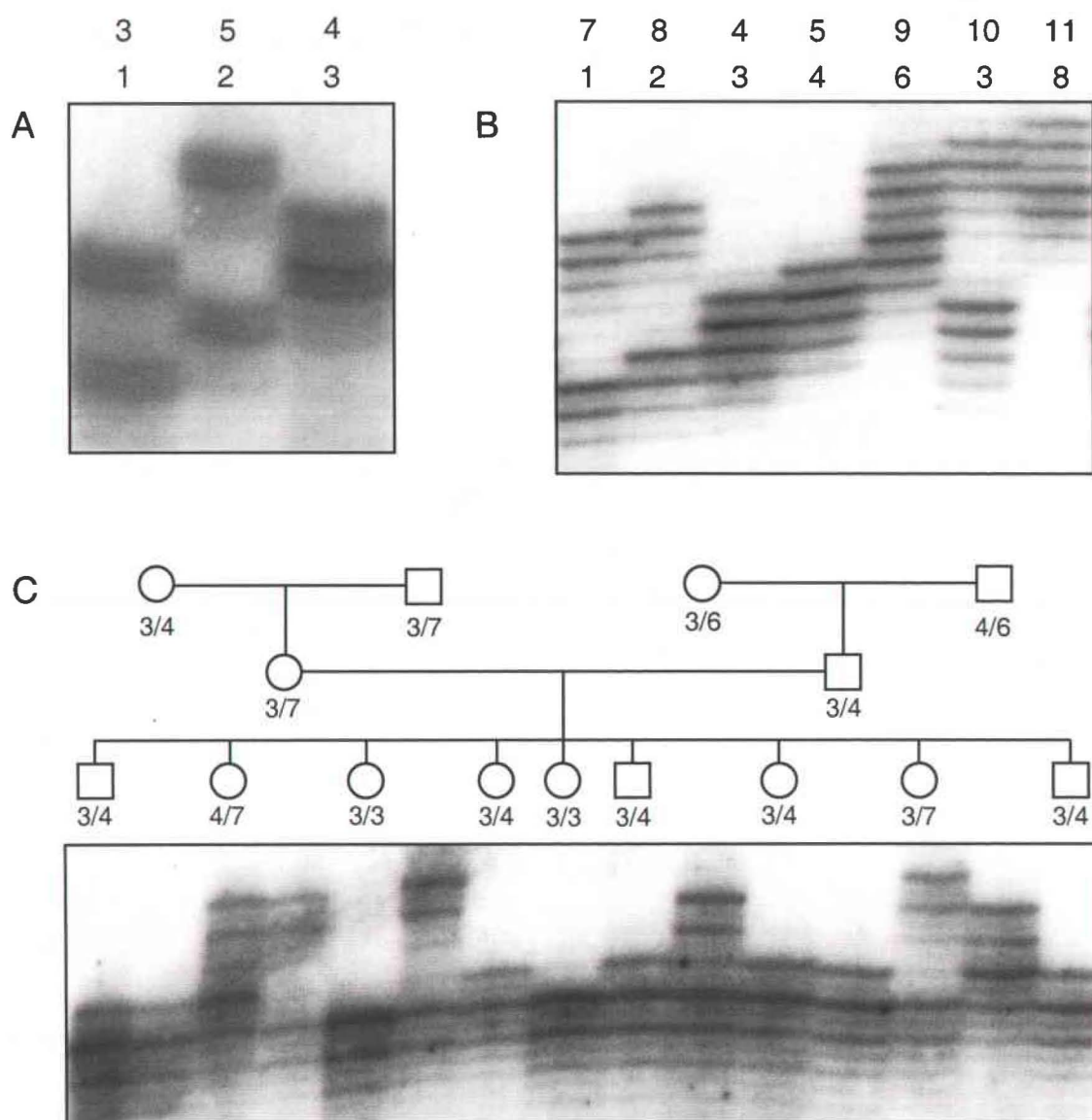
Figure 2.1. Characterization of novel microsatellites lms1 and lms15. Different alleles of the two novel (CA) repeats at the human lysyl oxidase gene locus. A. Five alleles of lms1. B. Eleven alleles of lms15. C. Mendelian segregation of lms15 was confirmed in a 15-member, three generation Venezuelan population (CEPH#107). No expansion of this dinucleotide repeat was evident in this pedigree.

lms15 is located 7 kb telomeric to the LOX gene, placing the lysyl oxidase gene at 5q23.1, between D5S471 and D5S818 markers (Figure 2.2).

3. Significant Loss of Heterozygosity in Colon Tumor DNA Samples

The LOX gene locus at 5q23.1 was targeted for high density LOH mapping to assess the status of this region for genetic changes in 66 patients with colon cancer and 62 patients with esophageal cancer. Three microsatellites covering 40 kb around the LOX gene (lms1, D5S467 and lms15), and additional flanking centromeric (D5S346, D5S421 and D5S471) and telomeric (D5S490 and D5S642) markers that cover the region from 5q21.3 to 5q23.2, were used to screen for loss of heterozygosity (LOH) in matching blood and tumor DNA samples from the patient panels.

LOH and allelic imbalance at the three markers flanking the LOX gene in colon tumor DNA occurred at about the same frequency (all percentages are followed by absolute numbers in parentheses): 32.2% (10/31) at the lms1, 35.7% (15/42) at D5S467 and 31.2% (15/48) at the lms15 locus. At all these three loci combined, 38.1% (16/42) of patients showed allelic changes of one, two or all three microsatellite markers in colon tumor DNA samples, in cases when at least two of the markers were informative at the LOX gene locus. Of the total number of patients, 9.1% (6/66) were non-informative for any of the three LOX microsatellites.
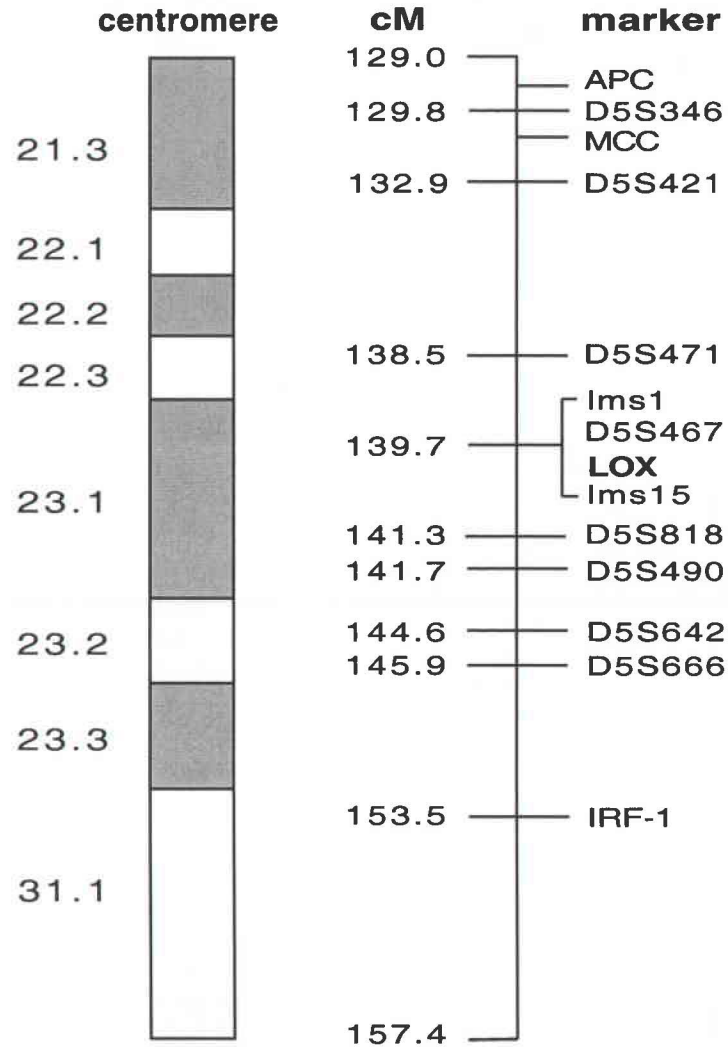
Figure 2.2. Chromosomal localization of the LOX gene at 5q23.1. Map positions and physical distances in centimorgans (cM) are indicated. lms1 and lms15 are novel microsatellites. The positions of the LOX, APC, MCC and IRF-1 genes and the relative positions of the microsatellite markers are also indicated

77

The most centromeric marker tested in this study, D5S346, located between the APC and MCC genes at q21.3 revealed 37.1% (23/62) LOH and allelic imbalance in all informative patients. The D5S421 marker at q21.3 showed 37.7% (23/61) LOH and allelic imbalance, and the third centromeric marker relative to the LOX gene, D5S471, demonstrated 36.4% (20/55) LOH and allelic imbalance. The marker telomeric to the LOX gene, D5S490 at q23.1, had a lower value of 23.8% (10/42) and the most telomeric microsatellite, D5S642 at q23.2, demonstrated 38.8% (19/49) LOH and allelic imbalance. Representative alleles and LOH for the microsatellite markers tested are shown in Figure 2.3a, and the summary of the microsatellites affected by LOH and allelic imbalance are shown in Figure 2.4. Interestingly, female patients showed much higher incidences of LOH at D5S642 compared to males. For the remaining markers, males had higher or similar incidences to females. These values were 33.3% for males and 34.5% for females for D5S346; 37.0% and 27.6% for D5S421; 44.0% and 26.9% for D5S471; 44.4% and 25.0% for lms1; 41.2% and 22.7% for D5S467; 47.6% and 22.7% for lms15; and 27.8% and 20.0% for D5S490. There was only one tumor sample, #43, which showed no amplification of either allele for markers lms15 and D5S642.

An additional 15.2% (10/66) of patients showed the presence of new alleles in their tumor DNA (MIN) and 70.0% (7/10) of these had new alleles either at several or at all informative markers, suggesting defects of DNA mismatch repair (Bronner et al, 1994). In general, most of the new alleles appeared to be shorter than the normal counterparts. Figure 2.3b illustrates the presence of new alleles in tumor #56 at most loci
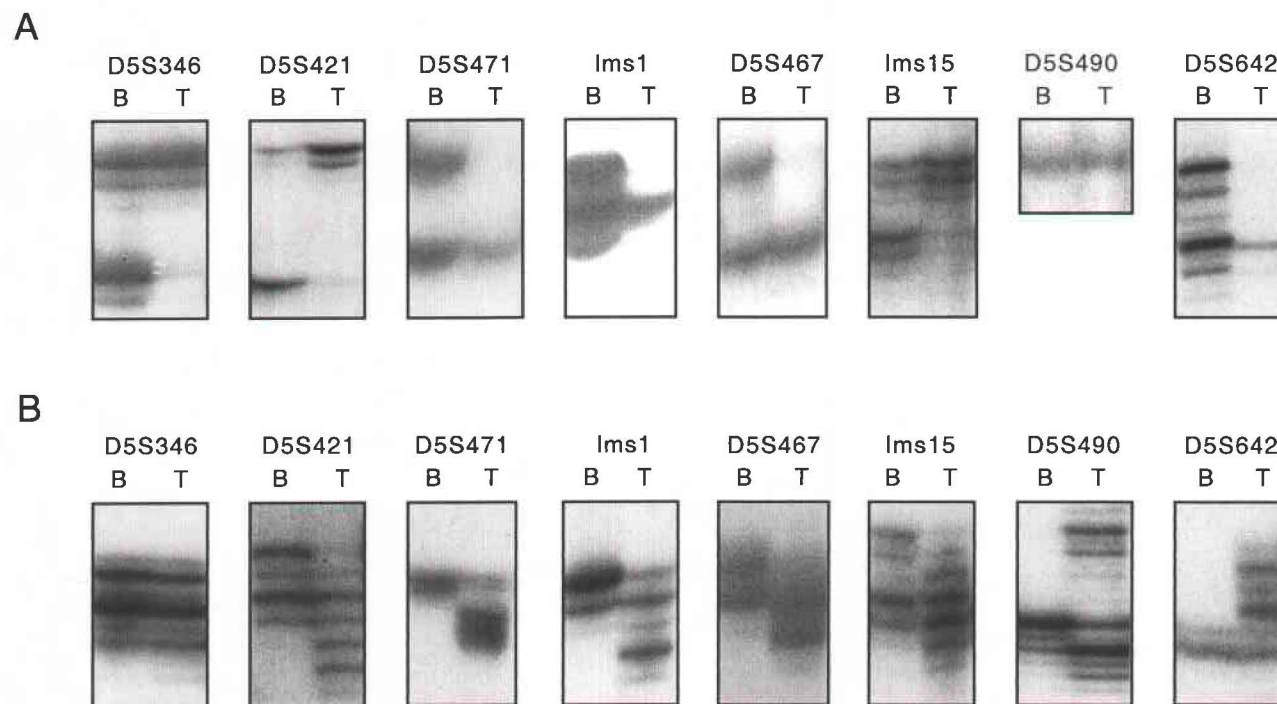
Figure 2.3. Representative loss of heterozygosity (LOH) and microsatellite instability (MI) at the LOX gene and flanking loci in colon cancer. Each panel contains an autoradiogram of the microsatellites PCR amplified from blood (B lanes) and tumor (T lanes) DNA. A: All informative markers tested in tumor DNA relative to blood DNA samples demonstrated LOH in tumor #19. B: Microsatellite instability was detected at all markers tested in tumor #56 except for D5S346.
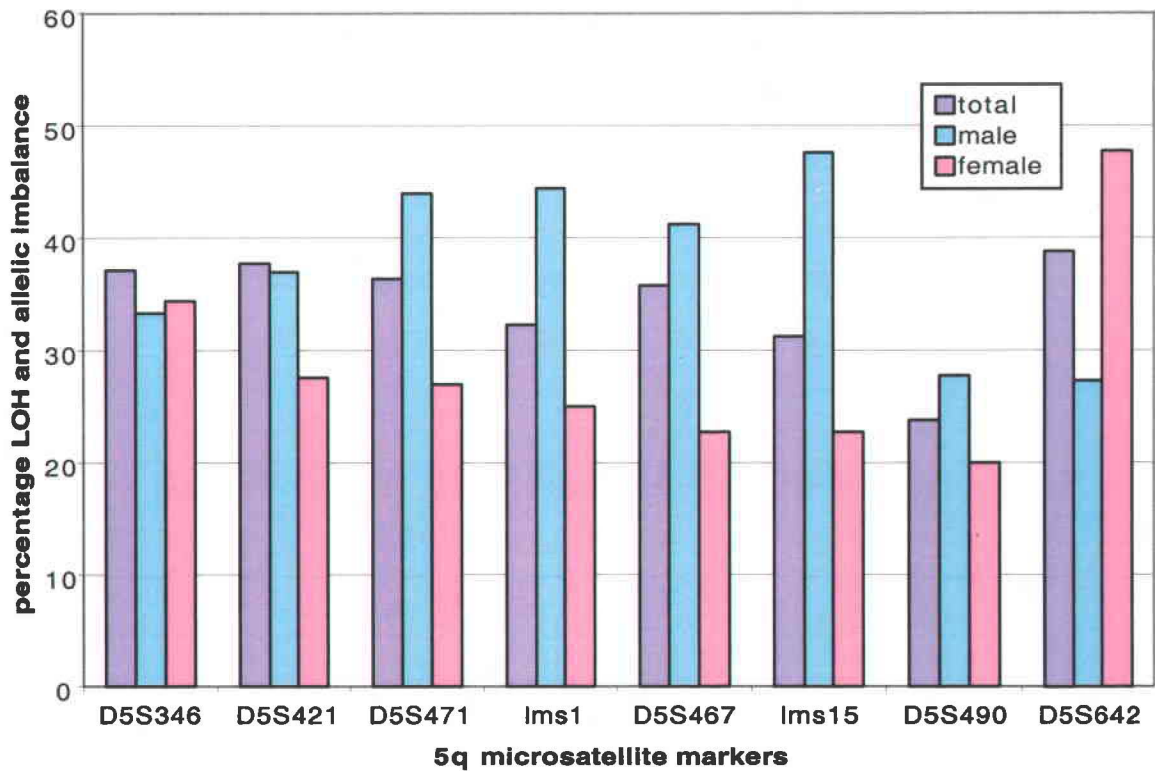
Figure 2.4. Loss of heterozygosity and allelic imbalance at chromosome 5q21.3-q23.2 in colon cancer. Significant LOH and allelic imbalance observed in tumor DNA samples at the LOX gene locus with lower frequency at flanking centromeric and telomeric microsatellite markers. Tumor samples from males had higher frequency LOH at all the microsatellite markers except D5S346 and D5S642.

tested, and the summary of the microsatellites affected by MIN is shown in Figure 2.5.

Except for markers D5S346 and D5S490, females had a much higher incidence of MIN

than males. These values were 7.4% for males and 3.4% for females for D5S346; 7.4%

and 13.8% for D5S421; 8.0% and 15.4% for D5S471; 11.1% and 20.0% for lms1; 11.8%

and 22.7% for D5S467; 9.5% and 22.7% for lms15; 11.1% and 10.0% for D5S490; and

9.1% and 17.4% for D5S642. The results of the microsatellite analysis for each of the

colon samples are shown in Figure 2.6.

The APC/MCC gene loci at 5q21.3 and the LOX gene loci at 5q23.1 were

simultaneously affected in 33.3% (22/66) of tumor samples by LOH, indicating that a

relatively large region of chromosome 5q was deleted in these cases. LOH at the

APC/MCC gene locus without loss at the LOX gene locus was observed in 3.0% (2/66)

of tumors. In comparison, 10.6% (7/66) of the patients showed loss at the LOX locus in

the absence of loss of the D5S346 marker at the APC/MCC locus.

No stage A tumors tested in this study demonstrated LOH, allelic imbalance or

microsatellite instability. LOH and allelic imbalance associated with the LOX gene was

observed in stage B and higher grade tumors. Tumors that demonstrated microsatellite

instability were all stage B, and most (75%) were located in the right colon.

Analysis on approximately 50% of the esophageal panel was completed. The

markers within the LOX locus, lms1, D5S467 and lms15, showed LOH or allelic
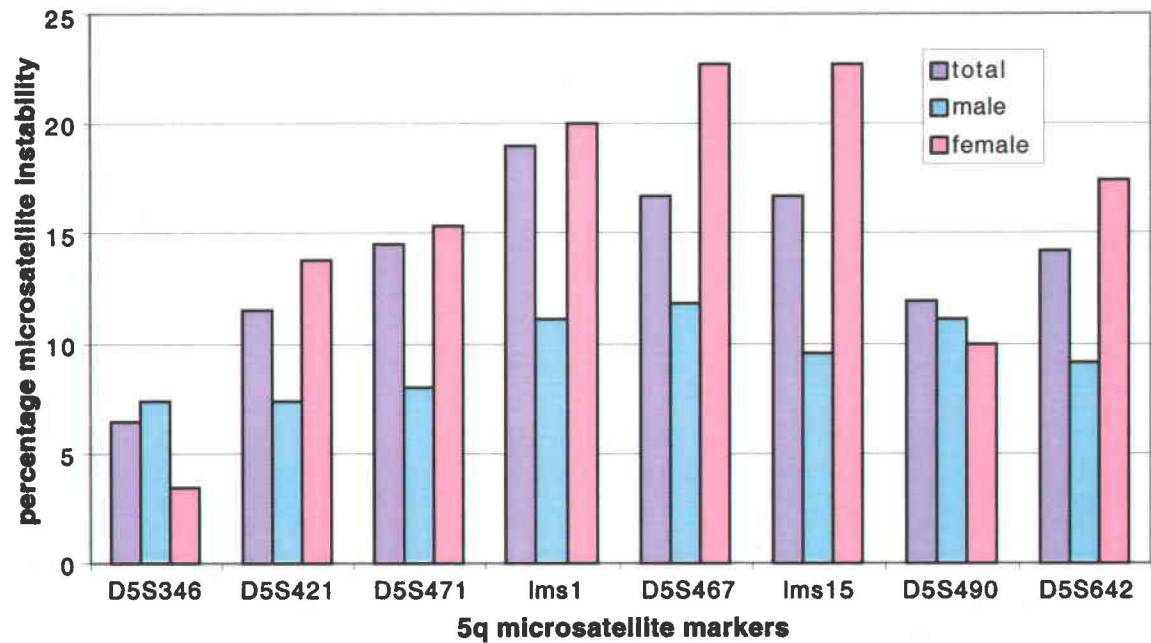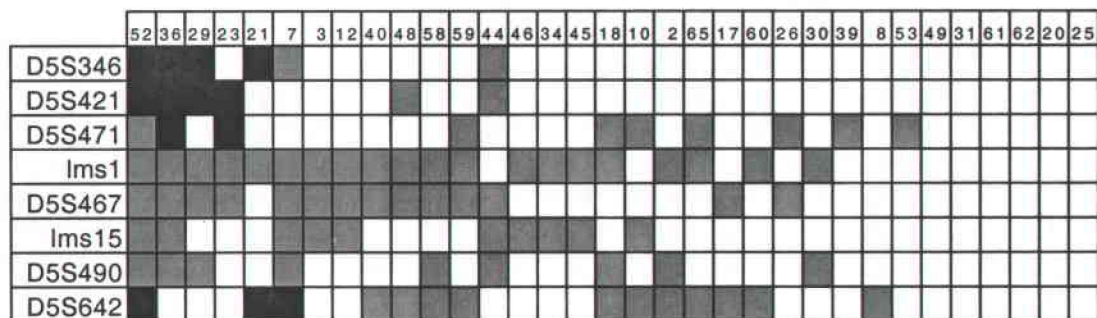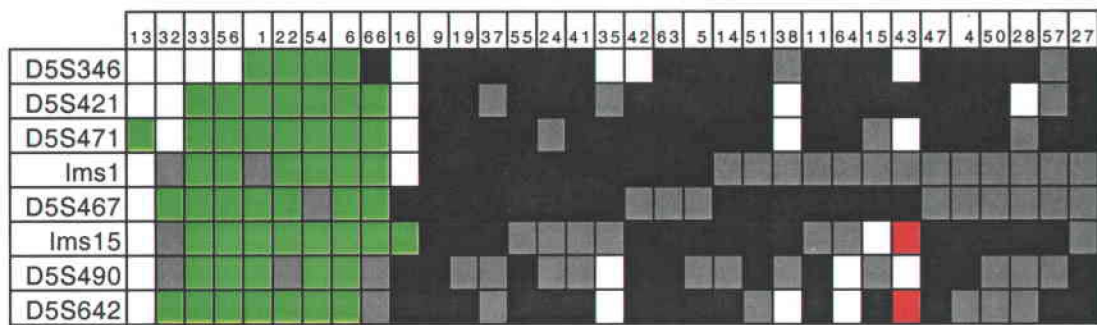
Figure 2.5. Microsatellite instability at chromosome 5q21.3-q23.2 in colon cancer.

Tumor samples from females had higher frequency MIN at all the microsatellite markers except D5S346 and D5S490.

Figure 2.6. Analysis of microsatellites at the LOX gene locus and flanking markers in colon tumors. Microsatellites are noted in the left margins and the patient number is noted at the top. Approximately 15% of tumor samples demonstrated MIN and greater than 30% demonstrated LOH and allelic imbalance.

imbalance in 35.3%, 21.4% and 22.2%, respectively (Figure 2.7). Microsatellite D5S346 at the APC/MCC locus demonstrated 20.7% change. The highest LOH (36.0%) is seen in marker D5S490, followed by lms1 (35.1%) and D5S471 (33.3%). Due to the low percentage of LOH in the two markers closest to the lysyl oxidase gene, studies directed at *LOX as a candidate tumor suppressor in esophageal cancer, will not be pursued.*

4. Reduced LOX mRNA Levels in Colon Tumors

A matched normal/tumor cDNA array was hybridized to a LOX cDNA radiolabeled probe to evaluate LOX expression levels in tumors relative to matched normal colonic tissue. The array contained 11 matched samples, all of which were adenocarcinoma, except for one benign tumor. All the normal colon samples demonstrated expression of LOX and there was down-regulation of LOX expression in 7 of the 10 adenocarcinoma samples and in the benign tumor (Figure 2.8). Interestingly, all three samples that did not show down-regulation were female, and is consistent with the observation that females have lower incidence of LOH in the chromosomal region surrounding LOX. The array allowed for determination of decreased LOX mRNA levels in a panel of colon tumor samples of which the LOX allele status was not known.

To evaluate whether reduced LOX levels were correlated with LOH of the LOX gene region, RT-PCR of LOX mRNA was performed on colorectal tumor tissues that were analyzed for LOH. Tumor samples were divided into two groups: Group-1 demonstrated either loss of heterozygosity or allelic imbalance at two or more 5q21.3-
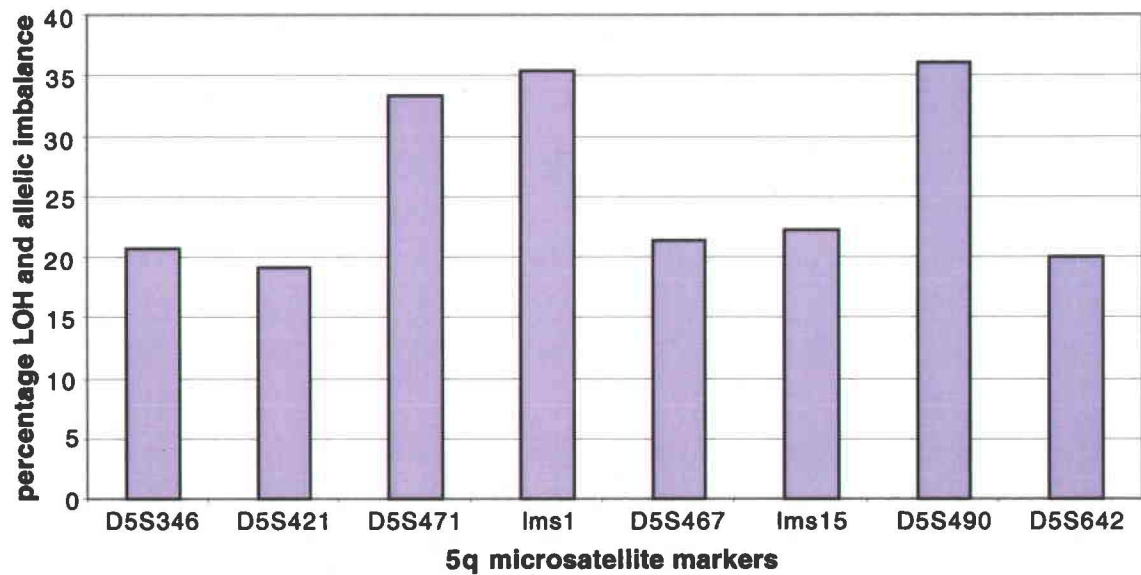
84

Figure 2.7. Loss of heterozygosity and allelic imbalance at chromosome 5q21.3-q23.2 in esophageal cancer. Significant LOH and allelic imbalance observed in tumor DNA samples at markers D5S471, lms1 and D5S490, centromeric and telomeric to the LOX gene locus, respectively. The two markers closest to and flanking the LOX gene, D5S467 and lms15, did not have significant microsatellite alterations.
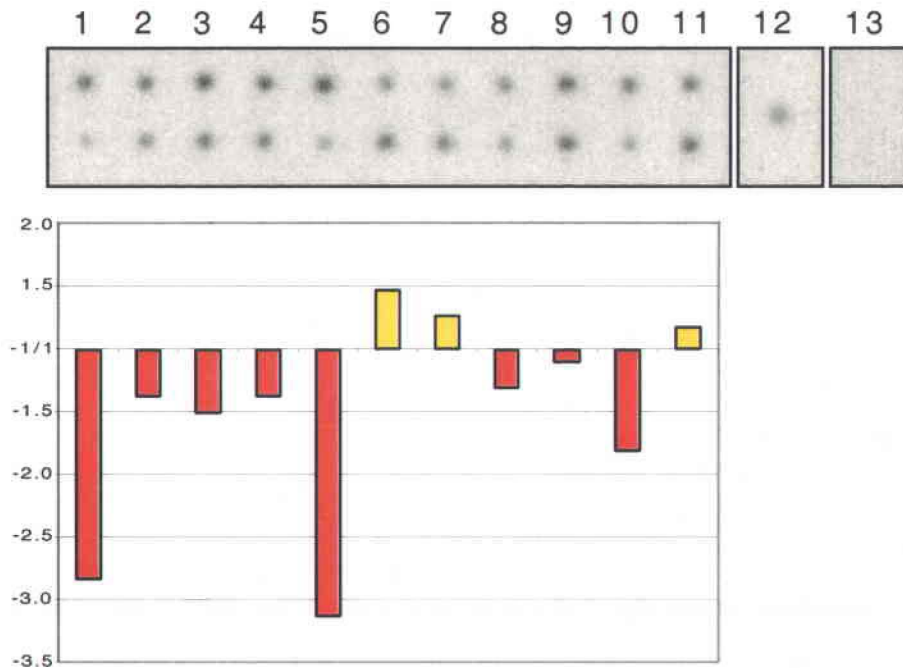
Figure 2.8. Reduced LOX mRNA levels in matched normal and tumor tissue from colon. A Matched/Normal Tumor Expression Array (Clontech) was analyzed for LOX mRNA expression. The upper row of samples 1-11 are from normal colon tissue and the lower row of samples are from matching colon tumors. Sample 1: benign tumor; samples 2-11: adenocarcinoma; sample 12: positive control of genomic DNA; sample 13: negative control of yeast total RNA. Patients of samples 2, 6 and 8 also had metastases. Samples 1-4, and 9 were from male patients. The bar graph demonstrates fold down-regulation (red) or up-regulation (yellow) of LOX expression in colon tumor compared to its matched normal tissue.

23.1 microsatellites, and Group-2 demonstrated no alterations of these microsatellites. The conserved region of the LOX mRNA encoding the cytokine receptor-like (CRL) domain (Figure 1.2, 1.3), corresponding to sequences encoded by exons 5-6, was amplified using RT-PCR from total RNA extracted from these tumor tissue samples.

The LOX mRNA was detected in all Group-2 RNA samples (not shown) but there was a significant reduction of the LOX mRNA in 6 out of 8 tumor tissue samples in Group-1 (Figure 2.9). There was an equal distribution of males and females both in the samples that did not show reduction (1 sample each), and in those that did show significant reduction (3 samples each). Two internal controls were used in these experiments: β-catenin mRNA, known to be up-regulated in colon cancer due to loss of APC or β-catenin mutations (Morin et al, 1997), was amplified in all tumor samples in Group-1, but was not detected in any of the tumor samples in Group-2 (not shown). GAPDH mRNA was present in all samples. The six samples that demonstrated significant reduction in LOX mRNA expression were evaluated for mutations.

5. Somatic Mutations of the LOX Gene in Colon Tumors

a. *Deletion of LOX Allele*

A previously characterized *Pst* I polymorphic site within the first exon of the LOX gene (Csiszar et al, 1993) enabled us to monitor the deletional status of this exon in each allele of the tumor DNA samples of patients who demonstrated heterozygosity for this polymorphism. The low frequency of 13% for the A allele in the general population
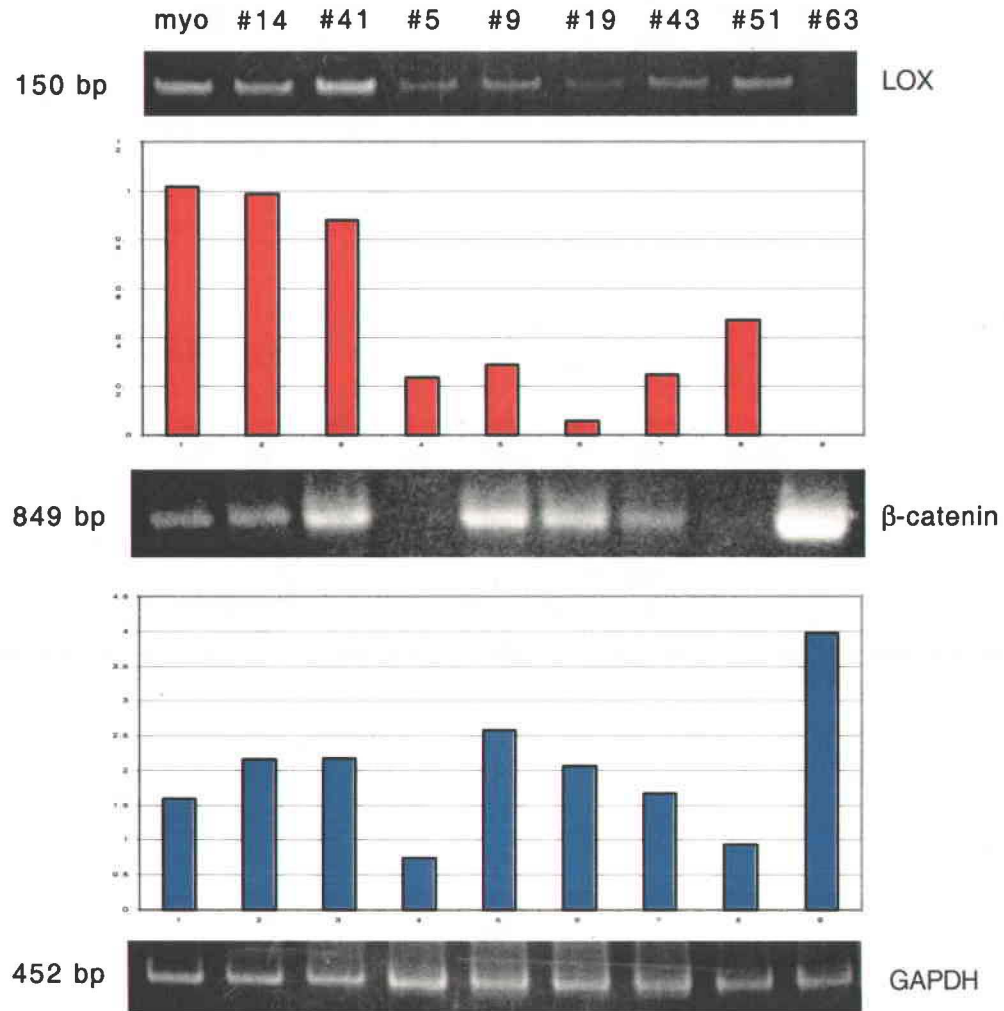
87

Figure 2.9. Reduced LOX mRNA levels in colon tumors demonstrating LOH. Total RNA from tumor samples demonstrating LOH were analyzed by RT-PCR for the presence of LOX, β-catenin and GAPDH mRNA. Lane 1: positive control of human smooth muscle cell RNA (myo); lanes 2-9: RNA samples from colon tumors that demonstrated LOH or allelic imbalance at the LOX gene locus, patient number indicated. Patients #14, #9, #43 and #51 are male. The sizes of the amplified products are indicated in bp on the left, and the identity of the amplified sequence is indicated on the right of the panels.

88

left only 4 informative, heterozygous patients that also showed microsatellite changes. Two (#24 and #52) demonstrated LOH of the microsatellites in the LOX gene locus or in flanking markers, and two (#56 and #66) demonstrated MIN. Of these, patient #52 and patient #66 showed loss and reduction of the A allele and G allele, respectively (Figure 2.10). The remaining allele of each of two tumor samples, allele A, represented as the 145 and 75 bp bands in patient #52, and allele G, represented as the 221 bp band in patient #66, were evaluated for mutations.

b. *Southern Blot Analysis of the LOX Gene*

Work previous to this dissertation involved Southern blot analysis of 14 matched normal blood and colon tumor samples, including patients #51, #52 and #66, to detect deletions or rearrangements. *Pst*I digested blood and tumor DNA samples, run on an agarose gel and transferred to nylon membrane, were hybridized to a radiolabeled 3' lysyl oxidase cDNA probe and exposed to X-ray film. In tumor #52, the 4.5 kb fragment containing exons 4 and 5, and the 11 kb fragment containing exons 6 and 7 of the LOX gene were absent, and an aberrant 9 kb fragment was detected (Figure 2.11). This was determined to be a 3' end rearrangement involving exons 5-7. Patient #51 and #66 did not show any aberrant banding patterns.

c. *Exon Deletions Within the LOX Gene*

Along with flanking intronic sequences, the first 5 exons of the LOX gene that encode important functional domains of the LOX protein, including the signal peptide,
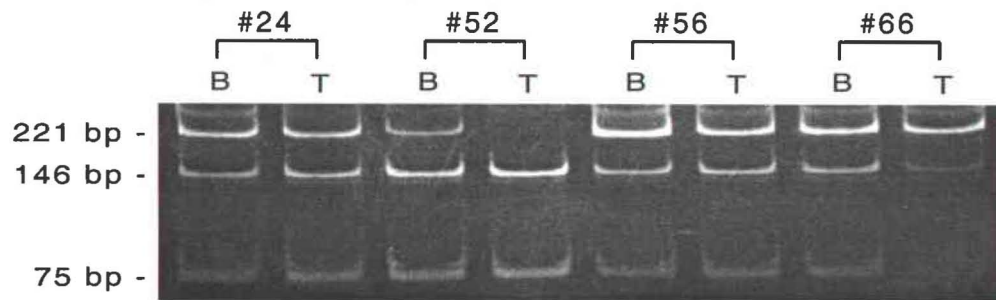
Figure 2.10. Deletion of one LOX gene allele detected using a G/A polymorphism.
A *Pst*I polymorphic site within exon 1 of the LOX gene was PCR amplified from
blood (B) and tumor (T) DNA samples of the informative patients #24, #52, #56 and
#66 who also demonstrated microsatellite changes. The amplified products were
digested with *Pst*I restriction enzyme and separated on a non-denaturing polyacryla-
mide gel. The major G allele is represented as an undigested 221 bp product, and the
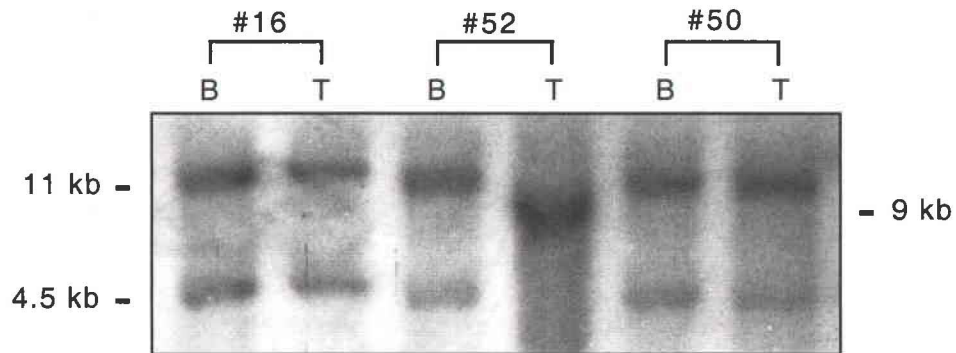minor A allele is represented as two digestion products of size 146 and 75 bp.
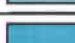
Figure 2.11. Southern blot analysis of the LOX gene in tumor DNA samples. A
Southen blot of *Pst*I digested blood (B) and tumor (T) DNA samples that showed
LOH at the LOX locus, was hybridized to a lysyl oxidase cDNA probe. The sizes of
the expected hybridizing genomic DNA fragments are indicated in kb on the left of
the panel, and the size of the aberrant fragment is indicated in kb on the right of the
panel.

processing site, copper-binding domain and part of the cytokine receptor-like domain

(Figure 1.3), were PCR amplified to evaluate the presence of intragenic mutations. The

identity of each of the amplified products from the six samples that demonstrated reduced

LOX expression and the two samples that demonstrated loss of one allele of exon 1, was

confirmed by sequence analysis. Exon 1 could not be amplified in 5 of the 6 tumor

samples that demonstrated low levels of LOX mRNA and LOH of the LOX gene locus.

Exon 2 could not be amplified in 3 of the samples, 2 of which also lacked exon 1

amplification (Figure 2.12). The amplification of these exons from the matched normal

blood DNA samples excluded the possibility of polymorphisms that may have interfered

with amplification.

d. *Mutational Analysis of LOX DNA and mRNA*

Sequence analysis of the amplified exons revealed one mutation in tumor #66.

The mutation was in the sequence encoded by exon 4, at codon 332, and consisted of a T

to A substitution that changed a TAT codon to a TAA stop codon (Figure 2.13). As this

patient already demonstrated loss of one LOX allele using a *Pst*I polymorphism within

exon 1, mRNA from tumor #66 was RT-PCR amplified for the sequence corresponding

to exons 1-4, and confirmed the presence of the inactivating exon 4 mutation in the

remaining allele.

Alterations of both LOX gene alleles were detected in all eight of the samples that

demonstrated reduced LOX mRNA expression or loss of exon 1, and represented 12.1%

	lms1	D5S467	LOX							lms15
			Exon 1	Exon 2	Exon 3	Exon 4	Exon 5	Exon 6	Exon 7	
#5	[LOH/allelic imbalance]	ni	[Homozygous deletion]	+	+	+	0	0	0	[LOH/allelic imbalance]
#9	[LOH/allelic imbalance]	[LOH/allelic imbalance]	[Homozygous deletion]	[Homozygous deletion]	+	+	0	0	0	[LOH/allelic imbalance]
#19	[LOH/allelic imbalance]	[LOH/allelic imbalance]	[Homozygous deletion]	[Homozygous deletion]	+	+	0	0	0	[LOH/allelic imbalance]
#43	ni	[LOH/allelic imbalance]	+	[Homozygous deletion]	+	+	0	0	0	[Homozygous deletion]
#51	ni	[LOH/allelic imbalance]	[Homozygous deletion]	+	+	+	0	0	0	[LOH/allelic imbalance]
#63	[LOH/allelic imbalance]	ni	[Homozygous deletion]	+	+	+	0	0	0	[LOH/allelic imbalance]
#66	[Microsatellite instability]	[Microsatellite instability]	[LOH/allelic imbalance]	+	+	[Mutation]	+	0	0	[Microsatellite instability]
#52	ni	ni	[LOH/allelic imbalance]	+	+	+	[Homozygous deletion]	[Homozygous deletion]	[Homozygous deletion]	ni

Legend:

- [blue] LOH/allelic imbalance
- [green] Homozygous deletion
- [pink] Mutation
- [yellow] Microsatellite instability

- ni — non-informative
- + — at least one allele present
- 0 — exon not tested

Figure 2.12. A spectrum of mutations within the LOX gene and flanking microsatellite markers in sporadic colon tumors. Patient numbers are noted on the left. On the top are the microsatellites markers and the exons for the LOX gene. Homozygous deletions of the first six patients were scored as a failure of these exons to amplify and thus represent either loss of both alleles or a mutation at the primer site. The homozygous deletion of the last patient was detected by Southern blot analysis. The mutation was detected by sequence analysis of individual exons.

329	330	331	332	333	334	335
Ser	Cys	Asp	Tyr	Gly	Tyr	His
TCC	TGT	GAC	TAT	GGC	TAC	CAC
TCC	TGT	GAC	TAA			
Ser	Cys	Asp	**STOP**			
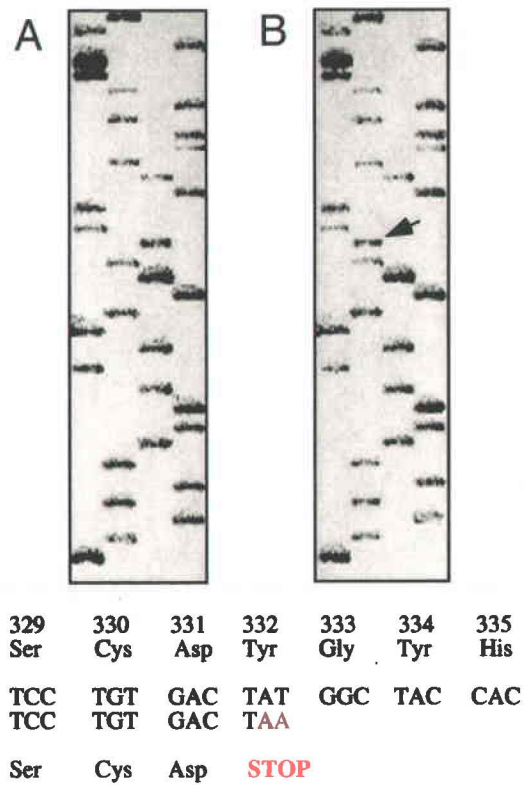
Figure 2.13. Inactivating point mutation within the LOX gene. Exon 4 was PCR amplified from tumor #66 which demonstrated MIN and loss of one allele of exon 1 of the LOX gene. The normal sequence is shown in (A) and the sequence from tumor #66 is shown in (B) and demonstrates a T to A change as indicated by the arrow. The numbers and abbreviated amino acids below the panel refer to codons within the LOX mRNA sequence.

(8/66) of the tumors. These results and the microsatellite status of markers flanking the

LOX gene of these same tumor samples are summarized in Figure 2.12.

D. DISCUSSION

Previous studies had reported loss of heterozygosity of chromosome 5q21-31 in

colon cancer (Mertens et al, 1997), and 5q23-31.1 in esophageal cancer (Peralta et al,

1998). Collectively, this area includes the APC and MCC genes at 5q21 (Kinzler et al,

1991a) and the IRF-1 gene at 5q31 (Itoh et al, 1991) that have already been established to

have a role in cancer development. The high frequency of loss encompassing

chromosome 5q22-23 in colon cancer and 5q23 in esophageal cancer indicated that

additional tumor suppressor genes may also reside in this area, but no tumor suppressor

gene at this chromosomal loci has been identified. In addition, there have been no reports

of a more comprehensive evaluation of this chromosomal region or of genes that have

mapped to this area. The lysyl oxidase gene was mapped to 5q23.3-31.2 (Mariani et al,

1992; Hamalainen et al, 1991), and based on the evidence of LOX as a modulator of *ras*

and the observed decrease of LOX expression in transformed cells and progressive

prostate and breast cancer (reviewed in II.A), LOX was hypothesized to be a tumor

suppressor gene candidate involved in both colon and esophageal cancer. The results

presented in this chapter have confirmed significant loss of heterozygosity in

microsatellite markers flanking the LOX gene locus in colon tumors, demonstrated

reduced LOX gene expression in colon tumors and for the first time, identified somatic

mutations within the remaining LOX allele.

Detailed LOH analysis was accomplished by the use of previously characterized

microsatellites between 5q21.3 and 23.2, and three microsatellites flanking the LOX

gene. Two microsatellites were novel and were characterized to be polymorphic and thus

useful for the LOH study. Identification of the third microsatellite as D5S467 allowed for

the more precise localization of the LOX gene to chromosome 5q23.1 compared to the

previously identified 5q23.3-31.2 (Mariani et al, 1992; Hamalainen et al, 1991).

Microsatellite analysis of the LOX locus in the esophageal tumor panel revealed

no significant LOH in the markers closest to LOX, D5S467 and lms15. No significant

LOH was observed at marker D5S346 and indeed, the APC gene has been shown not be

involved in esophageal cancer (Shibagaki et al, 1994; Aoki et al, 1994; Powell et al,

1994). Based on the significant LOH of the markers centromeric and telomeric to the

LOX gene, it is likely that the 5q23 tumor suppressor candidates involved in esophageal

cancer lie close to lms1, 20 kb centromeric to the LOX gene, and D5S490.

Interesting gender-associated patterns emerged from the microsatellite analysis in

the colorectal tumors. The higher incidence of LOH at D5S642 in females (47.8%)

compared to males (27.3%) is consistent with reports of myeloid disorders that affect

mainly women and involve 5q31 (Peterson, 1996). Another interesting observation was

the higher incidence of LOH in males and of MIN in females for most of the

microsatellite markers. The lower incidence of LOH in females was also reflected in the

matched normal/tumor array, as the three samples that did not show down-regulation

were all from female patients. Microsatellite instability was previously observed to be more frequent among younger male and older female patients with colorectal cancer (Breivik et al, 1997), consistent with this cohort. Estradiol has been reported to be a weak carcinogen and weak mutagen capable of inducing various chromosomal and genetic lesions, including gene mutations and microsatellite instability (Liehr, 2000), but the exact mechanism of this mutagenic activity is not understood.

Microsatellite markers lms15 and D5S642 could not be amplified from the DNA of patient #43. However, the microsatellite between these markers had two alleles present, and several exons of the LOX gene could be amplified. Rather than deletion of these markers from both chromosomes with the intervening marker remaining intact, it is more likely that there were sequence alterations that prevented the primers from amplifying the sequence properly. For the remainder of the samples, at least one identifiable allele from the normal and tumor DNA could be amplified for each of the microsatellite markers evaluated.

Microsatellite analysis demonstrated significant loss of heterozygosity at the LOX locus in colon cancer. Significant LOH extended from the most centromeric marker, D5S346 at 5q21.3, located between the APC and MCC genes, to the three microsatellites closest to the LOX gene at 5q23.1. Marker D5S490 that also maps to chromosome 5q23.1, telomeric to the LOX gene, did not have significant LOH. The percentage LOH seen at the most centromeric marker, D5S346 at 5q21.3 is consistent with previous

reports (Tomlinson et al, 1998; Iacopetta et al, 1994), and validates the LOH seen at the LOX locus in colon tumors. As with other reports, microsatellite instability was observed mainly from tumors of the right colon (Breivik et al, 1997; Liu et al, 1995), and from tumors graded stage B indicating a better prognosis (Liu et al, 1995). The significant level of LOH at the LOX gene locus confirmed the likely existence of a tumor suppressor gene in this region involved in colon cancer.

Due to the lack of microsatellites within the LOX gene, microsatellites surrounding the LOX gene were used. Although it is generally accepted that the LOH of flanking microsatellites markers indicate the concomitant loss of the area between the markers, it is possible that the LOX gene could be unaffected. To resolve this possibility, a previously characterized *Pst*I polymorphic site within the first exon of the LOX gene (Csiszar et al, 1993) was used to monitor the deletional status of both LOX alleles at exon 1 in the four patients who demonstrated heterozygosity for this polymorphism. Tumors from patient #52 and #66 both showed loss of one lysyl oxidase allele. By extrapolation, this indicated that a sizable proportion of the tumor samples that demonstrated LOH had deletion of one allele of the LOX gene, and that tumor samples that demonstrated MIN of the microsatellite markers could also have a deletion.

Since tumor suppressor genes are, by definition, recessive, loss of LOX gene expression was a prerequisite for this gene to be considered a candidate. Reduced levels of LOX mRNA were observed in 70% (7/10) of colon adenocarcinomas whose LOH

status of the LOX gene was not known, and in 75% (6/8) of colorectal tumors that demonstrated LOH of markers flanking the LOX gene. The other 25% (2/8) of these samples may not have sustained deletions of the LOX gene despite LOH of the flanking markers, similar to patient #24 who demonstrated LOH of the LOX locus but still retained both alleles of LOX exon 1. Of the six colon tumors with known LOH of the LOX locus, one had undetectable levels of LOX mRNA, four had LOX mRNA levels less than 30%, and one sample had a LOX mRNA level of approximately 50% of the positive control. The low, but not absent, level of expression may be either due to the remaining LOX allele, or from residual normal cells included in the tumor samples during RNA isolation. As the presence of normal cell DNA was seen in most samples during the microsatellite analysis, it is likely that the low level of expression was due to residual normal cells. Therefore, in the tumor cells, the LOX allele not affected by deletion as indicated by LOH, must be inactivated for LOX to be considered a tumor suppressor candidate. Indeed, mutational analysis, focused on the tumors that demonstrated significantly reduced levels of LOX mRNA, revealed that a range of somatic mutations affected the LOX gene.

It should be noted that since the mutation analysis was focused on those samples that demonstrated reduced LOX mRNA levels or LOH of exon 1 by RFLP, it is possible that mutations that did not result in dramatic reduction of LOX expression were not detected in this study. Mutation analysis demonstrated 5' intragenic alterations or deletions, a 3' end rearrangement and a point mutation resulting in a premature stop

codon. The tumor with the premature stop codon in exon 4 also had loss of the other allele by RFLP analysis, resulting in two null alleles, and MIN of flanking microsatellites. These different mutational mechanisms of mismatch repair, deletion of one LOX allele with perhaps loss of a larger portion of the chromosome as suggested by LOH of the most telomeric marker D5S346, and a point mutation in the remaining allele, is in contrast to a review by Lengauer et al (1998) that suggested that instability at the chromosomal level and nucleotide level may be mutually exclusive. Other reports have indicated that colorectal cancers without MIN do not show high rates of mutation as do RER+ phenotype cells, but instead have loss of chromosome material as a consequence of mitotic recombination or aberrant mitotic segregation (Bhattacharyya et al, 1994), leading to the loss of approximately 25% of randomly chosen alleles in contrast to those with MIN that often lose none (Aaltonen et al, 1993).

Although this study focused on characterizing the loss or reduced function of lysyl oxidase in colon tumors as a result of deletions and mutations affecting the LOX gene, a well-documented tumor suppressor gene in colon cancer pathogenesis, the APC gene, as well as the MCC gene, which is also a possible tumor suppressor, map close to the LOX locus and a microsatellite marker, D5S346, at the APC/MCC gene locus was utilized in this study. Many of the tumors demonstrated LOH of both the D5S346 marker and the LOX locus, and although loss of function of neither the APC gene nor the MCC gene was evaluated in this study, based on LOH and the elevated levels of β-catenin mRNA, it is likely that the APC and the MCC genes are also inactivated. The

100

contribution of LOX gene deletions relative to the inactivation of APC and MCC could not be determined.

The results of this study have demonstrated that: 1) through high density microsatellite analysis, the lysyl oxidase gene locus is affected by a significant level of loss of heterozygosity, indicating that a tumor suppressor gene is likely to reside in this chromosomal region; 2) the majority of colon tumors exhibit a reduction and even absence of LOX gene expression, similar to the inactivation of a tumor suppressor gene; and 3) that this decrease in mRNA expression is due, at least partly, to somatic mutations affecting the LOX gene. These results indicate that the LOX gene is part of the cascade of mutations affecting chromosome 5q, and that the loss of LOX expression is associated with the pathogenesis of colon cancer, and support the hypothesis that the lysyl oxidase has a role as a tumor suppressor gene.

The publication of this data (Csiszar et al, 2002) was the first to demonstrate genetic events, namely LOH, deletions and mutations of the LOX gene, as a mechanism for the reduction of LOX gene expression that had been observed in cancer cell lines and tumor tissues by many investigators (see II.A). Recently, another mechanism for the silencing of the LOX gene has been reported in gastric cancer. Epigenetic changes, which include DNA methylation and modification of histones, are another major mechanism that contributes to modification of expression patterns necessary for tumorigenesis (Plass, 2002). In mammals, DNA methylation occurs mostly to a cytosine located next to a

guanine (5'-CpG-3') (Riggs and Jones, 1983) in long CG-rich sequences, and involves

the covalent addition of a methyl group to the 5' position of the cytosine ring (Bird,

1992). Aberrant methylation of CpG islands is the most commonly studied epigenetic

mechanism leading to transcriptional silencing of tumor suppressor genes (Garinis et al,

2002). CpG islands are sequences longer than 200 bp with a GC content over 50%,

compared to a genome-wide average of 40%, and an observed/ expected ratio of CpG of

0.6 or greater (Takai and Jones, 2002; Gardiner-Garden and Frommer, 1987). They are

found in the 5' region of certain genes, extending from the promoter region into the first

exon and sometimes into intron 1 (Antequera and Bird, 1993).

In the human lysyl oxidase gene sequence, a large CpG island spans the region

upstream of exon 1 extending to intron 2 (Martins et al, 2001). Methylation of the

promoter of LOX, and its consequent transcriptional silencing was observed in 11 of 24

primary gastric cancers with diffuse-type histology and 6 of 9 gastric cancer cell lines

(Kaneda et al, 2002). This study evaluated only the presence of methylation and did not

address if other mechanisms of gene inactivation were involved. Methylation of one gene

allele can be accompanied by LOH, mutation or methylation of the other allele to cause

complete loss of expression (Garinis et al, 2002). In my study, the colon tumor samples

that demonstrated LOH of the LOX gene locus and reduced expression of LOX, all had

somatic mutations, thus in this small subset of 6 samples, the inactivation of the LOX

gene was accounted for. In addition, decreased LOX mRNA expression was not observed

in the small subset of samples that did not demonstrate LOH of flanking microsatellites,

indicating that methylation of the LOX promoter was not involved in these samples. It is possible that, by chance, we missed samples whose expression was decreased by methylation, or that the combination of LOH and methylation is not a major mechanism involved in colon tumor pathogenesis.

Although several mechanisms of LOX gene inactivation have been described (Csiszar et al, 2002; Kaneda et al, 2002), it is not known what the consequence of this inactivation is and how it plays a role in cancer development. Multiple hypotheses on the possible function of LOX in cancer, including roles in the extracellular matrix, metastasis and chromatin regulation, will be discussed in Chapter IV.

CHAPTER III

LOSS OF HETEROZYGOSITY AND ALTERED EXPRESSION OF LOXL2 IN COLORECTAL AND ESOPHAGEAL TUMORS

A. INTRODUCTION

The lysyl oxidase-like 2 (LOXL2) gene is the third member of the lysyl oxidase gene family. At the time of its description by Saito et al (1997), it was found to be unique in protein structure from its predecessors LOX and LOXL, by the presence of 4 SRCR domains (Figure 1.3). With the discovery of the LOXL3 (Huang et al, 2001; Jourdan-Le Saux et al, 2001; Maki and Kivirikko, 2001) and LOXL4 (Asuncion et al, 2001; Ito et al, 2001; Maki et al, 2001) genes, it was apparent that these three members, LOXL2, LOXL3 and LOXL4, shared identical domain organization, and possibly similar function. All five LOX family members share the amino acid sequence that creates the unique LTQ co-factor of this family, and the copper-binding domain, both of which are necessary for amine oxidase activity. Indeed, catalytic activity has been demonstrated for LOX (Smith-Mungo and Kagan, 1998; Kagan et al, 1995; Eyre et al, 1984), LOXL (Borel et al, 2002; Csiszar, 2001) and LOXL4 (Ito et al, 2001), and is theoretically possible for LOXL2 to also have this function.

The first report describing LOXL2 hypothesized a role in cell adhesion or matrix-cell communication. This was based on the observation that LOXL2 mRNA was highly expressed in various adherent tumor cell lines, including astrocytoma, fibrosarcoma and

104

cervical adenocarcinoma, but down-regulated in non-adherent cell lines, including

cervical adenocarcinoma, erythroleukemia, T-cell leukemia, gastric carcinoma, and lung

small cell carcinoma. Loss of expression was hypothesized to confer the ability for the

cell to ignore extracellular signals and separate from its adjoining neighbor cells in order

to metastasize (Saito et al, 1997). *Ras-* transformed cells, which are adherent but

demonstrate less adhesion and more anchorage independence than their non-transformed

counterparts, also express decreased levels of LOXL2. Using subtractive suppression

hybridization to contrast differential gene expression profiles in immortalized rat

embryonic fibroblasts and HRAS-transformed cells, LOXL2 was identified as a *ras*

transformation target that is down-regulated nearly 60-fold (Zuber et al, 2000).

The down-regulation of LOXL2 expression was also demonstrated in ovarian

cancer in two separate reports using different methods of gene expression profiling. Ono

and co-workers (2000) used a cDNA microarray of 9121 genes to evaluate expression

patterns of 5 serous and 4 mucinous ovarian tumors against corresponding normal

ovarian tissue. LOXL2 was one of 115 genes found to be differentially expressed

between the two tumor types, as its expression was down-regulated only in the serous

adenocarcinomas. Similarly, Hough and co-workers (2000) demonstrated at least ten-fold

down-regulation of LOXL2 in the three high grade serous ovarian tumors compared to

nontransformed ovarian epithelia that were evaluated using serial analysis of gene

expression.

The lysyl oxidase-like 2 gene has been mapped to chromosome 8p21.2 to p21.3 (Jourdan-Le Saux et al, 1998), a chromosome region that demonstrates loss in both colon cancer (Lerebours et al, 1999; Arai et al, 1998; Cunningham et al, 1993) and esophageal cancer (Hu et al, 2000; Shibagaki et al, 1994). In addition, colon carcinoma cells with loss of 8p21 have suppressed tumorigenicity and invasiveness when normal chromosome 8p21 is introduced (Tanaka et al, 1996). Although the evidence indicates the presence of a tumor suppressor at 8p21, only one candidate thus far has emerged for each cancer. However, only one of 12 colorectal cancer cell lines demonstrated loss of expression of EXTL3 (Arai et al, 1999) and although 2 of 3 esophageal cancer cell lines had reduced FEZ1 expression, sequence aberrations could only be found for 4 of 72 primary squamous cell carcinomas and none of the esophageal cancer cell lines (Ishii et al, 1999). Neither candidate has been supported by additional reports.

Due to the evidence for the downregulation of LOXL2 as a *ras*-transformation target and in serous ovarian adenocarcinomas, involvement of its family member, lysyl oxidase, in cancer, and the evidence for the existence of a tumor suppressor at chromosome 8p21, to which the LOXL2 gene localizes, LOXL2 was hypothesized to be a candidate tumor suppressor gene. Therefore, to investigate this possibility, the LOXL2 gene was evaluated for loss of heterozygosity and for alterations in mRNA and protein expression in a cohort of colorectal and esophageal tumors.

B. MATERIALS AND METHODS

1. Patient population

For a description of the colon and esophageal tumor panel, please see Section II.B.1.a and b, respectively. Instead of the 66 consenting patients from Chapter II, the colon tumor panel for this study consisted of 65 consenting patients. However, this did not change the percentage composition of the panel in terms of gender, age or stage.

2. Culture of Human Cell Lines

For methodology of seeding frozen cell stocks, maintenance and passage of cultured cells, please see II.B.2.a and b.

a. *Cell Types*

All cell lines were derived from human subjects and grown in their respective media supplemented with 10% FBS and 1% PSN (penicillin/streptomycin/neomycin) mixture. The carcinoma cell lines were obtained from American Type Culture Collection (Manassas, Virginia). HCT-116 (colon carcinoma) was grown in McCoy's 5A medium. The colon adenocarcinoma cell lines, DLD-1 and HCT-15, were grown in RPMI (Roswell Park Memorial Institute) 1640 medium. The normal colon epithelial cell line, CRL-1831, was grown in Ham's F-12/DMEM (Dulbecco's Modified Eagle Medium) supplemented with 25 mM HEPES (N-2-hydroxyethylpiperazine-N'-2-ethane sulfonic acid; Invitrogen), 10 ng/mL cholera toxin, 0.005 mg/mL insulin and transferrin, and 100 ng/mL hydrocortisone (all from Sigma). The addition of HEPES improves pH control

between pH 6.7 and 8.4, and reduces undesirable fluctuation of pH due to tissue metabolism that may lead to inhibition of growth. Myo (smooth muscle), hos (human osteosarcoma) and ras (*ras*-transformed hos) cell lines were grown in DMEM. All media was obtained from Invitrogen. None of the cells were used more than 3 months in culture.

b. *Preparing Frozen Cell Stocks*

Frozen cell stocks are important to avoid senescence and prevent genetic drift. To prepare frozen cell stocks, cultured cells that were 80-90% confluent were trypsinized, resuspended and centrifuged as described in II.B.2.b. The pelleted cells were resuspended in their respective media supplemented with 10% FBS, 1% PSN and 10% DMSO. DMSO is a cryoprotective agent that reduces the freezing point and allows for a slower cooling rate, which reduces the risk of ice crystal formation and cell damage. One mL aliquots of the resuspended cells were placed in cryovials, placed in -20°C for approximately 40 minutes, then transferred to -80 °C for at least one hour but no longer than overnight. The cells were then transferred to the Locator6Plus cryo biological storage system (Barnstead/Thermolyne, Dubuque, Iowa).

3. Isolation of Nucleic Acids

For methodology of DNA extraction from blood and tissue, RNA extraction from tissue and cultured cells, isolation of recombinant DNA plasmids and quantitation of nucleic acids, please see II.B.3.a-e.

a. *Purification of PAC Clone*

PAC (plasmid artificial chromosome) clone 17460, which contained most of the

LOXL2 gene, was obtained from Genome Systems Inc (St. Louis, Missouri) and

prepared according to their PAC manual. The PAC library was constructed by ligating a

partial *Sau*3A I digest of human genomic DNA to the *Bam*HI site of the PAC vector, then

introduced into NS3516 bacterial cells by electroporation in order to generate a 16.5 kb

plasmid with a 120 kb genomic insert. The PAC clone plasmid was isolated using

standard alkaline lysis.

Bacteria harboring the PAC clone were seeded into 10 mL of LB medium with 25

µg/mL of kanamycin (Sigma) and incubated at 37°C with vigorous shaking and grown

overnight to stationary phase. Five mL of overnight culture was mixed with 5 mL of

40% glycerol and aliquoted into cryovials for long term storage at -80 °C. Four 125-mL

Erlenmeyer flasks with 75 mL of LB medium were then inoculated with 1.25 mL each of

the remaining overnight culture. This was incubated at 37°C with vigorous shaking for

1.5 hours, at which point IPTG (isopropylthio-β-D-1-galactoside; Sigma) was added for a

final concentration of 0.5 mM. IPTG inactivates the *lac* repressor and leads to induction

of the lytic operon resulting in an increase of the copy number of the plasmid from a

single copy per cell to approximately 20 copies per cell. Because amplification in the

presence of IPTG can lead to instability in recombinants carrying repetitive sequences of

genomic DNA, cultures are induced for only a short period of time. After incubation for

an additional 5 hours, the culture was divided into 30 mL aliquots and centrifuged at

10,000xg (8000 rpm in Sorvall Super T21 with SL-50T rotor; Kendro) for 10 minutes. The cell pellet could be frozen at this step without damage to the PAC plasmid.

Each cell pellet was completely resuspended in 1 mL of GTE buffer (50 mM glucose, 10 mM EDTA, 5 mM Tris-Cl, pH 8.0), followed by the addition of 1.5 mg of lysozyme. Lysozyme hydrolyzes the 1,4-β links between *N*-acetylmuramic acid and *N*-acetyl-D-glucosamine, found in the cell walls of certain bacteria. After incubation at RT for 5 minutes, 2 mL of freshly made 1% SDS/0.2 M NaOH solution was added to open the bacterial cell wall, denature chromosomal DNA and proteins, and release plasmid DNA into the supernatant. The solution was inverted gently, as the PAC clones are large enough to be sensitive to shearing, followed by incubation on ice for 5 minutes. To return the solution to neutral pH and precipitate the SDS-coated complexes, 1.5 mL of 3 M KAc (60 mL 5 M KAc, 11.5 mL glacial acetic acid, 28.5 mL ddH$_2$O) was added, the tube was sealed with parafilm and mixed gently by inversion. After incubation on ice for 5 minutes, the precipitated bacterial debris was pelleted by centrifugation at 8000 rpm for 10 minutes.

The supernatant was transferred to a new tube and RNase A (Sigma) was added for a final concentration of 50 μg/mL. RNase A cleaves at the 3' side of uracil or cytosine phosphate bonds. After incubation at 37°C for 60 minutes, an equal volume of phenol:chloroform:isoamyl alcohol (25:24:1) was added to remove proteins from the nucleic acids. The combination of phenol and chloroform, both of which denature

110

proteins, results in more efficient removal of proteins. In addition, chloroform facilitates the separation of the aqueous and organic phases, and the isoamyl alcohol reduces foaming during extraction. The mixture was inverted 10 times then centrifuged at 3250 x g (3000 rpm) for 20 minutes. The upper aqueous phase was transferred into a new tube and an equal volume of chloroform:isoamyl alcohol (24:1) was added to remove residual phenol. The inversions and centrifugation was repeated. The upper aqueous phase was again reserved, and the DNA was precipitated by the addition of an equal volume of isopropanol. The DNA was pelleted by centrifugation at 8000 rpm for 10 minutes, rinsed twice in 70% ethanol, allowed to air dry and resuspended in 100 μL of ddH$_2$O.

b. *Concentration of Nucleic Acids*

In certain cases, it is necessary to have nucleic acids at a specific concentration. For example, the RNA for Northern blot analysis needed to be at least 2 μg/μL in order to load 10 μg into the wells of the formaldehyde-agarose gel. Concentration of the RNA was accomplished by spin dialysis through a porous membrane using Microcon YM-3 (Millipore, Bedford, MA). During this spin dialysis protocol, the RNA solution to be concentrated is centrifuged through a hydrophilic, nonabsorbent, porous membrane. Macromolecules larger than the pores are retained in the upper reservoir, and concentrated to the desired volume. A Microcon YM-3 cartridge, which retains single-stranded nucleotides larger than 10 bases, was placed in one of the two vials provided. The desired microgram amount of nucleic acids was placed in the cartridge and the vial was centrifuged at 14,000 x g (11,000 rpm in Eppendorf Centrifuge 5417R; Brinkmann

111

Instruments, Inc., Westbury, NY) until the desired volume was obtained. The reservoir

was removed from the vial, inverted into a new vial and centrifuged at 1000 x g (3000

rpm) for 2 minutes to recover the concentrated nucleic acids.

4. Isolation of Proteins

a. *Protein Collection from Cultured Human Cell Lines*

Three different timed collections were performed. Cell cultures of the normal

colon epithelial cell line, CRL-1831, and the colon cancer cell line, DLD-1, were

changed to serum-free media when approximately 70% confluent (pre-confluent), 90%

confluent (confluent) and four days past confluency (post-confluent). Media was

removed, rinsed once with 1 x PBS and replaced with 3 mL of serum-free media for a T-

25 flask. Serum-free media was made using the appropriate media and all the additives

normally used except for fetal bovine serum. The proteins were collected after three days

in serum-free media. For each time point, proteins were collected from the conditioned

cell media (CCM), the extracellular matrix (ECM) and the cell layer (CL), following the

protocol of Debeer et al, 2002.

For the CCM collection, media was removed and placed immediately on ice with

15 µL of protease inhibitor cocktail (104 mM AEBSF, 80 µM Aprotinin, 2.1 mM

Leupeptin, 3.6 mM Bestatin, 1.5 mM Pepstatin A, 1.4 mM E-64 (Sigma)). The protease

inhibitor cocktail is optimized for mammalian tissues and contains a mixture of protease

inhibitors with a broad specificity for the inhibition of serine, cysteine, aspartic and

aminopeptidases. From this, 500 µL was saved for Bradford quantitation, and the remainder was divided equally into three microfuge tubes. The volume of media was noted and to this, 10 µL of StrataClean Resin (Stratagene, La Jolla, CA) was added to bind and concentrate the proteins. This was rocked on a platform for 30 minutes at 4°C, and then centrifuged in a microcentrifuge at maximum speed for 1 minute. The supernatant was removed to another tube, 20 µL of 2x Laemmli buffer (120 mM Tris-HCl, pH 6.8, 20% glycerol, 200 mM DTT, 4% SDS, 0.05% bromophenol blue) was added to the StrataClean Resin and the proteins were stored at -20°C until needed.

For the ECM collection, after the media was removed from the flask, the cells were rinsed with 1x PBS, and then 1.5 mL of 10 mM EDTA was added. The flask was allowed to rock for 5 minutes at RT, then the solution was collected and placed on ice. From this, 160 µL was saved for Bradford quantitation and the remainder was divided equally into two microfuge tubes. The volume was noted and to this, 10 µL of Strata Clean Resin was added. The samples were then processed similarly to the CCM samples.

For the CL collection, 1 mL of Mammalian Protein Extraction Reagent (M-PER, Pierce, Rockford, IL) with 26 µL of protease inhibitor was added to the cell layer after removal of the EDTA solution. M-PER contains a unique detergent that dissolves cell membranes at low concentrations for complete cell lysis without protein denaturation. The flask was allowed to rock for 5 minutes at RT until all cells were in suspension. The solution was agitated by pipetting, collected, and then centrifuged at maximum speed for

5 minutes. The supernatant was transferred to a microfuge tube, and 20 μL of 2x

Laemmli buffer was added to the insoluble pellet. Both soluble and insoluble fractions

were stored at -20°C until needed.

The supernatant from the CCM and ECM collections after treatment with

StrataClean Resin was subject to acetone precipitation in case the resin did not bind to the

LOXL2 protein. An aliquot of 300 μL of supernatant was mixed with 1.2 mL (4 volumes)

of acetone that had been prechilled to -20°C. The mixture was incubated for 1 hour at -

20°C, and then centrifuged at 18,000 x g (14,000 rpm in the Beckman Microfuge 18

Microcentrifuge) for 10 minutes. The supernatant was discarded, the pellet was allowed

to air dry then was resuspended in 10 μL of 2x Laemmli buffer, noting the final volume.

b. *Bradford Quantitation of Proteins*

Bovine serum albumin (BSA) was dissolved in 1x PBS to make protein standards

of concentrations 5, 10, 15, 20 and 25 μg/mL. In a 96-well plate, 160 μL of each of the

protein standards, in addition to 1 x PBS alone, were prepared in triplicate wells resulting

in wells with 0, 0.8. 1.6, 2.4, 3.2 and 4.0 μg of protein. Triplicate wells of 160 μL each

were also prepared from the reserved CCM and plain cell media used to grow the cells. A

single well of 160 μL was prepared for the reserved ECM, and triplicate wells of 2 μL

each of soluble CL were prepared with 158 μL of ddH2O. To each of the wells, 40 μL of

Bio-Rad Protein Assay Dye Reagent Concentrate (Hercules, CA) was added. The Bio-

Rad protein assay is based on the Bradford dye-binding procedure. Coomassie Brilliant

114

Blue G-250 is a triphenylmethane dye that forms strong but not covalent complexes with the basic and aromatic amino acids in protein. Uptake of dye by protein results in a color change to blue, detected by absorbance at wavelength 600 nm. The intensity of color change is proportional to the amount of proteins with molecular weight greater than 3,000-5,000, and thus the proteins in solution can be quantitated against the protein standard. The plate was incubated for at least 5 minutes at RT, and then absorbance was measured using the Polarstar Optima plate reader (BMG Labtechnologies, Durham, NC).

To determine the protein concentration of the samples, the average OD value of each of the protein standards were inputted with the known µg amount of protein in order to produce a protein assay standard curve utilizing the GraphPad Prism 3.0 program (GraphPad Software, Inc., San Diego, CA). The average OD of the unknown samples was compared to the protein standard curve and the estimated protein amounts were calculated by the program. For the CCM collection, the concentration of the protein was determined by subtracting the estimated protein amount of the plain media from the CCM. To calculate the concentration of the StrataClean Resin-purified protein, the adjusted CCM value and the unadjusted ECM protein amount was divided by 160 µL to calculate the amount of protein per µL of solution, then multiplied by the volume of the CCM or ECM in each tube prior to the addition of the StrataClean Resin for the total amount of protein per tube. This value was then divided by 30 µL to determine the final protein concentration per µL. For the soluble CL, the estimated protein amount was

halved to determine the protein concentration per μL. The protein concentration of the insoluble CL could not be determined.

5. Sequence Analysis

Sequence analysis was performed as described in II.B.8.c-d utilizing 32.5 fm of isolated PAC DNA and the primer LOXL2-ms1: GCT GAG TAC AGA CGC TGA TGC.

6. *Characterizing the LOXL2 Microsatellite for Loss of Heterozygosity Analysis*

Concurrent to this dissertation work, sequence analysis of PAC 17460 identified a microsatellite within intron 4. The area flanking the microsatellite was sequenced to design primers to PCR amplify this marker for loss of heterozygosity analysis. The sequences of the primers are as follows: LOXL2-ms1 (GT strand): GCT GAG TAC AGA CGC TGA TGC; LOXL2-ms2 (CA strand): GGT GAT GAG TGA TCG ACG GTC. End-labeling of primers was performed as described in II.B.4.b. The PCR reaction was performed as described in II.B.4.c except that the final nucleotide concentration was 124 μM. The thermocycle profile was an initial denaturation of 94°C for 3 minutes, 30 cycles of denaturing at 94°C for 30 seconds, annealing at 55°C for 30 seconds and extension at 72°C for 30 seconds, followed by a final extension of 72°C for 7 minutes. The PCR products were subject to denaturing polyacrylamide gel electrophoresis, autoradiography, quantitation and evaluation as described in II.B.4.d-f.

7. cDNA Array Analysis

The human LOXL2 cDNA clone used in this study was previously described (Jourdan-Le Saux et al, 1999) and was created by PCR-amplification of a 1.36 kb cDNA fragment which was cloned into a kanamycin-resistant plasmid, transformed into *E.coli* and stored as glycerol stocks in -80°C. The frozen glycerol stock was streaked onto LB-kanamycin (50 µg/mL) plates and incubated overnight at 37°C. Individual colonies were picked the following day and inoculated into 3 mL of LB-kanamycin media, and placed in a 37°C incubator-shaker overnight to stationary phase. The plasmid was isolated by the WIZARD mini-prep kit as described in II.B.3.d, then digested with *Eco*RI and *Kpn*I in NEB I Buffer (New England Biolabs, Inc., Beverly, MA). Isolation, purification and random-labeling of the cDNA probe were performed as described in II.B.5.b-d. Hybridization of the LOXL2 cDNA probe to the Matched Normal/Tumor Expression Array (Clontech), and subsequent phosphorimage analysis was performed as described in II.B.5.e-f.

8. Northern Blot Analysis

A Northern blot of RNA isolated the esophageal cancer cell lines WHCO1, WHCO3, WHCO5 and WHCO6, derived from primary squamous cell carcinoma, was received from University of Cape Town, South Africa. A Northern blot of the cell lines described in III.B.2.a was made and analyzed as follows.

a. *Preparation of Samples*

Total RNA was isolated from the normal cell lines derived from colon epithelia

(CRL-1831) and smooth muscle (myo), and from the cancer cell lines derived from colon

adenocarcinoma (DLD-1, HCT-116 and HCT-15), osteosarcoma (hos) and *ras*-

transformed hos (ras), using the protocol as described in II.B.3.c. After quantitation of the

isolated RNA as described in II.B.3.e, the samples, if needed, were concentrated using

spin dialysis as described in III.B.3.b to achieve a concentration of 2 μg/μL.

b. *Formaldehyde agarose gel electrophoresis*

Northern analysis is used to measure the amount and size of transcribed RNAs

from eukaryotic genes and to estimate their abundance. All apparatus used were treated

with RNase Away (Molecular BioProducts, Inc., San Diego, CA) and rinsed with DEPC-

treated ddH$_2$O before use. Agarose gels were prepared in a total volume of 100 mL with

1 x MOPS (20 mM 3-(N-morpholino)propanesulfonic acid) buffer and an agarose

concentration of 1.2%. Although Tris is an excellent buffer for standard agarose and

acrylamide gel electrophoresis, it is a primary amine and cannot be used with

formaldehyde. Formaldehyde forms unstable Schiff bases with the imino group of

guanine residues, and maintains RNA in the denatured state by preventing intrastrand

base pairing. The agarose and buffer were microwaved until completely dissolved. When

cooled to approximately 50°C, 5.1 mL of 37% formaldehyde was added for a final

concentration of 2.2 M, accounting for evaporation. The high concentration of

formaldehyde compensates for loss of formaldehyde by diffusion into the gel during

electrophoresis. The gel was poured into a sealed gel platform with gel comb, and allowed to sit for 1 hour. The gel was placed in an electrophoresis tank with enough 1 x MOPS buffer to cover the gel to a depth of 1 mm.

Ten micrograms of total RNA from each sample were mixed with 3 volumes of RNA loading buffer (50% deionized formamide, 2.2 M formaldehyde, 1 x MOPS buffer, 0.03% bromophenol blue, 0.03% xylene cyanol, 20 µg/ml ethidium bromide). The formamide in the loading buffer eliminates secondary structures in single-stranded RNA and allows for migration rate through agarose gels that is proportional to the $\log_{10}$ of its size, and the formaldehyde in the gel maintains RNA in its denatured state. Ethidium bromide is added to the sample instead of the gel as formaldehyde-agarose gels containing ethidium bromide emit a pinkish-purple glow when exposed to UV light that prevents visualization of RNA bands. The samples were denatured at 80°C for 5 minutes then placed on ice for 5 minutes before loading. Electrophoresis was carried out at 25V until both xylene cyanol and bromophenol blue had migrated into the agarose, then increased to 100V for the remainder. After electrophoresis, the gel was photographed with a ruler under ultraviolet light using Polaroid 667 film. The location of the RNA ladder was marked with punctures through the agarose by a 22-gauge syringe needle.

c. *Transfer of RNA to Solid Support*

The gel was hydrolyzed by shaking immersion twice in a solution of 50 mM NaOH for 15 minutes at RT. Alkaline treatment of the gel partially hydrolyzes the RNA

119

and increases the speed and efficiency of transfer of RNAs larger than 2.3 kb. At this point, it is possible to transfer as nucleic acids in alkaline solution become covalently fixed to charged nylon membranes. However, alkaline transfer can generate a high level of background, so following alkaline treatment, the gel was neutralized by shaking immersion twice in a solution of 0.5 M Tris-HCl, pH 7.5; 1.5 M NaCl for 15 minutes at RT. The Hybond-N+ membrane was soaked in 10 x SSC for 10 minutes. The RNA was transferred overnight by upward capillary transfer, then irreversibly bound to the membrane by UV cross-linking using identical methodology as described in III.B.5.b.

d. *Hybridization of cDNA probe to Northern Blot*

The LOXL2 probe was prepared as described in III.B.5.d. The membrane was prehybridized for two hours at 42°C with ExpressHyb solution. The LOXL2 cDNA probe was thoroughly mixed with another aliquot of ExpressHyb solution, then used to replace the prehybridization solution. Following overnight hybridization, the membrane was washed four times in 2x SSC, 0.05% SDS for 10 minutes each at RT, then twice in 0.1x SSC, 0.1% SDS at 50°C for 20 minutes each. The membrane was then sealed in a Seal-a-meal bag and placed in a phosphor cassette. Following phosphorimage analysis as described in II.B.5.f, the probe was allowed to decay until undetectable by phosphorimage analysis and reprobed with a GAPDH cDNA fragment (Clontech).

120

9. Western Blot Analysis

a. *SDS-Polyacrylamide Gel Electrophoresis*

Electrophoresis of proteins requires conditions that ensure dissociation of the proteins into their polypeptide subunits. The strongly anionic detergent SDS is used in combination with a reducing agent (DTT) and heat to dissociate the proteins prior to electrophoresis. The denatured proteins bind SDS and become negatively charged, and because the amount of SDS bound is almost always proportional to the molecular weight of the polypeptide independent of sequence (about 1.4 g of SDS per 1 g of polypeptide), SDS-polypeptide complexes migrate through polyacrylamide gels based on size. However, modifications to the polypeptide backbone, such as glycosylation, have significant impact on the apparent molecular weight and are not a true reflection of the mass of the polypeptide chain.

SDS-PAGE is carried out with a discontinuous buffer system in which the running buffer and the buffer within the gel are of different pH and ionic strength. The sample and the stacking gel contain Tris-Cl, pH 6.8, the running buffers contain Tris-glycine, pH 8.3, and the resolving gel contains Tris-Cl, pH 8.8. The chloride ions in the sample and stacking gel form the leading edge of the moving boundary, and the trailing edge is composed of glycine molecules. Between the leading and trailing edges of the moving boundary is a zone of lower conductivity and steeper voltage gradient. The polypeptides migrate in this zone, through the stacking gel of high porosity, and are deposited in a very thin zone on the surface of the resolving gel. In the resolving gel, the

higher pH causes ionization of glycine which migrates through the stacked polypeptides and travels through the resolving gel immediately behind the chloride ions. Freed from the moving boundary, the SDS-polypeptides migrate through the resolving gel in a zone of uniform voltage and pH, and a separated according by size through molecular sieving determined by concentration of polyacrylamide and ratio of acrylamide:bis-acrylamide.

A pair of 10 x 10.6 cm glass plates, one notched and one square, were thoroughly cleaned and dried with Kimwipes. The gel plates were placed together with the clean sides facing inwards, with spacers measuring 1.0 mm thick, and the glass sandwich was placed in the gel frame of the Hoefer miniVE vertical electrophoresis system (Amersham Pharmacia Biotech) with the notched plate facing the buffer chamber, and clamped into place. After ensuring that the bottom of the sandwich was flush with the guide feet, the bottom sealing plate was placed in the closed position and placed upright on the bench.

The 8% resolving gel mixture, which is able to resolve proteins of sizes 30-120 kDa, was made of 3.75 mL of 40% polyacrylamide (29% acrylamide:1% bis acrylamide), 3.8 mL of 1.5 M Tris, pH 8.8, 150 μL of 20% SDS, 150 μL of 10% APS and 6 μL of TEMED in a final volume of 15 mL for two gels. The acrylamide solution was poured into the gap between the two plates, and was immediately overlaid with 1 mL of ddH20 and rocked back and forth 8-10 times. The water overlay prevents oxygen from diffusing into the gel and inhibiting polymerization, and the rocking ensures even distribution for a smooth, linear resolving surface. The gel frame was placed in an upright position and

allowed to polymerize for 45 minutes. After polymerization was complete, the water

overlay was poured off into a Kimwipe wick. The 5% stacking gel mixture was made of

622 μL of 40% polyacrylamide (29:1), 630 μL of 1.0 M Tris, pH 6.8, 50 μL of 20% SDS,

50 μL of 10% APS and 5 μL of TEMED in a final volume of 5 mL for two gels. The

stacking gel mixture was poured over the polymerized resolving gel and the comb was

inserted completely. The depth of the stacking gel should be the length of the teeth plus 1

cm. The gel was placed in an upright position and allowed to polymerize for 1 hour

before use. After polymerization was complete, the comb was removed, the bottom

sealing plate was placed in the open position, and the gel frame was placed in the

electrophoresis tank. The tank and upper buffer chamber was filled with 1x Tris-glycine

electrophoresis buffer (25 mM Tris, 250 mM glycine, pH 8.3, 0.1% SDS).

SDS-polyacrylamide gels are not prerun prior to loading samples as this

procedure would destroy the discontinuity of the buffer systems. Each of the samples

were placed in new microfuge tubes: for the CCM samples treated with StrataClean

Resin, 3 μg of protein was prepared; for the ECM samples treated with resin, 7.5 μg was

prepared; for the insoluble CL samples, 5 μL was prepared; for the acetone-precipitated

CCM and ECM samples, 10 μL was prepared; and for the soluble CL samples, 10 μg of

protein with 10 μL of 2x Laemmli buffer was prepared. The samples were boiled for 5

minutes then immediately placed on ice. The samples were loaded on the gel, avoiding

the last lane on either end, which was loaded instead with 2x Laemmli buffer to prevent

gel distortion, and run at 13 mA per gel until the bromophenol blue had run off the gel.

b. *Transfer of Protein to Solid Support*

Electrophoretic transfer of the proteins from the gel to a solid support was accomplished using the "semi-dry" method. In this method, the gel is sandwiched horizontally between the membrane and Whatman 3MM paper saturated with transfer buffer as a reservoir. The direct contact with the electrodes yields high field strengths and rapid transfer. Polyvinylidene fluoride (PVDF) membrane is mechanically strong and binds proteins six-fold more tightly than nitrocellulose. Unlike nylon, there is less background and proteins immobilized on PVDF can be seen with standard stains.

For each gel, two sheets of Whatman 3MM paper and two sheets of Protean XL extra-thick blot paper (Bio-Rad) was cut to dimensions 7.5 x 8.5 cm. Immobilon-P PVDF membrane (Millipore) was cut to dimensions 7.3 x 8.3 cm. The membrane was equilibrated by soaking in methanol for 30-60 seconds, followed by 2-3 washes in ddH_2O over 2 minutes and at least 5 minutes in transfer buffer (48 mM Tris, 39 mM glycine, 0.037% SDS, 20% methanol). One sheet of blot paper was soaked completely in transfer buffer then placed on the bottom anode plate of the Transblot SD semi-dry transfer system (Bio-Rad). One sheet of Whatman paper, also soaked in transfer buffer, was placed on the blot paper, followed by the equilibrated membrane, ensuring that there were no bubbles between any of the layers. The gel frame was disassembled and the glass plates were pried apart such that the gel adhered to one plate. With a razor blade, the stacking portion of the gel was removed and the sides of the gel were removed such that it fit within the dimensions of the membrane. A small volume of transfer buffer was

added to the membrane to ensure that it was moist, then the gel was pried off the glass

plate with the razor blade and allowed to drop onto the membrane. The gel was quickly

adjusted so that it was centered on the membrane, then the other sheet of Whatman paper

was soaked in transfer buffer and placed on the gel. The other sheet of blot paper, also

soaked in transfer buffer, was placed over the Whatman paper, and any excess buffer

surrounding the sandwich was removed. The upper cathode plate of the Transblot was

placed on the sandwiches, followed by the Transblot cover. The proteins were allowed to

transfer for about 75 minutes at 10 V and 1 mA /cm^2 surface area contacting the plate.

While the proteins were transferring, at least 50 mL of blocking reagent (1 x PBS

(137 mM NaCl, 4.3 mM Na$_2$HPO$_4$•7H$_2$O, 2.7 mM KCl, 1.4 mM KH$_2$PO$_4$) with 5%

wt/vol non-fat dry milk (Carnation, Nestle Food Company, Glendale, CA) and 0.2%

Tween-20 (Fisher Scientific)) per blot was prepared. The blocking reagent prevents non-

specific adsorption of the immunological reagents to the membrane by the binding of

milk protein to the areas of the blot where no protein is present. The Tween-20 detergent

prevents protein aggregation. The blocking reagent was placed on a stir plate for at least

one hour to ensure that the dry milk was completely dissolved to prevent increased

background on the blot. After transfer of proteins, the blots were notched at one corner

for orientation, then placed in a container with 30-40 mL of the blocking reagent and

placed on a shaker. If more than one blot was placed in the container, the blots were

placed back-to-back. The remainder of the blocking reagent was placed at 4°C. After the

blots were allowed to block for at least one hour at RT, the blots could be stored overnight at 4°C or probed immediately for detection of target protein.

c. *Detection of LOXL2 Protein*

During the entire probing and detection process, the blots were not allowed to dry at any time. The blocking reagent was removed from the blots with 5 brief washes with ddH$_2$O, ensuring that the ddH$_2$O was not poured directly on the membrane that would remove some of the bound milk proteins and cause increased background. The ddH$_2$O was added to the container, swirled around and removed. Following the five washes, the blots were placed in 1 x PBST (1 x PBS with 0.2% Tween-20) and placed on a shaker for at least 5 minutes at RT. Each blot was then placed in a small container of dimensions similar to the blot, and the primary antibody solution was added. The primary antibody solution was prepared by diluting the reserved blocking reagent with 1 x PBST such that the final solution was 2.5% milk. For each blot, 10 μL of the LOXL2 antibody was added to 10 mL of the prepared solution for a final antibody dilution of 1:1000. The remainder of the 2.5% milk-PBST solution was stored at 4°C.

The LOXL2 antibody was designed against the C-terminal end sequence EHFSGLLNNQLSPQ. The polyclonal antibody was made by Sigma Genosys (The Woodlands, TX) and consisted of collection of pre-immune serum from two New Zealand White Rabbits, 4 immunizations with the peptide antigen prior to the first production bleed, an additional immunization prior to the second production bleed. Each

antibody collection was affinity purified against the peptide by the company. Prior to use for experimental purposes, the antibody was tested against *in vitro* expressed full length LOXL2 and LOXL3 constructs, and was shown to specifically recognize LOXL2.

The blots in primary antibody solution were placed on the shaker at low speed for at least 1 hour at RT. The blots were then placed in a larger container and the primary antibody solution was removed by five brief washes in ddH$_2$O and one wash in 1 x PBST for at least 5 minutes at RT with agitation as described above for removal of blocking solution. The blots were placed back in the small containers, and the secondary antibody solution was added. The secondary antibody solution was prepared by adding 2 μL of secondary antibody (provided in the ECL Plus Western Blotting Reagent Pack, Amersham Biosciences UK, Buckinghamshire, England) in 10 mL of the solution consisting of 2.5% milk in 1 x PBST for a final dilution of 1:5000. The secondary antibody recognizes rabbit proteins, including the primary antibody that was generated in rabbits, and is conjugated to horseradish peroxidase (HRP) for detection purposes.

The blots in secondary antibody solution were placed on the shaker at low speed for exactly 1 hour at RT. The blots were then placed in a larger container and the secondary antibody solution was removed by five brief washes in ddH$_2$O and one wash in 1 x PBS for at least 5 minutes at RT with agitation. The blots were removed from the 1 x PBS, and 5 mL of detection solution was applied directly to each membrane and allowed to incubate for 1 minute at RT. The ECL Western Blotting Detection Reagent

(Amersham Biosciences UK) was prepared immediately before use by combining 2.5 mL

each of Detection Reagent 1 and Detection Reagent 2 for each blot. One solution contains

hydrogen peroxide and the other contains luminol. Working quickly to capture maximum

signal, excess solution was removed and the membranes were then arranged between the

leaves of a sheet protector, placed in a cassette and exposed to Kodak X-OMAT AR film

overnight. The film was processed as described in II.B.4.e.

The HRP that is conjugated to the secondary antibody, catalyzes the transfer of

two electrons from peracid to hydrogen peroxide, to generate H_2O and an oxidized

enzyme form. The subsequent oxidation of luminol yields an excited form of 3-amino-

phthalate. As this compound returns to ground state, blue light is emitted at 428 nm and

this chemiluminescent reaction can be captured on X-ray film. Enhancers in this reaction

increase the quantity and duration of light emitted in this otherwise low-efficiency

reaction to make it several fold more sensitive than radioactive detection methods.

Intense bands can be detected within seconds, while fainter bands need longer exposure.

10. Immunohistochemical Analysis

a. *Description of Slides*

Human tissue microarray slides containing formalin-fixed, paraffin-embedded

tissue sections from colorectal cancer, esophageal cancer, normal colon and rectum, and a

test array slide with a variety of normal and cancer tissues were obtained from

Superbiochips Labs (South Korea) through Imgenex Corporation (San Diego, CA).

128

Paraffin-embedded tissue sections of normal esophagus tissue as well as esophageal cancers demonstrating LOH of the LOXL2 gene were obtained from University of Cape Town, South Africa.

The colon tumor array slide contained 56 adenocarcinoma samples. The composition of the panel was 35.7% female and 64.3% male, with an age range of 35-78 years of age and an average age of 56.7 years of age with a standard deviation of 11.0 years. The composition by site was 33.9% right (proximal) colon, 14.3% transverse colon and 51.8% left (distal) colon. The composition of the colon tumor panel by stage was 46.4% stage II, 44.6% stage III and 9% stage IV; and by pathology was 8.9% mucinous, 3.6% poorly differentiated, 64.3% moderately differentiated and 23.2% well differentiated.

The esophageal tumor array slide contained 50 squamous cell carcinoma samples. The composition of the patient panel was 8.0% female, 90.0% male and 2.0% not reported, with an age range of 42-75 years of age and an average age of 59.0 years of age with a standard deviation of 8.1 years. The composition by stage was 32% stage II, 58% stage III, 4% stage IV and 6% not reported; and by pathology was 10% poorly differentiated, 54% moderately differentiated, 34% well differentiated and 2% not reported.

b. *Preparation of Slides*

Fixation and paraffin embedding of tissues allows for preservation of tissue and cell architecture, and archival for future studies. However, the strong chemicals involved in this process may modify amino acid side chains and eliminate the desired epitope, or modify proteins in the local environment of the target protein, preventing antibody access. To improve antibody detection on fixed, paraffin-embedded tissues, an antigen retrieval method was utilized after paraffin removal to attempt to expose antigens that would otherwise be masked. Antigen retrieval methods are designed to renature protein antigens and break local barriers to antibody access.

The paraffin-embedded slides were dried for 20 minutes in an Precision oven (Winchester, VA) at 60°C. The paraffin was then removed by 3 washes in fresh xylene for 10 minutes each. Multiple Coplin jars were used to simultaneously process the slides for each step. The tissues were then rehydrated by immersion through graded series of ethanol. Two washes each with 100% and 95% ethanol, and one wash with 70% ethanol were performed for 5 minutes per wash, followed by three 5-minute washes in 1x PBS, pH 7.4 (0.137 M NaCl, 0.0027 M KCl, 0.0119 M phosphates; Fisher Scientific). The slides were placed on a paper towel, and the excess PBS was removed from the margins of the slide by blotting with Whatman filter paper (Fisher Scientific).

To unmask antigens, the slides were immersed in 0.1 M Na citrate buffer, pH 6.0, and microwaved on high power for 5 minutes. More citrate buffer was added if

necessary, then the slides were microwaved on medium power for 5 minutes, followed by low power for 5 minutes. The slides were then immersed in cold 1x PBS, pH 7.4 to stop the antigen retrieval process. The slides were removed to a paper towel, and excess PBS was removed by blotting with Whatman filter paper.

c. Detection of LOXL2 Protein

Fluorescent methods of detection allows for high resolution but fade with time. Two materials were used to minimize this problem. First, Vectashield Mounting Media for Fluorescence (Vector Laboratories, Inc., Burlingame, CA) was used in the final mounting of slides to prevent rapid loss of fluorescence and photobleaching during microscopic examination, and to minimize fading during storage. Second, Alexa Fluor secondary antibodies (Molecular Probes, Inc, Eugene, OR) were chosen as it is brighter, much more photostable and has fluorescence independent of pH ranging from 4 to 10, in comparison to fluorescein. As the primary LOXL2 antibody was produced in rabbit, a secondary goat anti-rabbit IgG antibody was used. The rabbit-specific anti-IgG antibodies are raised against IgG heavy and light chains, affinity purified, adsorbed against the bovine, goat, mouse, rat and human IgG to minimize cross-reactivity, and labeled with an Alexa Fluor dye. Because the secondary antibody was produced in goat, normal goat serum was used to block the slides prior to incubation with the primary antibody.

The slides were placed in a chamber lined with wet paper towels. The sections were covered with 5% normal goat serum (NGS; Pierce) in 1x PBS for 30 minutes at RT.

The excess NGS was removed by blotting with Whatman filter paper, then the sections were covered with rabbit anti-human LOXL2 antibody diluted to 1:300 in 1% NGS, 1x PBS, for 2 hours at RT. The slides were washed three times in TPBS (0.1% Triton X-100 (Fisher Scientific) in 1x PBS) for 5 minutes each, blotted with Whatman paper, then placed into the moist slide chamber. The sections were covered with Alexa Fluor 488 labeled goat anti-rabbit IgG antibody diluted to 1:200 in 1% NGS, 1x PBS, for 45 minutes at RT. The slides were washed three times in 1x PBS for 5 minutes each, then blotted with Whatman paper. One drop of Vectashield mounting medium for fluorescence with DAPI (1.5 μg/mL) was placed in the center of the section. DAPI (4',6 diamidino-2-phenylindole) is a DNA counterstain that produces a blue fluorescence, and is incorporated into the mounting media. A premium cover glass (Fisher Scientific) was applied and the mounting media was allowed to disperse over the entire section. The cover glass was permanently sealed around the perimeter using non-clear nail polish.

c. *Evaluation of Slides*

The slides were evaluated with the Zeiss Laser Scanning Microscope LSM 5 Pascal (Carl Zeiss, Inc., Thornwood, NY). The DAPI was detected with excitation at 360 nm and emission at 460 nm. Alexa Fluor 488 was detected with excitation at 488 nm and emission at 518 nm. The slides of normal tissues were evaluated under 40x, 63x and 100x magnification. Images were captured using the LSM 5 Pascal software, version 3.0. The tumor tissue slides were evaluated under 63x magnification. The maximum number of LOXL2-expressing cells per field were recorded and scored as follows: 0: no LOXL2-

132

expressing cells noted; 1: 1-5 LOXL2-expressing cells/field; 2: 6-10 LOXL2-expressing cells/field; 3: 11-20 LOXL2-expressing cells/field; 4: 21-40 LOXL2-expressing cells/field; and 5: more than 41 LOXL2-expressing cells/field. The tumor specimens were also scored for auto-fluorescent elastic fibers as follows: -: complete absence of elastic fibers or presence of only scattered fine immature elastic fibers; +: presence of thick mature elastic fibers and scattered fine immature elastic fibers. Statistical analysis was performed using GraphPad Prism 3.0 (GraphPad Software Inc., San Diego, CA). Three way analysis was performed using Kruskal-Wallis test and two way analysis was performed using the Mann-Whitney test. A P value less than 0.05 was considered statistically significant.

C. RESULTS

1. Identification of a Polymorphic Microsatellite Marker Within the LOXL2 Gene

Concurrent to this dissertation work, sequence analysis of PAC clone 17460 (Jourdan-Le Saux et al, 1999) identified a partial sequence element of CA-dinucleotide repeats within intron 5 of the LOXL2 gene. This was the only CA-repeat identified by sequencing of exons 4-14 and all introns except intron 9 which was too large to be PCR amplified (Jourdan-Le Saux et al, 1999). Sequence analysis of the area flanking this microsatellite revealed a 22-dinucleotide repeat (Figure 3.1). A comparison of the sequence within the Genbank database at that time revealed that the microsatellite was a previously unidentified marker. A recent BLAST search revealed that it is currently an unnamed marker within the complete sequence of the human chromosome 8 clone RP11-
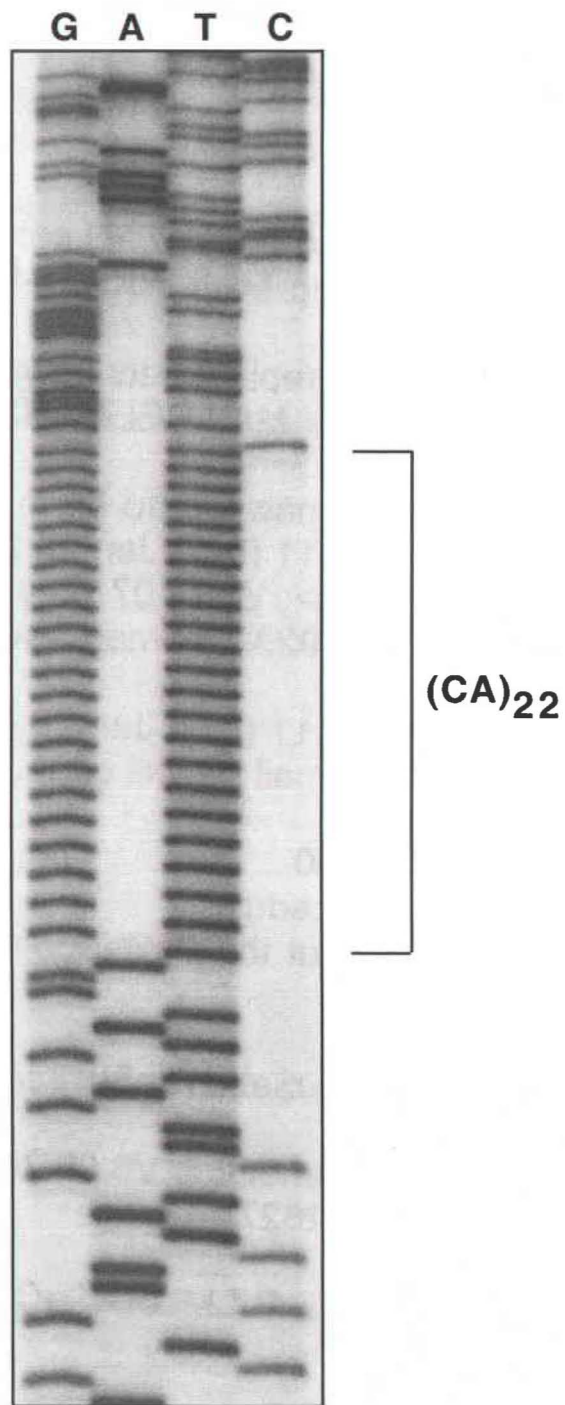
Figure 3.1. A CA dinucleotide repeat within intron 5 of the lysyl oxidase like-2 gene. Sequence analysis of PAC Clone 17460 revealed an allele of 22 CA repeats.

134

177H13. This microsatellite was found to be polymorphic in our populations of interest. Thirteen alleles were detected, with the number of repeats varying from 15 to 27 (Figure 3.2). Mendelian segregation of different alleles, without expansion, was confirmed in a 15-member, three generation Venezuelan population (CEPH#107).

2. Significant Loss of Heterozygosity in Colon and Esophageal Tumors

In the colon tumor panel, 14 patients (21.5%) were non-informative for the microsatellite marker within intron 5 of the LOXL2 gene. Of the individuals who were informative (51 patients), 33.3% (17 patients) demonstrated loss of heterozygosity (Figure 3.3a). An additional 15.7% (8/51) of informative patients demonstrated the presence of new alleles in their tumor DNA (MIN) (Figure 3.3b). In general, most (6/8) of the new alleles appeared to be shorter than their normal counterparts. As with the microsatellites utilized in the LOX study in Chapter II, males demonstrated a higher incidence of LOH: 47.3% in males and 25.9% in females; and a lower incidence of MIN at the LOXL2 marker: 5.3% in males and 22.2% in females (Figure 3.3).

No stage A tumors tested in this study demonstrated LOH, allelic imbalance or microsatellite instability. LOH and allelic imbalance associated with the LOX gene was observed in stage B and C. Individuals with stage D colon cancer were non-informative for this microsatellite marker. Tumors that demonstrated microsatellite instability were all stage B, and mainly (66%) located in the right colon.

135
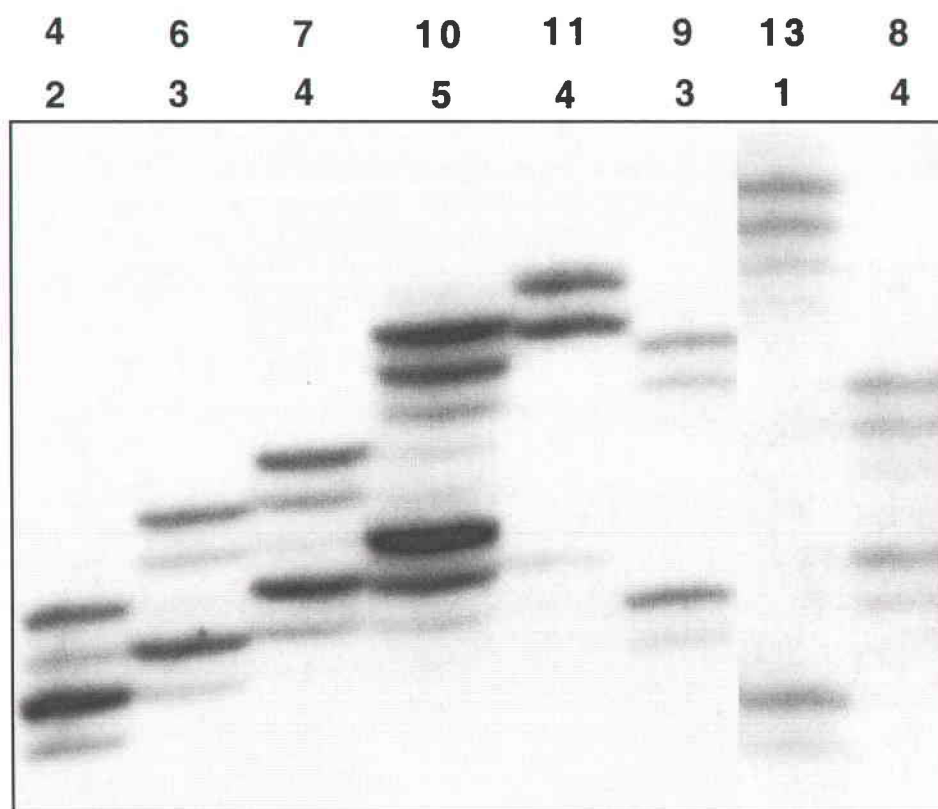
Figure 3.2. Characterization of the polymorphic nature of the LOXL2 microsatellite. Thirteen alleles of the LOXL2 microsatellite were observed in the colon and esophageal tumor panels.
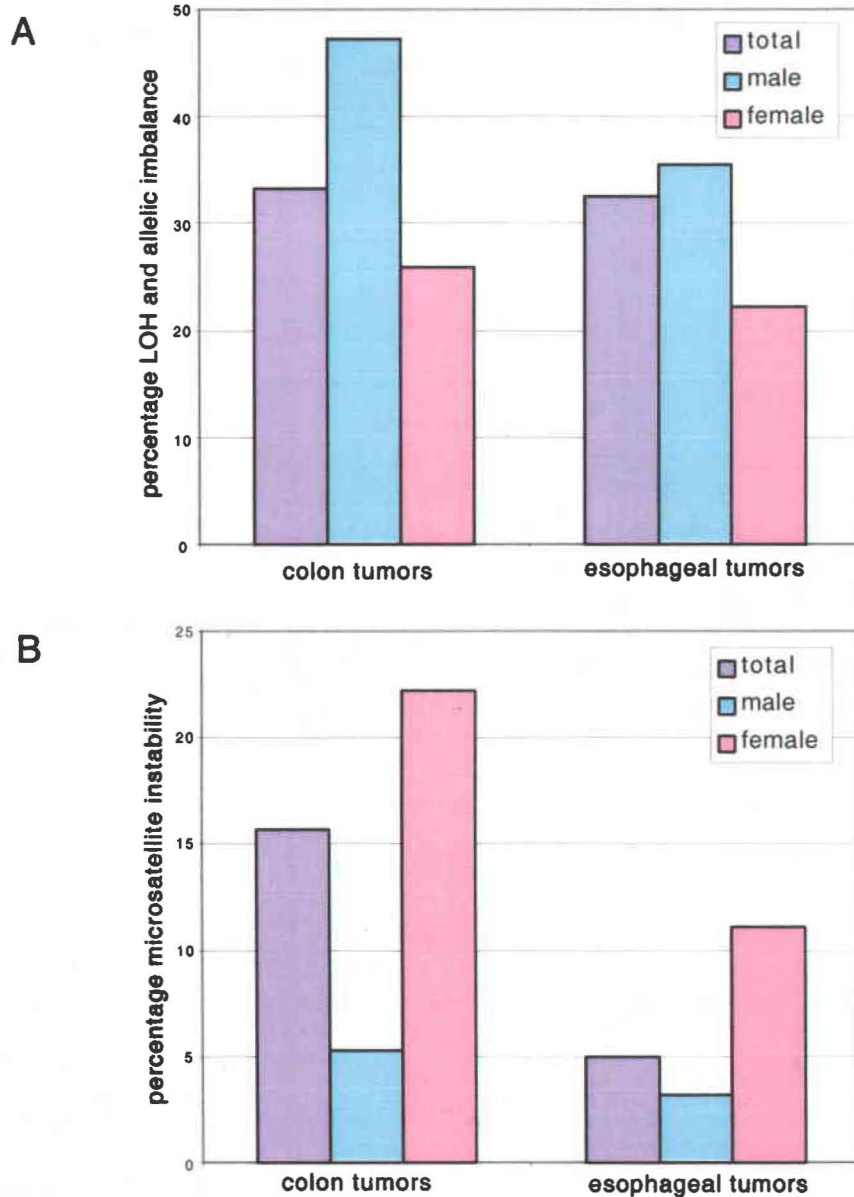
Figure 3.3. Microsatellite changes at the LOXL2 microstallite in colon and esophageal cancer. A. Significant LOH and allelic imbalance observed in tumor samples using a microsatellite within intron 5 of the LOXL2 gene. Males demonstrated higher incidence of LOH. **B.** Microsatellite instability within the LOXL2 gene. Females demonstrated higher frequency of MIN.

137

In the esophageal tumor panel, 22 patients (35.5%) were non-informative for the LOXL2 marker. Of the individuals who were informative (40 patients), 32.5% (13 patients) demonstrated loss of heterozygosity (Figure 3.3a). An additional 5% (2/40) of informative patients demonstrated the presence of new alleles (MIN) (Figure 3.3b). As with the colon tumor samples, males demonstrated a higher incidence of LOH: 35.5% in males and 22.2% in females, and a lower incidence of MIN: 3.2% in males and 11.1% in females (Figure 3.3).

No Stage 0 tumors were informative for this microsatellite marker. The one individual with a Stage 1 tumor had LOH, but no microsatellite changes were observed in Stage 2 tumors. Of the Stage 3 tumors, which made up 83% of the panel, 31% demonstrated LOH and 3% demonstrated MIN. Individuals with LOH and MIN composed 25% each of the Stage 4 patients.

3. LOXL2 mRNA Expression in Colon Tumor cDNA and Cultured Cell Lines

A matched normal/tumor cDNA array was hybridized to a LOXL2 cDNA radiolabeled probe to evaluate LOXL2 expression levels in tumors relative to matched normal colonic tissue. The array contained 11 matched samples, all of which were adenocarcinoma, except for one benign tumor. All of the normal colon samples demonstrated expression of LOXL2, and the expression levels were variable with an average deviation (average of the absolute deviations of the data points from their mean) 2.7 fold larger than the mean. When compared to their matched tumor sample, seven of

138

the samples had changes of expression from baseline less than 2 fold. Of the 4 samples

that demonstrated changes of more than two fold, three were less than four-fold (Figure

3.4). The one tumor sample that had nine-fold down-regulation of LOXL2 expression,

had much higher expression of LOXL2 in the matched normal sample compared to the

other normal colon samples. This wide variation in expression in the normal colon tissue

cDNA samples indicated that LOXL2 may be expressed only in certain cell types or in

certain histological regions of the colon. Therefore, to evaluate the expression

specifically in tumor cells, cultured human cell lines were used.

The normal fetal colon epithelial cell line CRL-1831 demonstrated detectable

LOXL2 mRNA expression, compared to the near absence of LOXL2 mRNA that was

observed in the three colon carcinoma cell lines tested, the HCT-116 colon carcinoma,

and the two adenocarcinoma cell lines, HCT-15 and DLD-1 (Figure 3.5). HCT-15 and

DLD-1 are from the same genetic origin as determined by DNA fingerprinting, but are of

different clonal origin based on marker chromosomes and numerical changes. LOXL2

mRNA expression was also detected in the control smooth muscle cell line (myo), and in

the human osteosarcoma (hos) cell line. The *ras*-transformed hos cell line (ras)

demonstrated a down-regulation in transcription compared to hos (Figure 3.5a).

However, all the esophageal squamous cell carcinoma cell lines as well as the normal

esophageal tissue expressed LOXL2 (Figure 3.5b).
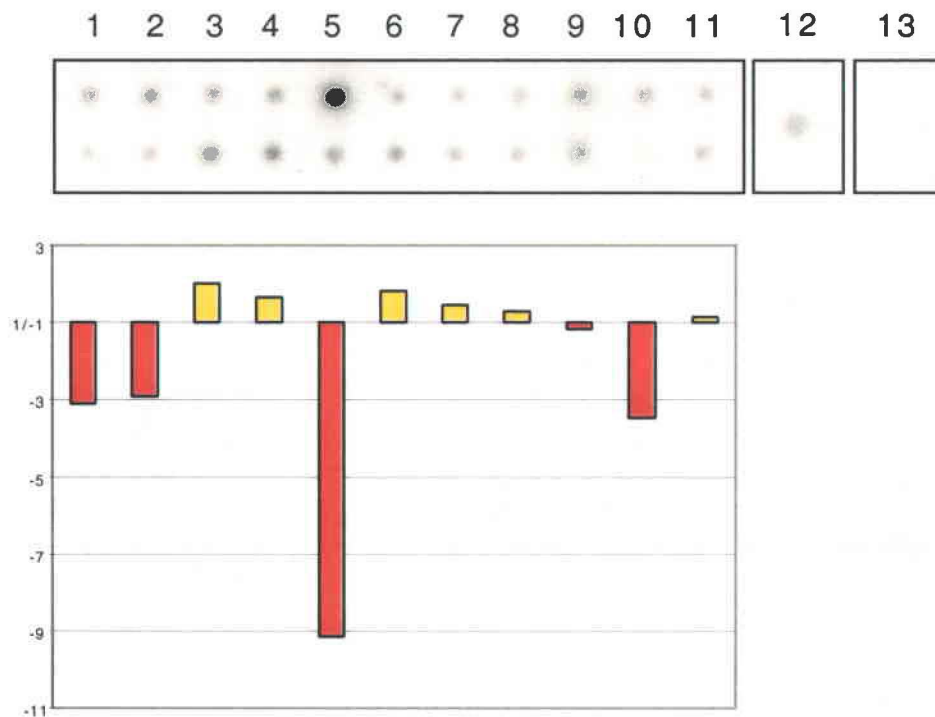
Figure 3.4. Reduced LOXL2 mRNA levels in matched normal and tumor tissue from colon. A Matched/Normal Tumor Expression Array (Clontech) was analyzed for LOXL2 mRNA expression. The upper row of samples 1-11 are from normal colon tissue and the lower row of samples are from matching colon tumors. Sample 1: benign tumor; samples 2-11: adenocarcinoma; sample 12: positive control of genomic DNA; sample 13: negative control of yeast total RNA. Patients of samples 2, 6 and 8 also had metastases. Samples 1-4, and 9 were from male patients. The bar graph demonstrates fold down-regulation (red) or up-regulation (yellow) of LOXL2 expression in colon tumor compared to its matched normal tissue.

140
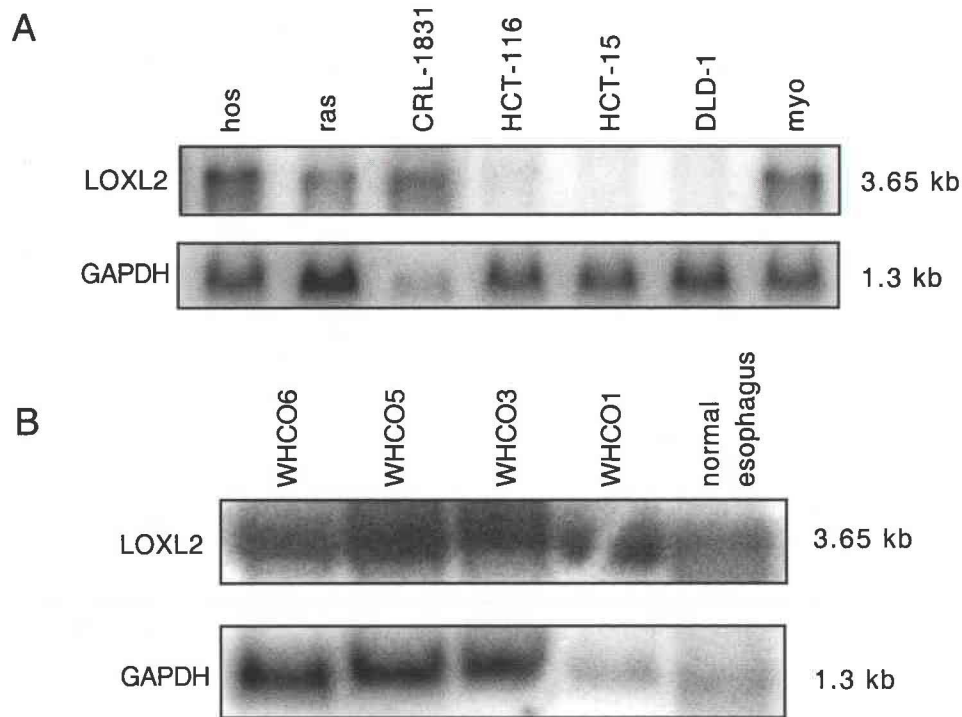
Figure 3.5. Northern blot analysis of LOXL2 mRNA expression in various human cell lines. A. A Northern blot containing 10 µg of total RNA isolated from cultured human osteosarcoma (hos), *ras*-transformed hos (ras), normal colon epithelial cells (CRL-1831), colon cancer (HCT-116, HCT-15, DLD-1) and smooth muscle (myo) cell lines. **B.** A Northern blot containing 5 µg of total RNA isolated from cultured human esophageal squamous cell carcinoma cell lines, WHCO6, WHCO5, WHCO3 and WHCO1, and from normal esophagus tissue. Both blots were hybridized to ^{32}P-labeled LOXL2 cDNA probe and GAPDH probe.

To confirm that the mRNA levels observed in the colon cell lines were consistent with protein expression, proteins were isolated from CRL-1831 and DLD-1 for Western blot analysis. Three collections from different stages of confluency were obtained as LOX protein expression in multiple cell types is detected by Western blot analysis only during post-confluency. The antibody designed against the C-terminal end of LOXL2 was shown to specifically recognize a LOXL2 construct (Figure 3.6). Expression of LOXL2 protein was detected in the StrataClean Resin-purified CCM and in the insoluble CL collection of CRL-1831 cells harvested at pre-confluency, confluency and post-confluency (Figure 3.7). There appeared to be no difference in the amount of LOXL2 protein expression at the different stages of confluency. No LOXL2 expression was detected in the CCM supernatant collection, either the StrataClean Resin-purified ECM or ECM supernatant collection, or in the soluble CL collection. Minimal, if any, LOXL2 expression was detected in DLD-1 cells.

Northern and Western blot analysis indicated loss of expression of LOXL2 in colon cancer cell lines compared to the normal colon epithelial cell line. LOXL2 expression was not lost in any of the esophageal squamous carcinoma cell lines evaluated. However, the use of the normal colon epithelial cell line, did not explain the wide variation in expression in normal colon samples as demonstrated by the cDNA array. To determine if other cell types or histological regions of the colon expressed LOXL2, the localization of LOXL2 protein expression in normal colon tissue as well as in normal esophageal tissue was evaluated.
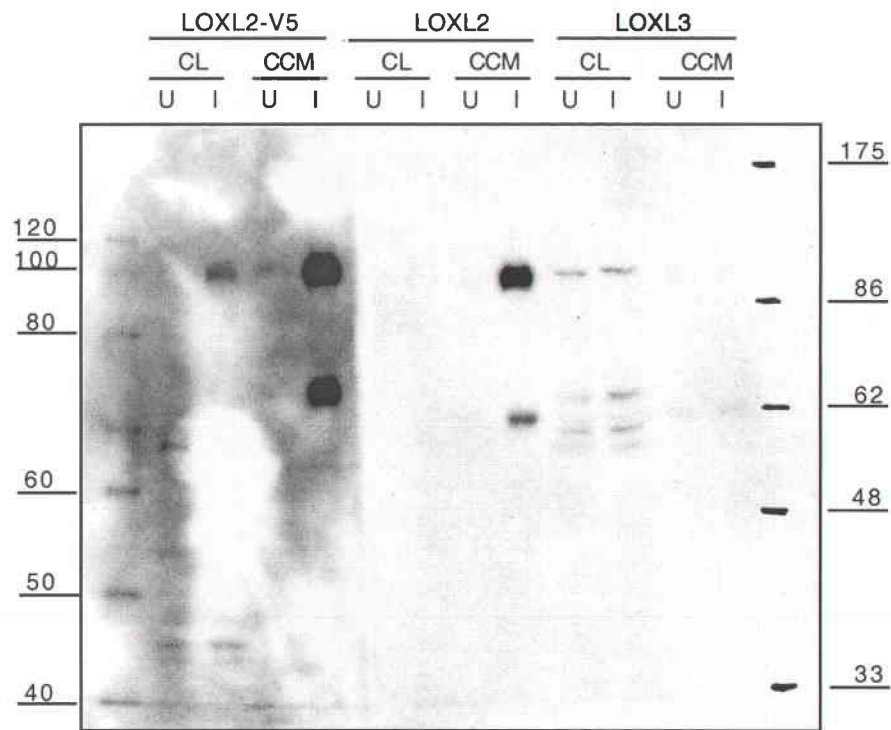
Figure 3.6. Specificity of the LOXL2 Antibody. Human LOXL2 and LOXL3

cDNA were cloned into pIND-V5-6His inducible mammalian expression vector

to generate either LOXL2 fused to a V5-6xHis epitope tag (LOXL2-V5) or full-

length LOXL2 OR LOXL3. Constructs were expressed in a human embryonic

kidney cell line (HEK 293-EcR) containing the inducible transcriptional activator.

The cells were uninduced (U) or induced for 24 hours (I). Proteins were collected

from the insoluble cell layer (CL) and cultured cell media (CCM). Presence of

the LOXL2-V5 construct was detected by a V5 antibody (1:5000). The LOXL2

antibody (1:2000) recognizes both the LOXL2 V5 and LOXL2 construct, but not

the LOXL3 construct. (Courtesy of Dr. Keith Fong)
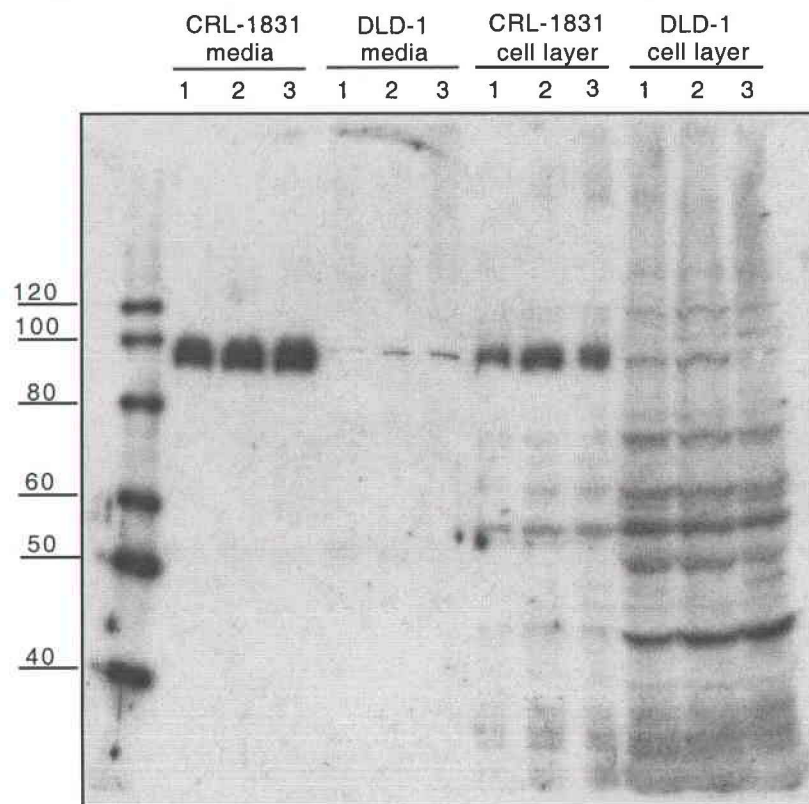
Figure 3.7. Western blot analysis of LOXL2 protein expression in human colon cell lines. Proteins collected from the media and insoluble cell layer of cultured human colon epithelial cells (CRL-1831) and colon adenocarcinoma cells (DLD-1) at preconfluency (1), confluency (2) and post-confluency (3) were used for Western blot analysis. Three μg of media proteins and 5 μL of insoluble cell layer proteins were loaded.

144

4. Localization of LOXL2 Protein in Normal Human Colon and Esophagus

Tissue array analysis of various normal tissues revealed that in the mucosa of the large colon, expression of LOXL2 was limited to few scattered but specific cells predominately in the base of the tubular glands (Figure 3.8a). This localization pattern explains the wide variation in expression seen in the cDNA array. The mucosa of the colon consists of four types of cells: absorptive cells, mucous-secreting goblet cells, stem cells that give rise to the absorptive and goblet cells, and enteroendocrine cells. Based on the shape and frequency of the cells expressing LOXL2, they are most likely enteroendocrine cells. These cells are scattered throughout the mucosa from the stomach to the large intestine, and secrete a variety of peptide hormones (Kierszenbaum, 2002). Analysis of normal human esophageal tissue revealed that LOXL2 localized to the outer layer of stratified squamous epithelium of the esophageal mucosa (Figure 3.8b).

The absence of LOXL2 expression in the colonic epithelial cells of the crypts of the tubular glands which give rise to adenocarcinoma indicated that perhaps colon adenocarcinoma cells would not express LOXL2 as well. This pattern is observed by Northern and Western blot analysis of the colon cancer cell lines. In normal esophageal mucosa, LOXL2 was expressed in the squamous epithelial cells, though mainly in the most outer layers. The basal epithelial cells which are mitotically active and which likely give rise to the esophageal squamous cell carcinoma, did not express LOXL2. However, all of the esophageal squamous cell carcinoma cell lines did express abundant LOXL2, indicating that perhaps an upregulation of LOXL2 occurs in the development of this type

145
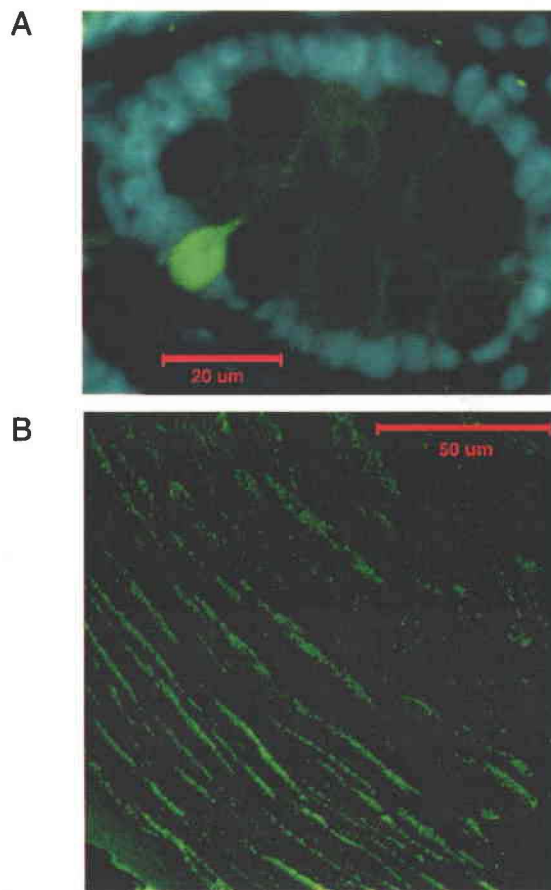
Figure 3.8. Immunohistochemical analysis of LOXL2 in normal colon and esophageal tissues. A normal colon tissue array (ImGenex) and slides of normal esophageal tissue (University of Cape Town, South Africa) were stained with LOXL2 antibodies (1:300 dilution) and Alexa Fluor 488 (green fluorescence). **A.** Cross-section of a tubular gland of the colonic mucosa reveals LOXL2 localization to the enteroendocrine cells. Nuclei were counterstained with DAPI (blue). **B.** In normal esophageal tissue, LOXL2 localizes to the outer later of the stratified squamous epithelium.

of tumor. To evaluate these possibilities, immunohistochemistry on tissue arrays of colon adenocarcinoma as well as esophageal squamous cell carcinoma was performed.

5. Increased Expression of LOXL2 in Colon and Esophageal Tumors

In the colon adenocarcinoma samples, although the tubular gland structure was observed in nearly all of the specimens, only one gland of one sample demonstrated the expression of LOXL2 in a single enteroendocrine cell. However, although there was loss of normal LOXL2 localization, for the remainder of the samples of the colon and esophageal tumor arrays, the presence of LOXL2-expressing tumor cells were noted in the majority of the specimens, and in one esophageal tumor, the LOXL2-expressing cells appeared to be infiltrating a blood vessel (Figure 3.9). The number of LOXL2-expressing cells per field were scored, averaged and evaluated for correlation with tumor stage, tumor differentiation and the presence of elastosis. For the colon tumors, the tumor site was also evaluated for any correlation with the number of LOXL2-expressing cells.

For the tumor stage, there were less LOXL2-expressing cells with higher stage for both the colon adenocarcinomas and esophageal squamous cell carcinomas, although this was not statistically significant (Table 3.1). For the colon tumors, the site of the tumor

Table 3.1. Correlation of LOXL2 Expression by Tumor Stage

	Stage II	Stage III	Stage IV
Colon Tumors	2.1	1.8	1.6
Esophageal Tumors	3.0	2.7	2.5

147
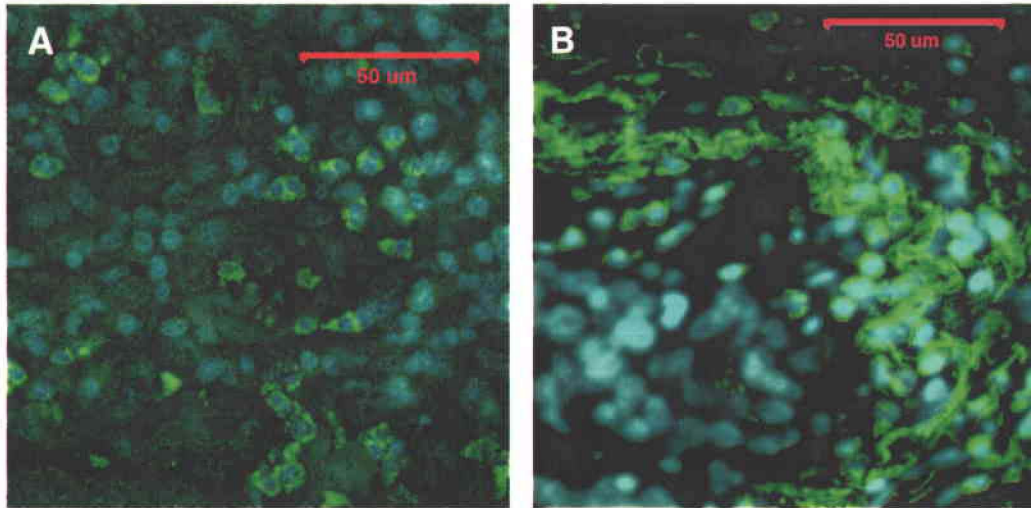
Figure 3.9. Immunohistochemical analysis of LOXL2 in colon adenocarcinoma and esophageal squamous cell carcinoma. One colon cancer tissue array and one esophageal cancer tissue array (ImGenex) were stained with LOXL2 antibodies (1:300 dilution) and Alexa Fluor 488 (green fluorescence). Nuclei were counterstained with DAPI (blue). **A.** Multiple LOXL2-expressing tumor cells in colon adenocarcinoma. **B.** The auto-fluorescent elastic fibers outline the structure of the blood vessel wall. LOXL2-expressing tumor cells are seen outside and within the blood vessel wall as well as within the lumen of the blood vessel which has been infiltrated with tumor cells.

was also not significant in relation to the amount of LOXL2-expressing tumor cells.

However, when evaluated for tumor differentiation, there was a statistically significant (P

<0.05) difference in the colon tumor samples (Table 3.2). There were less LOXL2-

Table 3.2. Correlation of LOXL2 Expression by Tumor Differentiation

	Well	Moderate	Poor/Mucinous
Colon Tumors	0.9*	2.1	2.6
Esophageal Tumors	3.0	2.7	2.6

*P<0.05

expressing tumor cells noted in the well differentiated colon tumors compared to the

moderately differentiated, poorly differentiated and mucinous tumors. Due to the

presence of auto-fluorescent elastic fibers, the presence or absence of elastosis could also

be evaluated. There were more LOXL2-expressing tumor cells with absent elastosis,

although it was not statistically significant (Table 3.3).

Table 3.3. Correlation of LOXL2 Expression by Elastosis

	Presence of Elastosis	Absence of Elastosis
Colon Tumors	1.6	2.0
Esophageal Tumors	2.5	3.1

In some tumors, no LOXL2-expressing cells were noted. Similar tumors may

have given rise to the colon cancer cell lines with near absent LOXL2 expression. The

absence of expression in some cases may be due to loss of heterozygosity accompanied

by another mechanism. To determine if tumors with LOH of the LOXL2 gene are more

149

likely to have absent or low expression of LOXL2, tissues of five esophageal tumors demonstrating LOH were evaluated. Of these five, two samples had LOXL2-expressing tumor cells (scored 2 and 5). The other three samples lacked LOXL2 expression, which was a higher proportion than seen in the esophageal tissue array (4/50).

D. DISCUSSION

Previous studies have reported loss of heterozygosity of chromosome 8p21.2-21.3 in colon cancer and esophageal cancer (Hu et al, 2000; Lerebours et al, 1999; Arai et al, 1998; Shibagaki et al, 1994; Cunningham et al, 1993), to where the LOXL2 gene has been mapped (Jourdan-Le Saux et al, 1998). Based on the evidence of LOXL2 as a *ras*-transformation target (Zuber et al, 2000), and the down-regulation of LOXL2 in serous ovarian adenocarcinomas (Hough et al, 2000; Ono et al, 2000), LOXL2 was hypothesized to be a tumor suppressor gene candidate involved in both colon and esophageal cancer. The results presented in this chapter have indicated that although the LOXL2 gene exhibits significant loss of heterozygosity in colon and esophageal tumors, LOXL2 expression is increased in tumors and is associated with poorly differentiated or mucinous colon tumors and absent elastosis, both indicators of poor prognosis.

Loss of heterozygosity analysis was accomplished by the use of an intragenic microsatellite marker within intron 5 of the LOXL2 gene. This microsatellite was novel and characterized to be polymorphic and thus useful for microsatellite analysis. Similar gender-associated patterns were observed for the LOXL2 microsatellite as was for the

150

microsatellite analysis of the LOX gene locus described in Chapter II. There was a higher incidence of LOH in males and of MIN in females for the colon tumor panel, which is consistent with the previous observation of more frequent MIN in older female patients with colorectal cancer (Brevik et al, 1997). The esophageal tumor panel also demonstrated this pattern, although the incidence of MIN in terms of gender has not been described, perhaps because of the predominance of males in this disease. However, the incidence of MIN has been reported to increase with histological severity in esophageal squamous cell carcinoma (Lu et al, 2003), consistent with my observation of MIN in 3% of the Stage 3 tumors and 25% of the Stage 4 tumors. In the colon panel, and as with other reports, microsatellite instability was observed mainly from tumors of the right colon (Breivik et al, 1997; Liu et al, 1995), and from tumors graded stage B indicating a better prognosis (Liu et al, 1995).

Significant LOH of 33.3% and 32.5% was observed for the colon tumor panel and esophageal tumor panel, respectively. In addition, analysis of cultured colon cancer cell lines, revealed near absence of LOXL2 mRNA expression in the three cell lines evaluated compared to presence of LOXL2 expression in normal fetal colon epithelial cells. In addition, a down-regulation of LOXL2 transcription was demonstrated in the ras-transformed human osteosarcoma cell line compared to its matched non-transformed counterpart. This is consistent with, although not as dramatic as, the 60-fold down-regulation of LOXL2 in ras-transformed rat embryonic fibroblasts (Zuber et al, 2000).

151

The Northern blot results were confirmed at the protein level by Western blot analysis which detected LOXL2 expression as a 95 kDa band in the cultured cell media (CCM) and in the insoluble cell pellet of the normal colon epithelial cell line CRL-1831, but not in the colon adenocarcinoma cell line DLD-1. The multiple bands in the insoluble cell pellet of DLD-1 represent non-specific background bands which are not unusual when using a polyclonal antibody preparation that contain a wide range of antibodies that represent any recent and current antibody response of the animal at the time of harvest. Additional bands may also result from cross-reactions to another protein with a similar epitope as the sequence to which the antibody was designed. Although a BLAST search of the peptide sequence used to design the LOXL2 antibody did not reveal any matches, it is possible that there may be unknown proteins with similar sequence. The observed 95 kDa band was larger than the sequence-predicted 87 kDa protein. Western analysis of protein isolated from the expression of a full-length construct of LOXL2 yielded a band of 95 kDa, indicating that there may be post-translational modification of LOXL2.

In contrast to the expression studies done in cultured cell lines, the matched normal/tumor cDNA array did not reveal general down-regulation of LOXL2. The one sample that did show greater down-regulation than the other samples was due to the increased expression detected in the matched normal sample. This large variation in expression in the normal colon sample raised the possibility that LOXL2 is expressed only in certain regions or cells of the colon, and the large variation in expression was due

to the area of tissue sampled. This was confirmed by immunohistochemistry of tissue arrays that showed expression of LOXL2 only in the enteroendocrine cells of the colon.

Interestingly, the three other cell types of the colonic mucosa, the absorptive cells, goblet cells and stem cells, did not express LOXL2. If these epithelial cell types did not express LOXL2, why did the Northern analysis indicate that normal colon epithelial cells express LOXL2? There are two possibilities. The first is that the cell line used was of fetal origin while the tissue array used for immunohistochemistry was of normal colon samples from individuals aged 35-78 years of age. It is possible that there are developmental changes of LOXL2 expression in the colon. The other possibility is that the change in expression was due to 2-dimensional (2D) culturing of the normal colon epithelial cells. Using normal breast epithelial cells and breast cancer cells, it has been shown that there is little overlap in gene expression differences between non-tumorigenic and tumorigenic cells cultured in 2D compared to 3D, and of the few genes that are common between the two groups, nearly half show altered expression in opposite directions (Bissell et al, 2002). With the uncertainties inherent in using cell culture, the immunohistochemical analysis of the tumor tissue arrays gave more definitive evidence of the increase in LOXL2 expression in both colon and esophageal tumors.

In both the colon adenocarcinoma and the esophageal squamous cell carcinoma, the more mitotically active epithelial cells in the crypts of tubular glands of the colonic mucosa and the basal squamous cells of the esophageal mucosa that commonly give rise

153

to tumorigenic cells lacked LOXL2 expression. Although most of the correlations between the number of LOXL2-expressing cells and demographics of the tumors were not statistically significant, probably due to the low number of samples, two interesting trends were noticed. The first was that LOXL2-expressing tumor cells more were common in tumors lacking elastosis. Elastosis refers to the stromal reaction to tumors and is composed of aggregates of thick mature and fine immature elastic fibers (Fukushima et al, 2000). Elastosis is associated with improved prognosis in lung and breast (Fukushima et al, 2000; Vaiphei et al, 1990), and though it has been described in colon cancers (Martinez-Hernandez and Catalano, 1980), the association between elastosis and prognosis for colon cancer has not been studied.

The second interesting trend, which was statistically significant, was that LOXL2-expressing tumor cells were more common in less differentiated colon tumors. In the data, poorly differentiated adenocarcinoma and mucinous carcinoma were grouped as they have common characteristics including lower incidence, more advanced stage at diagnosis, aggressive behavior and high incidence of metastasis (Kanazawa et al, 2002). A lower grade of differentiation has also been observed in the invasive part of the tumor, although the main tumor is more differentiated (Kanazawa et al, 2002). This is similar to the observation of LOXL2-expressing tumor cells invading through a blood vessel wall. Could LOXL2 be involved in more aggressive behavior, including invasion? This possibility is supported by two reports. LOXL2 mRNA expression was found only in highly invasive/metastatic breast cancer cell lines MDA-MB-231 and Hs578T compared

154

to the poorly invasive/non-metastatic breast cancer cell lines T47D and MCF-7 (Kirschmann et al, 2002). Non-invasive MCF-7 cells, transfected with LOXL2 and injected into mammary fat pads of mice, were reported to infiltrate the pseudocapsules surrounding the tumor and invade adjacent tissues, including muscle, the vascular system and perineural space (Akiri et al, 2003).

What about previous reports about down-regulation of LOXL2 in ovarian carcinomas? In addition, although normal breast epitheilial cells express LOXL2 (Akiri et al, 2003), poorly invasive/non-metastatic breast cancer cell lines T47D and MCF-7 do not express LOXL2, indicating a down-regulation in these cells lines. Similarly, the HCT-116, DLD-1 and DLD-15 colon carcinoma cells do not express LOXL2. These three cell lines are epithelioid similar to the MCF-7 and T47D cells. HCT-116 is poorly invasive (Gohla et al, 1996) and the invasive variant of DLD-1 is nonepithelioid (Vermuelen et al, 1995). Could there be both processes happening – initial loss followed by re-expression? In this case, there can be loss of one allele by deletion, detected by loss of heterozygosity, and the temporary silencing of the second allele by promoter methylation. Certainly in the case of gastric cancers, LOX expression is silenced by promoter hypermethylation (Kaneda et al, 2002). To identify a CpG island within the promoter of the LOXL2 gene, the *Homo sapiens* chromosome 8 genomic contig sequence (NT023666) containing the entire LOXL2 gene spanning 107 kb of genomic sequence was evaluated. Analysis of the sequence from 21 kb upstream of exon 1 extending to the beginning of exon 2 with GrailEXP CpG Island Locator (http://compbio.ornl.gov/ grailexp/grailexp.cgi), revealed a

predicted CpG island of length 1150 bp, from the promoter region extending into intron 1, with a observed/expected ratio of 0.82 and a GC content of 67.61%. The methylation of LOXL2 may initially silence this gene, and further genetic alterations or alterations of the matrix surrounding the tumor may induce the re-expression of LOXL2. Indeed, LOXL2 expression can be induced in MCF-7 cells by co-culture with fibroblast conditioned media (Kirschmann et al, 2002). This may be similar to TGF-β, which appears to have a role in tumor suppression and promotion. Many early stage tumors lose sensitivity to TGF-β, yet TGF-β signaling is required during late tumor progression and metastasis (Grunert et al, 2003). This may also be occurring with LOXL2, whose expression is associated with invasiveness and metastasis.

Further studies aimed at characterizing the molecular role of LOXL2 in cancer cell invasion and metastasis will be discussed in Chapter IV.

CHAPTER IV

FINAL DISCUSSION AND FUTURE DIRECTIONS

Chapter II of this dissertation described significant loss of heterozygosity of the lysyl oxidase gene locus in colon cancer, with the closest microsatellite marker to the LOX gene having a LOH of 35.7%. In tumors demonstrating LOH, there was reduced LOX mRNA expression accompanied by inactivating mutations of the LOX gene in colon tumors. Chapter III also described significant loss of heterozygosity of the LOXL2 gene in colon and esophageal tumors, of 33.3% and 32.5% respectively. However, immunohistochemical analysis demonstrated increased LOXL2 protein expression in colon and esophageal tumors compared to normal colon and esophageal tissue. This was an extremely interesting though unexpected finding as all members of the LOX protein family have C-terminal homology and have been assumed to have similar functions. Certainly, LOX, LOXL and LOXL4 have all been described to have amine oxidase activity (Borel et al, 2002; Ito et al, 2001; Kagan, 1986). However, the premise of similar domain equals similar function does not necessarily pertain to proteins of the extracellular matrix (ECM).

In general, ECM proteins are multi-functional molecules with domains that are repeated or show phylogenetic similarity to domains from other proteins (Hohenester and Engel, 2002). This is certainly the case of the repeated SRCR domains in LOXL2, LOXL3 and LOXL4, and the cytokine receptor-like domain in all LOX proteins. In

vertebrates, basic ECM families were expanded by gene duplication (Hohenester and

Engel, 2002). This is supported by the observation of two LOX family members in

Drosophila melanogaster compared to at least five members in *Homo sapiens*. Following

gene duplication, however, the homologous domains evolve independently, thus

gradually changing their function and it is generally not possible to predict the function of

an extracellular domain based on its homology to a known domain (Hohenester and

Engel, 2002). The CRL domain does not exist in proteins other than in the LOX family,

and as a partial Class 1 cytokine receptor domain, may likely have a different function

than proteins containing the consensus sequence of Class 1 cytokine receptors. In

addition, the second SRCR domain of LOXL2, LOXL3 and LOXL4, which is the most

variable, likely defines the protein interaction and thus, its function. Therefore, the

function(s) of each of the LOX proteins should be analyzed separately with no

expectation of similar function.

So what are the predicted roles of the other LOX family members in cancer?

LOXL maps to chromosome 15q22, close to the PML gene involved in promyelocytic

leukemia (Goy et al, 2000). There have been sporadic reports on the gain of 15q22-25 in

malignant mesotheliomas and Barrett's adenocarcinoma (Krismann et al, 2002; Riegman

et al, 2001), and rearrangements in lung cancer and acute myelogenous leukemia (Park et

al, 2001; Melnick et al, 1999). Chromosome 15q22 does not demonstrate significant

LOH in any cancer, indicating that a tumor suppressor gene is unlikely to reside in this

locus. However, genome-wide screens for LOH may miss regions containing a possible

tumor suppressor. This is well demonstrated in the microsatellite analysis of the LOX

locus in esophageal cancer. Evaluation of only markers lms15 and D5S642 that do not

demonstrate significant LOH would miss the significant LOH of marker D5S490.

Therefore, a subset of the colon tumor panel was screened for LOH of the LOXL gene

utilizing a previously identified intragenic microsatellite (Kim et al, 1997). This showed

an insignificant 13.6% LOH, falling far below the 30% threshold that is commonly

accepted, indicating that LOXL is unlikely to be involved in colon tumor pathogenesis as

a tumor suppressor. Instead, LOXL appears to be involved in fibrotic processes, both in

lung and liver (Kim et al, 1999; Decitre et al, 1998), and is induced during the stromal

reaction of lung and breast tumors (Decitre et al, 1998).

LOXL3 has been shown, through a collaboration with Millenium (Cambridge,

MA) to have a general increase in expression in primary breast, lung and colon cancers,

as well as liver metastasis, compared to normal tissue of the same origin (Figure 4.1).

Indeed, LOXL3 maps to chromosome 2p13 (Jang et al, 1999), a region affected by

translocations and amplifications in B-cell lymphomas and neuroblastomas (Wessendorf

et al, 2003; Gozzetti et al, 2002; Palanisamy et al, 2002; Barth et al, 2001; Kim et al,

2001). LOXL4 has been mapped to chromosome 10q24 (Asuncion et al, 2001), a gene-

rich region affected by translocations and deletions in various types of cancer, including

cancers of the lung, prostate and brain (Leube et al, 2002; Chernova and Cowell, 1998;

Kim et al, 1998; Virmani et al, 1998). Recently, LOXL4 was reported to be

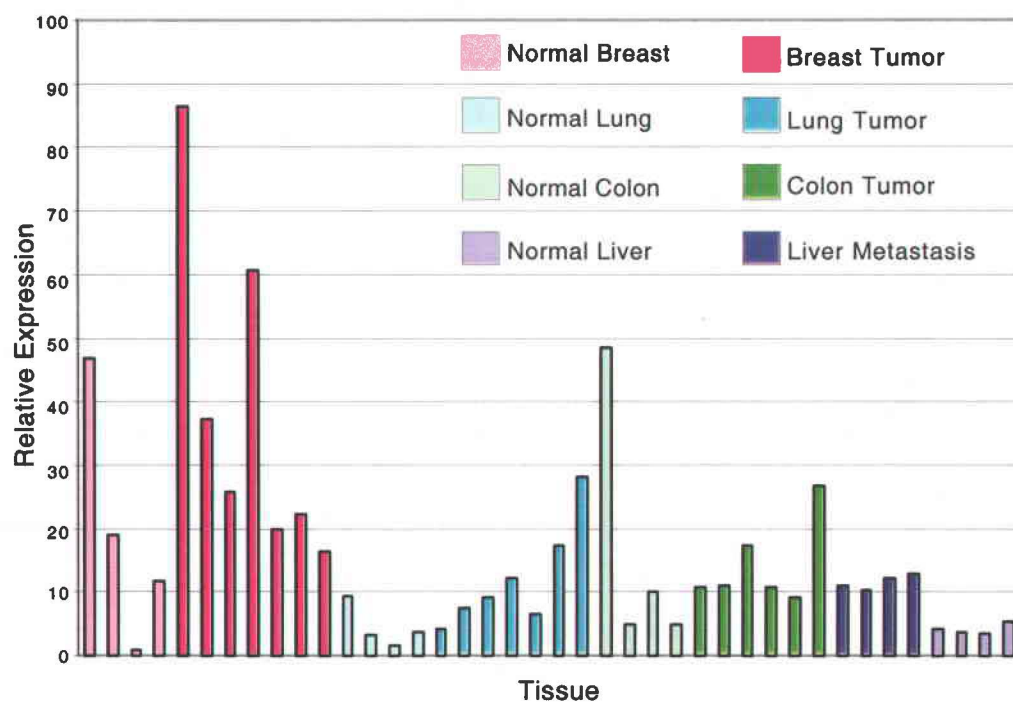overexpressed in human head and neck squamous cell carcinomas (Holtmeier et al,

Figure 4.1. LOXL3 expression in various normal and tumor tissues using real-time PCR. There is overall higher expression of LOXL3 mRNA in tumors from breast, lung and colon, as well as in liver metastases, compared to its respective normal tissue.

2003). These observations collectively indicate that the lysyl oxidase genes may have different functions with regards to pathogenesis of different tumor types.

What are the hypothesized functions of LOX in cancer? It is well known that lysyl oxidase is an extracellular enzyme that catalyzes the cross-linking of elastin and collagen, and thus loss of the lysyl oxidase protein could result in modulation of the extracellular matrix such that tumor growth and metastasis could occur. The extracellular matrix, which contacts the surface of the cell about every 20 nm (Bob Mecham, personal communication), is a critical component of tumorigenesis. Indeed, the importance of the ECM in transformation is indicated by the fact that lysyl oxidase and LOXL2 are only two of the many ECM genes down-regulated by *ras*-transformation. Collagen type III and fibronectin were identified by Kryzyzosiak and co-workers as down-regulated by *ras* transformation (1992). Recently, a genome-wide survey of *ras* transformation targets identified 20 down-regulated ECM genes. Besides LOX and LOXL2, fibronectin was identified (more than 100-fold decreased), as well as α2(I) collagen (more than 20-fold decrease), and several matrix metalloproteinases (MMPs) including MMP-1 (more than 100-fold decrease) and MMP-2 (more than 50-fold decrease) (Zuber et al, 2000). This coordinated down-regulation of several ECM genes is not limited to *ras* transformation. NIH 3T3 cells expressing mutant RET pro-oncogene proteins that are responsible for the dominant inherited cancer syndromes, multiple endocrine neoplasia types 2A and 2B, have decreased levels of LOX, type I collagen and TIMP3 (Watanabe et al, 2002).

Substrates of lysyl oxidase in the extracellular matrix have an effect in tumor

pathogenesis. The ECM protein, α2(I) collagen, is also a suppressor of *ras*

transformation. Transfection of α2(I) collagen into K-*ras* transformed NIH 3T3 cells,

resulted in flatter morphology, decrease anchorage independence, slower proliferation,

and suppressed tumorigenicity in nude mice (Travers et al, 1996). In fact,

farnesyltransferase inhibitors (FTI), an anti-cancer drug class that targets the

farnesylation of *ras* protein critical for *ras* activity (Leonard, 1997; Sebti and Hamilton,

1997; Kato et al, 1992), cause stable phenotypic reversion of *ras*-transformed rat

fibroblast cells due to upregulation of α2(I) collagen (Du et al, 1999). In addition,

aberrant expression of types I and type III collagens have been observed in breast cancer.

Fibroblastic cells of malignant tumor stroma had increased synthesis of these fibrillar

collagens, and formation of aberrant collagen bundles (Kauppila et al, 1998). These

collagen-producing fibroblasts associated with tumors are able to stimulate tumor

progression of immortalized normal prostate epithelial cells as evidenced by increased

growth, altered morphology and invasion (Olumi et al, 1999).

Does cross-linking of these ECM proteins by lysyl oxidase have an effect on its

role in cancer? This appears to be the case in elastin. Decreased lysyl oxidase activity

would lead to decreased cross-linking of elastin yielding an increase in soluble elastin.

Soluble elastin is able to interfere with tumor cell dissemination into elastin-rich tissues

of the skin, lung and blood vessels, by chemotaxis towards the soluble elastin gradient

and stimulation of adherence to insoluble elastin (Timar et al, 1995; Timar et al, 1991).

Although all the data reviewed so far indicates that a loss of LOX is a key feature

of tumorigenesis and even invasiveness, a recent study identified LOX as an up-regulated

gene in breast cancer metastasis (Kirschmann et al, 1999). Our subsequent study

demonstrated that LOX was responsible, at least partially, for the invasive ability of the

highly invasive/metastatic cell lines MDA-MB-231 and Hs578T. This was shown by the

decreased ability of MDA-MB-231 and Hs578T cell lines transfected by LOX antisense

oligos to invade through a collagen IV/laminin/gelatin matrix, to levels comparable to the

poorly-invasive/non-metastatic cell lines MCF-7 and T47D. This inhibition of

invasiveness was also produced by treatment of these cells by treatment with BAPN, a

specific and irreversible inhibitor of LOX amine oxidase activity. Transfection of MCF-7

with a sense construct of LOX caused a two-fold increase in invasiveness of the cells

(Kirschmann et al, 2002). Northern blot analysis of the two poorly-invasive/non-

metastatic cell lines, MCF-7 and T47D, and the two highly invasive/metastatic cell lines,

MDA-MB-231 and Hs578T, demonstrated that the mRNA expression of all the LOX

family members were found only in the invasive/metastatic cell lines (Figure 4.2).

Although these results appear to contradict previous observations with

transformed fibroblasts, cancer-derived cell lines and cancer tissues, this was the first

study to evaluate invasive cancer cell lines compared to non-invasive cancer cell lines.

Lysyl oxidase expression is associated with the epithelial-mesenchymal transition (EMT)

process. During EMT, there is a loss of epithelial morphology and the gain of

mesenchymal characteristics. This three step process involves first, the epithelial cells
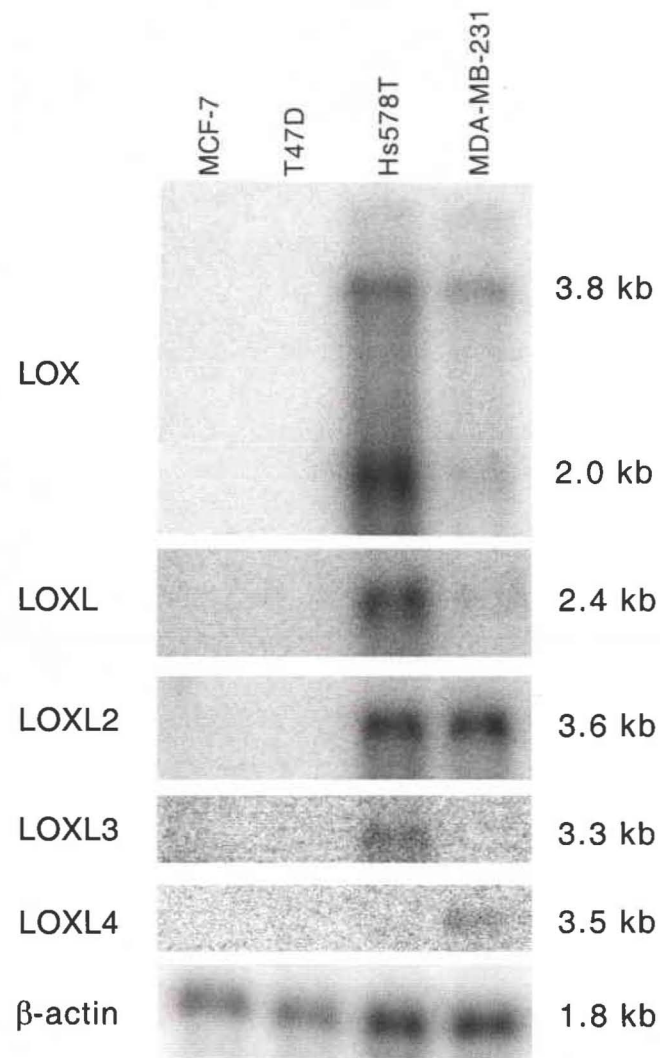
163

Figure 4.2. Northern blot analysis of the members of the lysyl oxidase family in four breast cancer cell lines. There is no expression of LOX, LOXL, LOXL2, LOXL3 and LOXL4 in the poorly-invasive/non-metastatic cell lines, MCF-7 and T47D. LOX and LOXL2 are expressed in both the highly invasive/metastatic cell lines, Hs578T and MDA-MB-231.

164

gaining a fibroblast-like phenotype; next, the down-regulation of epithelial-specific

proteins and the expression of mesenchymal proteins; and finally, the digestion of and

migration through the extracellular matrix (Grunert et al, 2003). EMT occurs during

critical phases of embryogenesis, particularly during gastrulation, and in the last steps of

tumorigenesis to facilitate metastasis. The global gene changes necessary to alter

phenotype and function during EMT may be induced by the activity of lysyl oxidase on

nuclear substrates.

Until recently, the only known *in vivo* substrates for lysyl oxidase were collagen

and elastin. However, the sequences surrounding the target lysine in these molecules do

not have homology, nor do they have similar secondary structures. This indicates that the

substrate specificity of LOX may be flexible. Indeed, recently, LOX was shown to cross-

link basic fibroblast growth factor *in vitro* (Li et al, 2003). Bovine lysyl oxidase

demonstrated activity against a variety of basic, globular proteins, including histone H1

(Kagan et al, 1983). This has been recently confirmed by Giampuzzi et al (2003), who

reported interaction between the carboxy-terminal portion of LOX and the

unphosphorylated form of histone H1, and to a lesser extent, an interaction with histone

H2 that does not require the carboxy-terminus of LOX. The authors suggest that LOX

may bind to H1 at lysine sites which would hinder the phosphorylation of the nearby

serine, or that the catalytic activity of LOX would cause deamination of lysines,

diminishing the overall positive charge. The former would lead to decreased

transcription, while an increase in the negative charge would lead to histone dissociation

from the DNA and increased transcription. H2 may act as a regulator of the cellular

location of LOX, delivering LOX to its substrate H1 (Giampuzzi et al, 2003). Thus, an

alteration in LOX expression levels would potentially yield transcriptional changes in

multiple genes important for the tumorigenesis. Indeed, intracellular overexpression of

mature, catalytically active lysyl oxidase is able to increase the activity of the $\alpha 1(III)$

collagen promoter up to 12 fold (Giampuzzi et al, 2000). We have also observed

alterations in transcription by modulating the activity of one of the two *Drosophila* lysyl

oxidases.

Drosophila melanogaster was evaluated as a possible model system to evaluate

the function of the lysyl oxidase proteins. In contrast to the five lysyl oxidase members in

human, there are only two lysyl oxidase orthologues found in *Drosophila melanogaster*

(Figure 4.3). Interestingly, the DmLOXL-1 and DmLOXL-2 proteins, which are

evolutionarily earlier than the mammalian lysyl oxidases, both have SRCR domains,

indicating that mammalian LOX and LOXL have arisen more recently in evolution. This

is consistent with the observation that elastin, one of the substrates of LOX, is only found

in vertebrates (Sage and Gray, 1977). Thus, the SRCR domains may be crucial in the

"original" function of these amine oxidases. The two *Drosophila* orthologues of lysyl

oxidase were found to have distinct spatial and temporal expression patterns. Northern

analysis revealed that Dmloxl-1 was expressed in all developmental stages, while

Dmloxl-2 mRNA was expressed only in adult flies (Figure 4.4). This allowed for a
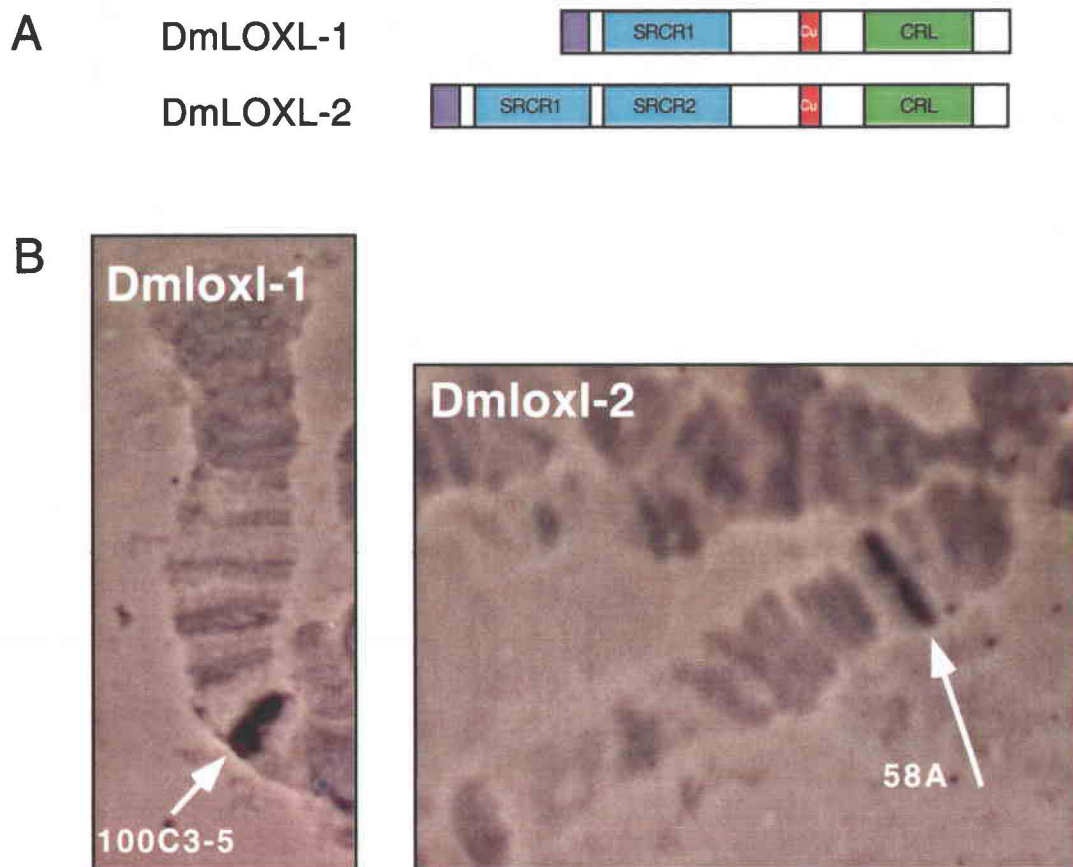
Figure 4.3. Domain organization and chromosomal localization of the
***Drosophila* lysyl oxidases.** A. The domain structure of the two *Drosophila* lysyl
oxidase orthologues, DmLOXL-1 and DmLOXL-2 They share the unique copper-
binding domain, shaded in red, and a cytokine receptor-like domain, shaded in
green, and the predicted extracellular signal sequence, shaded in purple, that is
common to all lysyl oxidase genes.. In addition, DmLOXL-1 has one SRCR
domain and DmLOXL-2 has two SRCR domains. B. ESTs of Dmloxl-1 and
Dmloxl-2 were labeled with digoxygenin and used as a probe for *in situ*
hybridization to Drosophila chromosomes by the modified Cambridge protocol.
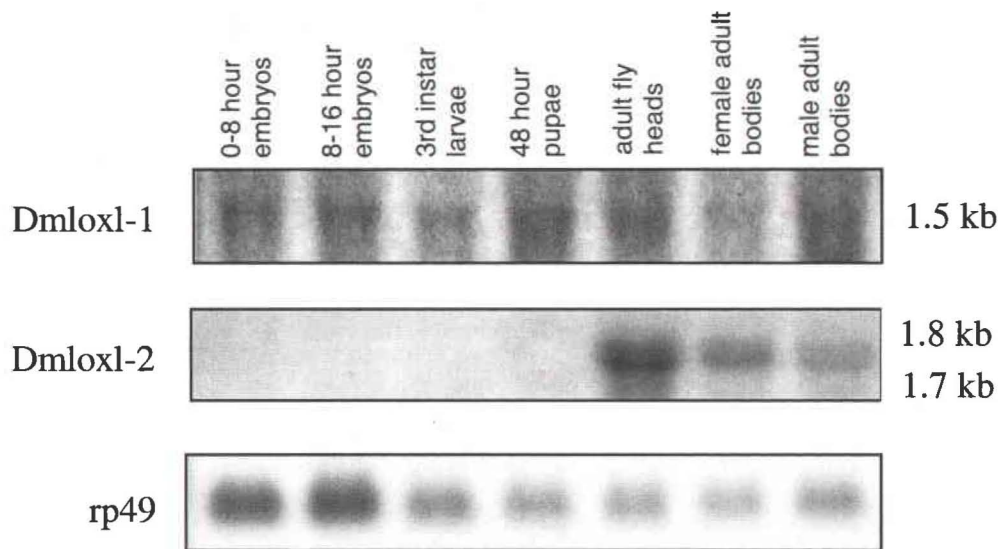
Figure 4.4. Northern blot analysis of the Drosophila lysyl oxidases at various developmental stages. Ten micrograms of total RNA from various developmental stages of Drosophila were used to make a Northern blot. Autoradiograms were obtained after hybridization with a ^{32}P-radiolabeled Dmloxl-1 EST probe, Dmloxl-2 EST probe and a cDNA probe of the ribosomal protein rp49. The 1.5 kb mRNA of Dmloxl-1 was detected in all developmental stages, while the 1.8 and 1.7 kb mRNA of Dmloxl-2 was detected only in adult flies.

unique model to study DmLOXL-1 alone as the only lysyl oxidase active in developing embryos and larvae.

Selective inhibition of DmLOXL-1 by βAPN treatment of embryos and larvae resulted in developmental delay and reduced expression of seven constitutively expressed ribosomal genes and the sgs3 glue gene (Molnar et al, 2003). In addition, males treated with βAPN demonstrated enhanced position effect variegation (PEV) while transgenic female flies overexpressing Dmloxl-1 demonstrated suppression of PEV. In PEV, a change in the chromatin structure through heterochromatization of euchromatic regions, has proven to be connected with gene inactivation (Jenuwein and Allis, 2001; Bhadra et al, 2000; Reuter and Spierer, 1992). The compact packaging, typical for heterochromatin, is extended into the adjoining euchromatic regions resulting in transcriptional repression of the affected loci, in this case the white (w^+) gene responsible for red eye color. Dominant mutations can either suppress or enhance variegation, as a result of elevated or repressed transcription of the w^+ gene, leading to flies with eye color of red or white, respectively (Reuter and Spierer, 1992). This alteration of variegation indicates that Dmloxl-1 is able to modify chromatin structure resulting in the increase in transcriptional activity. These results are consistent with the less tightly packed chromatin and the increase in activity of the α1(III) collagen promoter induced by LOX (Giampuzzi et al, 2000; Mello et al, 1995), and confirm this as a valid hypothesis of LOX function.

What of the hypothesized function of LOXL2? The possibility of a role of LOXL2 in invasion has been introduced in Chapter III. LOXL2 mRNA is highly expressed in invasive breast cancer cell lines (Figure 4.2). This mRNA expression pattern was confirmed by Western analysis using the same LOXL2 antibody as described in Chapter III, which also showed LOXL2 to be present in normal breast epithelial cells (Figure 4.5). The larger 150 kDa protein detected by the antibody was not detected by a second antibody designed against the same sequence, although both antibodies detect the lower 95-100 kDa protein. The association between increased LOXL2 (and LOX) expression and cancer cell line invasiveness was not only observed in breast cancer, but also noted in prostate (Kirschmann et al, 2002) and melanoma cell lines (Figure 4.6).

Western analysis of three invasive cell lines run on a lower percentage acrylamide gel than for Figure 4.5 revealed slight variations in the molecular weight observed, indicating a difference in mobility (Figure 4.7). This may be due to phosphorylation. Analysis of the LOXL2 protein through the Center of Biological Sequence Analysis at the Technical University of Denmark (www.cbs.dtu.dk/services) NetPhos 2.0 Server which predicts phosphorylation sites, revealed 14 predicted serine, 8 predicted threonine and 5 predicted tyrosine phosphorylation sites. Another post-translational modification that may be occurring in LOXL2 is glycosylation. The observed 95-100 kDa protein is larger than the expected 87 kDa predicted from the 774 amino acid sequence. Most secretory proteins contain one or more carbohydrate chains, and indeed lysyl oxidase undergoes N-glycosylation prior to secretion and cleavage. Using the NetNGlyc 1.0

170

Figure 4.5. Western blot analysis of LOXL2 protein expression in human breast cell lines. Proteins collected from the cultured cell media of the human mammary epithelial cell line HMEC, the highly invasive/ metastatic breast cancer cell lines Hs578T and MDA-MB-231, and the poorly invasive/non-metastatic cell line T47D, at preconfluency (1), confluency (2) and post-confluency (3) were used for Western blot analysis. Three µg of cultured cell media protein was loaded per lane onto an 8% polyacrylamide gel.

171
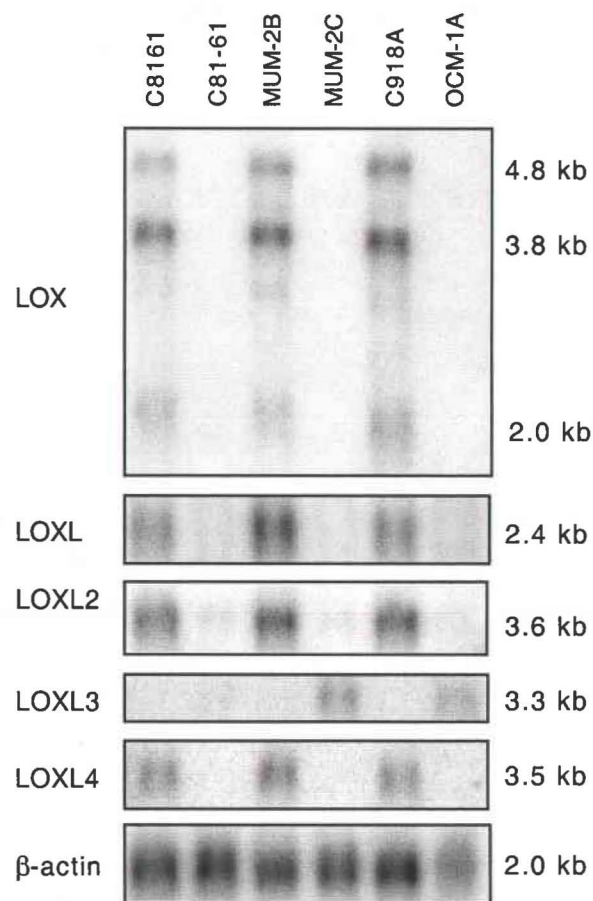
Figure 4.6. Northern blot analysis of the members of the lysyl oxidase family in melanoma cell lines. There is expression of LOX, LOXL, LOXL2 and LOXL4 in the invasive cutaneous (C8161) and uveal (MUM-2B and C918A) melanoma. The remaining cell lines are of non-invasive cutaneous (C81-61) and uveal (MUM-2C and OCM-1A) melanoma cell lines.
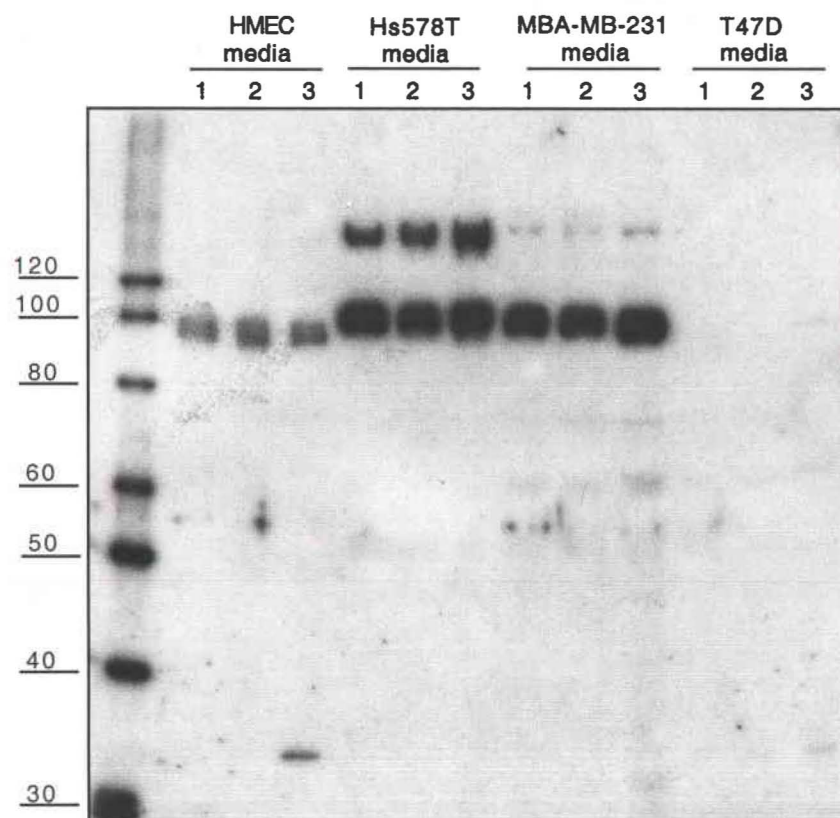
Figure 4.7. Western blot analysis of LOXL2 protein expression in invasive human cancer cell lines. Proteins collected from the cultured cell media of the highly invasive/metastatic breast cancer cell lines Hs578T (1), MDA-MB-231 (2), and the invasive melanoma cell line A375Pvar (3), at post-confluency were used for Western blot analysis. Three μg of cultured cell media protein was loaded per lane onto a 6% polyacrylamide gel.
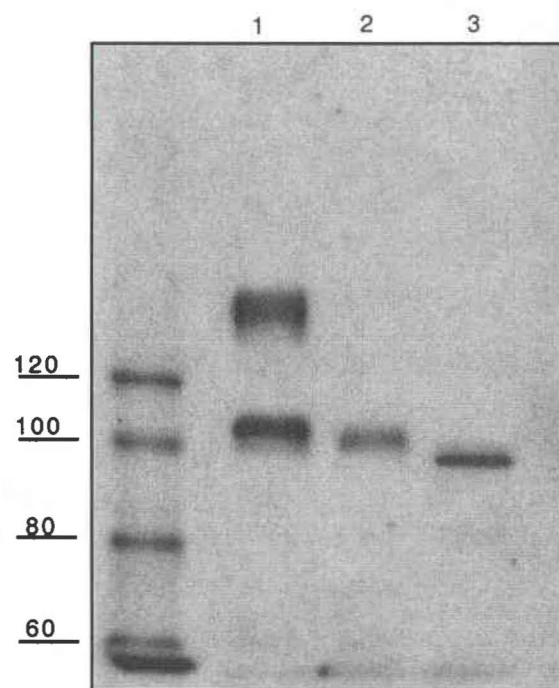
Server at the same website, three N-glycosylation sites were predicted. Would these post-translational modifications affect the function of the LOXL2 protein?

Indeed, the basic question of LOXL2 function has barely been explored. Very little is known about LOXL2 function, either in normal tissues or in cancer. To gain some perspective about function, immunohistochemistry of a multiple tissue array was performed. LOXL2 expression in normal breast tissue, consistent with the Western blot on normal mammary epithelial cells, was found only on the luminal surface of ductal epithelial cells (Figure 4.8). Besides the lumen of the mammary glands, LOXL2 localizes to the lumen of gastric glands in the body of the stomach, distal convoluted tubules of the kidney, prostatic glands of the prostate, and the trophoblast layer of the placenta that faces the maternal lacunae (Figure 4.9). Altered LOXL2 expression in colon cancer and esophageal cancer has been demonstrated in Chapter III, and we have found similar results in breast and lung cancer (Figure 4.8). Non-invasive MCF-7 breast cancer cells, transfected with LOXL2 and injected into mammary fat pads of mice, were reported to invade tissues adjacent to the tumor (Akiri et al, 2003). This report, in addition to our expression data showing LOXL2 upregulation in highly invasive/ metastatic cancer cell lines, indicates that LOXL2 confers invasive properties. This is consistent with LOXL2 upregulation in epithelial-mesenchymal transition (Kiemer et al, 2001).

In EMT, the loss of intercellular junctions and acquisition of cell motility, is accompanied by modification of the type of intermediate filaments expressed (Boyer et

174
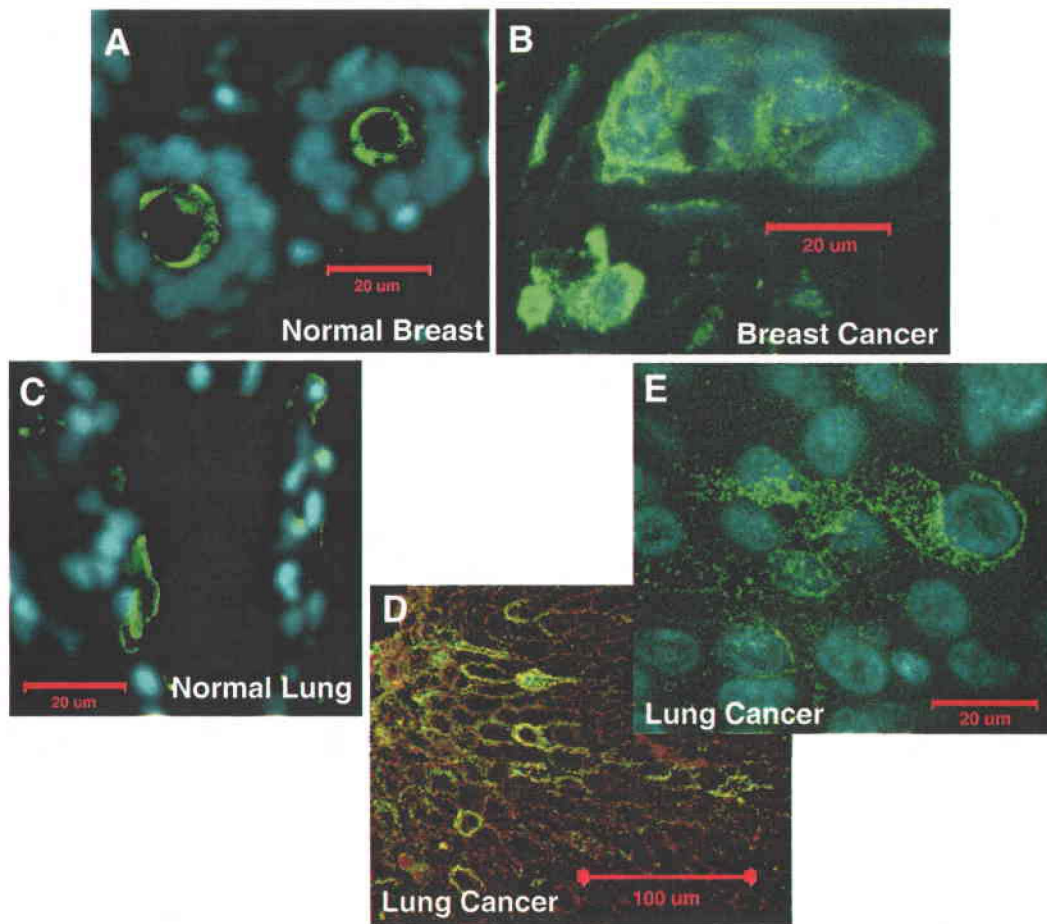
Figure 4.8. Immunohistochemical analysis of LOXL2 in normal tissues and tumors of the breast and lung. Multiple tissue arrays (ImGenex) were stained with LOXL2 antibodies (1:300 dilution) and Alexa Fluor 488 (green fluorescence). Nuclei were counterstained with DAPI (blue) except for D. **A.** LOXL2 localizes to the luminal surface of the mammary duct epithelial cells. **B.** In infiltrating ductal carcinoma of the breast, LOXL2 is expressed at the periphery of the breast cancer cells. **C.** LOXL2 is present in certain cells of the alveoli. **D, E.** Serial sections of the same lung squamous cell carcinoma show LOXL2 expression within the cytoplasm.

175
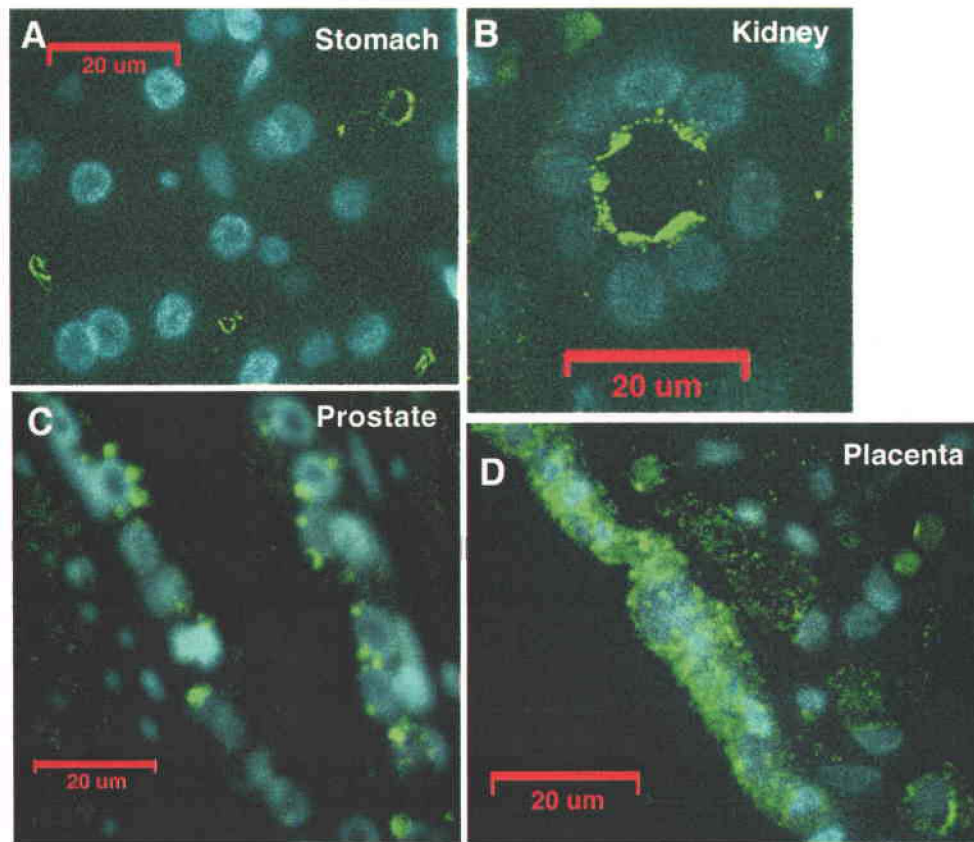
Figure 4.9. Immunohistochemical analysis of LOXL2 in various normal tissues.
Multiple tissue arrays (ImGenex) were stained with LOXL2 antibodies (1:300 dilution)
and Alexa Fluor 488 (green fluorescence). Nuclei were counterstained with DAPI
(blue). LOXL2 localizes to the luminal surface of the epithelial cells lining the: **A.** gas-
tric glands in the body of the stomach; **B.** distal convoluted tubule of the kidney; **C.**
prostatic glands of the prostate; and **D.** trophoblast layer of the placenta, including the
syncytiotrophoblast and cytotrophoblast layer.

al, 2000). In particular, the intermediate filament vimentin, which is normally restricted to mesenchymal cells in mature tissues, is expressed in epithelial cells during EMT along with cytokeratin, which is normally restricted to epithelial cells. This process was recapitulated by the development of a stable MCF-7 breast cancer cell line, termed MoVi, which expressed both vimentin and cytokeratin. MoVi cells demonstrated greater motility and invasiveness, while down-regulation of vimentin in the MoVi cells as well as the breast cancer cell line MDA-MB-231, which normally expresses both vimentin and cytokeratin, resulted in reduced motility and invasiveness (Hendrix et al, 1997). EMT may also be involved in the dedifferentiation program that leads to malignant carcinoma (Thiery, 2002). This reversion to an undifferentiated, embryonic-like phenotype, is accompanied by the expression of genes that are associated with different cellular phenotypes, and has been observed in aggressive tumor cells (Hendrix et al, 2003). Indeed, the expression of LOXL2 appears to be associated with less differentiated and aggressive tumors.

Future studies of this project will focus on LOXL2 as its role in invasiveness is supported by the most data. My long-term goal is to determine the molecular role(s) of LOXL2 in tumor development and metastasis. My immediate goal is to define the extent to which LOXL2 promotes cancer cell invasion. My hypothesis is that LOXL2 directly contributes to tumor development by promoting cancer cell invasiveness, through catalytic activity and its unique and novel protein domains. I plan to address my hypothesis through three specific aims:

Specific Aim 1: Identify if LOXL2 confers the ability of breast cancer cells to migrate and invade through the ECM

Rationale: LOXL2 has been shown, by our group and others, to be upregulated in highly invasive breast cancer cell lines and during EMT, which facilitates migration and invasion. Recently, the gain of *in vivo* invasive properties by non-invasive MCF-7 cells transfected with LOXL2 was reported. By recapitulating this process *in vitro*, we will be able to evaluate the function of the full length LOXL2 protein in promoting migration and invasion (Aim 1); the necessity of catalytic activity for this function (Aim 2); and the role of the novel CRL domain in contributing to this function (Aim 3). Breast cancer cell lines will be used as the model system as data supporting the role of LOXL2 in invasiveness was generated with these cell lines. We have previously shown that MDA-MB-231 and Hs578T express multiple LOX family members, but MCF-7 and T47D express none. To avoid the influence of other LOX family members, MCF-7 and T47D cells will be used. Invasion of cells through a basement membrane *in vitro* has been reported to correlate with invasive ability *in vivo* (Albini et al, 1987), so it is anticipated that transfection of LOXL2 into non-invasive breast cancer cells will result in measurable invasiveness. As invasiveness of a cell depends on two factors, migration and breakdown of the ECM, both these abilities will be evaluated. A full length LOXL2 cDNA construct will be transiently transfected into MCF-7 and T47D cells. Migratory and invasive ability will be evaluated on untransfected cells, cells transfected with empty vector, and cells transfected with the full length LOXL2 cDNA construct. Data will be compared to the

positive control of invasive Hs578T and MDA-MB-231 cells. LOXL2 protein expression in transfected cells will be confirmed by Western blot analysis. As an alternative strategy, purified LOXL2 from MDA-MB-231 and HS578T cells will be added to MCF-7 and T47D cells to evaluate the effect of exogenously added LOXL2 on cell migration and invasion. This will determine if it is extracellular LOXL2 that affects cell migration and invasion, and if LOXL2 produced by invasive cancer cell line can induce nearby non-invasive cells to adopt invasive properties. Another alternative strategy would be to use siRNA to selectively eliminate LOXL2 expression in Hs578T and MDA-MB-231 cells to evaluate the contribution of the LOXL2 protein in inducing cell migration and invasion.

Methodology: *Cell culture* of breast cancer cell lines will use RPMI media supplemented with 10% fetal bovine serum, 10 mM HEPES and 10 mM L-glutamine, and will be maintained as described in Chapter II. *A full length LOXL2 cDNA construct* has been generated and will be placed in an adenoviral expression system (Invitrogen) for transient transfections. Our collaborators have used the adenoviral system for transfection of GFP-LOX construct into MCF-7 cells at 99% efficiency (Dawn Kirschmann, personal communication). *Evaluation of migration and invasion* will use the FluoroBlok Systems (BD Biosciences, Bedford, MA) that quantitate in real-time fluorescence, cells that reach the lower chamber, either by migration through pores for the HTS FluoroBlok System, or by invasion through Matrigel for the BioCoat FluoroBlok Invasion System. Alternately, the MICS (membrane invasion culture system) chambers will be used. The methodology of these assays has been previously described (Maniotis et al, 1999; Hendrix et al, 1987)

and will be shared by our collaborators, Dr. Dawn Kirschmann and Dr. Mary Hendrix, from the University of Iowa. *Western blot analysis* will be performed on cultured cell media and cell layer extracts using the method described in Chapter III. The *C-terminal LOXL2 antibody* has already been generated and characterized to specifically recognize LOXL2, as described in Chapter III. *Immunoprecipitation of LOXL2 protein* will use UltraLink Immobilized Protein G (Pierce) that we have previously used to purify LOXL2. *siRNA* will be generated using the Dicer siRNA generation kit (Gene Therapy Systems, Inc., San Diego, CA) which mimics the natural RNA interference process by using recombinant human dicer enzyme to digest dsRNA into a pool of 22 bp siRNAs, simulating naturally occurring small temporal RNAs (stRNAs) and microRNAs (miRNAs) to degrade the homologous mRNA transcript. The mixture of siRNAs generated has a greater chance of success and is more efficient than the usual method of designing and testing several single siRNAs. This post-transcriptional gene silencing method eliminates gene expression more efficiently and effectively than the use of anti-sense transfection (McManus and Sharp, 2002) or the previously used long dsRNA which resulted in non-specific gene suppression due in part to an interferon response (Clemens, 1997).

Specific Aim 2: Establish if LOXL2 has amine oxidase activity and if this catalytic activity is necessary to induce cell migration and invasion

Rationale: Amine oxidase activity has been documented for LOX, LOXL and LOXL4. Although similar activity has yet to be shown for LOXL2, it contains the LTQ and copper-binding domain necessary for catalytic activity, and has close homology to LOXL4. In the first part of this aim, I plan to test the amine oxidase activity of purified LOXL2 protein, isolated by immunoprecipitation from MDA-MB-231 and Hs578T cultured cell media and cell layer. Alternatively, transient transfection of a LOXL2 cDNA construct into MCF-7 and T47D cells, followed by evaluation of the cultured cell media and cell layer for activity will be done. The addition of βAPN, a specific inhibitor of LOX, is used to indicate the amount of catalytic activity attributable to lysyl oxidase, but the effect of βAPN on LOXL2 is not known. As an alternative strategy to eliminate LOXL2 activity, siRNA will be used to silence LOXL2 expression and evaluate catalytic activity due solely to LOXL2, and by comparison with βAPN treatment, the effectiveness of βAPN inhibition can be determined. The use of siRNA will also address if βAPN has an effect on migration and invasion through a different mechanism than its inhibition of LOXL2. Loss of LOXL2 expression due to siRNA will be confirmed using Western analysis. In the second part of this aim, catalytic activity will be inhibited in transfected MCF-7 and T47D cells to evaluate whether LOXL2 amine oxidase activity is necessary for the ability to induce migration or invasion.

Methodology: In addition to methods described in Aim 1, *cell culture* will use phenol red-free media as phenol red interferes with the activity assay. *Amine oxidase activity will be measured using a fluorometric assay* (Palamakumbura and Trackman, 2002)

already implemented in our lab. This assay uses the synthetic substrate 1,5 diamino-

pentane (Sigma), and the generation of the side-product hydrogen peroxide, is detected

by Amplex Red (Molecular Probes). *Inhibition by BAPN* will be used in concentrations of

100 and 200 μM, which we have previously used to inhibit LOX activity, along with

solvent-only control. Catalytic activity will be inhibited in LOXL2-transfected MCF-7

and T47D breast cancer cells followed by evaluation for migratory and invasive ability.

Specific Aim 3: Determine the role of the individual LOXL2 protein domains in contributing to migratory and invasive action, focusing first on the CRL domain

Rationale: In aim 2, I expect LOXL2 amine oxidase activity to be necessary for

migratory and invasive action. However, my hypothesis is that amine oxidase activity

must be accompanied by protein-protein interaction in order for LOXL2 to induce

migration and invasion. Both the CRL and SRCR domains of LOXL2 are novel domains

that may be capable of protein interaction. These interaction domains could potentially

control activity and substrate specificity of the enzyme, and target LOXL2 to a specific

localization necessary for its function. I plan to initially focus on the C-terminal CRL

domain for the following reasons. The CRL domain is unique to the LOX family, and we

have recently found that the CRL domain of LOX is able to bind fibronectin, an

important component of the ECM. The CRL domain of LOXL2 may also interact with

ECM proteins and influence migration over the synthetic basement membrane. A LOXL2

construct with most of the CRL removed, but containing the tyrosine necessary for LTQ

182

formation and catalytic activity, will be evaluated for activity and its ability to induce

migration and invasion by transfection into MCF-7 and T47D cells. Results from this

aim, together with our concurrent yeast-two hybrid screen showing LOXL2 binding to

ECM molecules and growth factors, will support a functional role of the CRL domain.

Methodology: *Deletion analysis* will be done by creating a construct with most of the

CRL domain deleted but which still retains catalytic activity. Catalytic activity will be

evaluated as described in the methodology of Aim 2. This construct will be placed in an

adenovirus expression system, then transfected into MCF-7 and T47D breast cancer cell

lines, which will be evaluated for migration and invasiveness.

This dissertation has demonstrated the association between LOX and LOXL2

expression, and tumor development. There is strong evidence to indicate that LOXL2 is

involved in epithelial-mesenchymal transition and in inducing tumor cell invasiveness.

Through my future research strategy as outlined in my specific aims, the functional

aspects of this association will be addressed for LOXL2 and will describe the role of this

protein and its enzymatic activity in the critical but poorly understood process of tumor

invasion. The current and future studies have and will contribute to the general

understanding of cancer biology and to the function of one member of this very

interesting amine oxidase family.

REFERENCES

Aaltonen, L.A., Peltomaki, P., Leach, F.S., Sistonen, P., Pylkkanen, L., Mecklin, J.P., Jarvinen, H., Powell, S.M., Jen, J., Hamilton, S.R., Petersen, G.M., Kinzler, K.W., Vogelstein, B. and de la Chapelle, A. Clues to the pathogenesis of familial colorectal cancer. Science 1993; 260: 812-816.

Akagawa, M. and Suyama, K. Characterization of a model compound for the lysine tyrosylquinone cofactor of lysyl oxidase. Biochemical and Biophysical Research Communications 2001; 281: 193-199.

Akiri, G., Sabo, E., Dafni, H., Vadasz, Z., Kartvelishvily, Y., Gan, N., Kessler, O., Cohen, T., Resnick, M., Neeman, M. and Neufeld, G. Lysyl oxidase-related protein-1 promotes tumor fibrosis and tumor progression in vivo. Cancer Research 2003; 63: 1657-1666.

Albini, A., Iwamoto, Y., Kleinman, H.K., Martin, G.R., Aaronson, S.A., Kozlowski, J.M. and McEwan, R.N. A rapid *in vitro* assay for quantitating the invasive potential of tumor cells. Cancer Research 1987; 47: 3239-3345.

Almassian, B., Trackman, P.C., Iguchi, H., Boak, A., Calvaresi, D. and Kagan, H.M. Induction of lung lysyl oxidase activity and lysyl oxidase protein by exposure of rats to

cadmium chloride: properties of the induced enzyme. Connective Tissue Research 1991; 25: 197-208.

Antequera, F. and Bird, A. Number of CpG islands and genes in human and mouse. Proceedings of the National Academy of Sciences U.S.A. 1993; 90-11995-11999.

Anthony, C. Quinoprotein-catalyzed reactions. Biochemical Journal 1996; 320: 697-711.

Aoki, T., Mori, T., Du, X., Nishiira, T., Matsubara, T. and Nakamura, Y. Allelotype study of esophageal carcinoma. Genes, Chromosomes and Cancer 1994; 10: 177-182.

Arai, T., Akiyama, Y., Nagasaki H., Murase, N., Okabe, S., Ikeuchi, T., Saito, K., and Yuasa, Y. EXTK3/EXTR1 alterations in colorectal cancer cell lines. International Journal of Oncology 1999; 15: 915-919.

Arai, T., Akiyama, Y., Yamamura, A., Hosoi, T., Shibata, T., Saitoh, K., Okabe, S. and Yuasa, Y. Allelotype analysis of early colorectal cancers with lymph node metastasis. International Journal of Cancer 1998: 79: 418-423.

Arsura, M., Mercurio, F., Oliver, A.L., Thorgeirsson, S.S. and Sonenshein, G.E. Role of the IκB kinase complex in oncogenic Ras- and Raf-mediated transformation of rat liver epithelial cells. Molecular and Cellular Biology 2000; 20: 5381-5391.

Aruffo, A., Bowen, M.A., Patel, D.D., Haynes, B.F., Starling, G.C., Gebe, J.A. and

Bajorath, J. CD6-ligand interactions: a paradigm for SRCR domain function?

Immunology Today 1997; 18: 498-504.

Asuncion, L., Fogelgren, B., Fong, K.S.K., Fong, S.F.T., Kim, Y. and Csiszar, K. A

novel human lysyl oxidase-like gene (LOXL4) on chromosome 10q24 has an altered

scavenger receptor cysteine rich domain. Matrix Biology 2001; 20: 487-491.

Baker, S.J., Fearon, E.R., Nigro, J.M., Hamilton, S.R., Preisinger, A.C., Jessup, J.M.,

vanTuinen, P., Ledbetter, D.H., Barker, D.F., Nakamura ,Y., White, R. and Vogelstein,

B. Chromosome 17 deletions and p53 gene mutations in colorectal carcinomas. Science

1989; 244: 217-221.

Barth, T.F., Bentz, M., Leithauser, F., Stilgenbauer, S., Siebert, R., Schlotter, M.,

Schlenk, R.F., Dohner, H. and Moller, P. Molecular-cytogenetic comparison of mucosa-

associated marginal zone B-cell lymphoma and large B-cell lymphoma arising in the

gastro-intestinal tract. *Genes, Chromosomes and Cancer 2001; 31: 316-325.*

Bazan, J.F. Structural design and molecular evolution of a cytokine receptor superfamily.

Proceedings of the National Academy of Sciences USA 1990; 87: 6934-6938.

Bhadra, U., Pal-Bhadra, M. and Birchler, J.A. Histone acetylation and gene expression analysis of sex lethal mutants in *Drosophila*. Genetics 2000; 155: 753-763.

Bhattacharyya, N.P., Ganesh, A., Phear, G., Richards, B., Skandalis, A. and Meuth, M. Molecular analysis of mutations in mutator colorectal carcinoma cell lines. Human Molecular Genetics 1995; 4: 2057-2064.

Bhattacharyya, N.P., Skandalis, A., Ganesh, A., Groden, J. and Meuth, M. Mutator phenotypes in human colorectal carcinoma cell lines. Proceedings of the National Academy of Sciences U.S.A. 1994; 91: 6319-6323.

Binda, C., Mattevi, A. and Edmondson, D.E. Structure-function relationships in flavo-enzyme-dependent amine oxidations: a comparison of polyamine oxidase and monoamine oxidase. Journal of Biological Chemistry 2002; 277: 23973-23976.

Bird, A. The essentials of DNA methylation. Cell 1992; 70: 5-8.

Bissell, M.J., Radisky, D.C., Rizki, A., Weaver, V.M. and Petersen, O.W. The organizing principle: microenvironmental influences in the normal and malignant breast. Differentiation 2002; 70: 537-546.

Boak, A.M., Roy, R., Berk, J., Taylor, L., Polgar, P., Goldstein, R.H. and Kagan, H.M. Regulation of lysyl oxidase expression in lung fibroblasts by transforming growth factor-$\beta 1$ and prostaglandin E2. American Journal of Respiratory Cell and Molecular Biology 1994; 11: 751-755.

Bodmer, W., Bailey, C., Bodmer, J., Bussey, H., Ellis, A., Gorman, P., Lucibello, F., Murday, V., Rider, S. and Scambler, P. Localization of the gene for familial adenomatous polyposis on chromosome 5. Nature 1987; 328: 614-616.

Borel, A., Eichenberger, D., Farjanel, J., Kessler, E., Gleyzal, C., Hulmes, D.J., Sommer, P. and Font, B. Lysyl oxidase-like protein from bovine aorta: Isolation and maturation to an active form by bone morphogenetic protein-1. Journal of Biological Chemistry 2001; 276: 48944-48949.

Bose, K.K., Chakraborty, J., Khuder, S., Smith-Mensah, W.H. and Robinson, J. Lysyl oxidase activity in the cells of flexor retinaculum of individuals with carpal tunnel syndrome. Journal of Occupational and Environmental Medicine 2000; 42: 582-587.

Boyd, C.D., Mariani, T.J., Kim, Y. and Csiszar, K. The size heterogeneity of human lysyl oxidase mRNA is due to alternate polyadenylation site and not alternate exon usage. Molecular Biology Reports 1995; 21: 95-103.

188

Boyer, B., Valles, A.M. and Edme, N. Induction and regulation of epitheilial-mesenchymal transitions. Biochemical Pharmacology 2000; 60: 1091-1099.

Breivik, J., Lothe, R.A., Meling, G.I., Rognum, T.O., Borresen-Dale, A.L. and Gaudernack, G. Different genetic pathways to proximal and distal colorectal cancer influenced by sex-related factors. International Journal of Cancer 1997; 74: 664-669.

Bronner, C.E., Baker, S.M. and Morrison, P.T. Mutation in the DNA mismatch repair gene homologue hMLH1 is associated with heriditary non-polyposis colon cancer. Nature 1994; 368: 258 – 261.

Bronson, R.E., Calaman, S.D., Traish, A.M. and Kagan, H.M. Stimulation of lysyl oxidase (EC 1.4.3.13) activity by testosterone and characterization of androgen receptors in cultured calf aorta smooth-muscle cells. Biochemical Journal 1987; 244: 317-323.

Butler E, Hardin J and Benson S. The role of lysyl oxidase and collagen crosslinking during sea urchin development. Experimental Cell Research 1987; 173: 174-182.

Byers, P.H., Siegel, R.C., Holbrook, K.A., Narayanan, A.S., Bornstein, P. and Hall, J.G. X-linked cutis laxa: defective cross-link formation in collagen due to decreased lysyl oxidase activity. New England Journal of Medicine 1980; 303: 61-65.

189

Carter, E.A., McCarron, M.J., Alpert, E. and Isselbacher, K.J. Lysyl oxidase and collagenase in experimental acute and chronic liver injury. Gastroenterology 1982; 82: 526-534.

Chanoki, M., Ishii, M., Kobayashi, H., Fushida, J., Yashiro, N., Hamada, T. and Ooshima, A. Increased expression of lysyl oxidase in skin with scleroderma. British Journal of Dermatology 1995; 133: 710-715.

Chernova, O. and Cowell, J.K. Molecular definition of chromosome translocations involving 10q24 and 19q13 in human malignant glioma cells. Cancer Genetics and Cytogenetics 1998; 105: 60-68.

Chichester, C.O., Palmer, K.C., Hayes, J.A. and Kagan, H.M. Lung lysyl oxidase and prolyl hydroxylase: increases induced by cadmium chloride inhalation and the effect of β-aminopropionitrile in rats. American Review of Respiratory Disease 1981; 124: 709-713.

Chinoy, M.R., Zgleszewski, S.E., Cilley, R.E. and Krummel, T.M. Dexamethasone enhances ras-recision gene expression in cultured murine fetal lungs: Role in development. American Journal of Physiology: Lung Cellular and Molecular Physiology 2000; 279: L312-318.

Choung, J., Taylor, L., Thomas, K., Zhou, X., Kagan, H., Yang, X. and Polgar, P. Role of EP2 receptors and cAMP in prostaglandin E2 regulated expression of type I collagen $\alpha 1$, lysyl oxidase, and cyclooxygenase-1 genes in human embryo lung fibroblasts. Journal of Cellular Biochemistry 1998; 71: 254-263.

Chung, D.C. and Rustgi, A.K. DNA mismatch repair and cancer. Gastroenterology 1995; 109: 1685-1699.

Clemens, M.J. PKR - a protein kinase regulated by double-stranded RNA. International Journal of Biochemistry and Cell Biology 1997; 29: 945-949.

Contegiacomo, A. Palmirotta, R., De Marchis, L., Pizzi, C., Mastranzo, P., Delrio, P., Petrella, G., Figliolini, M., Bianco, A.R., Frati, L., Cama, A. and Mariani-Costantini, R. Microsatellite instability and pathological aspects of breast cancer. International Journal of Cancer 1995; 64: 264-268.

Contente, S., Kenyon, K., Sriraman, P., Subramanyan, S. and Friedman, R.M. Epigenetic inhibition of lysyl oxidase transcription after transformation by *ras* oncogene. Molecular and Cellular Biochemistry 1999; 194: 79-91.

191

Contente, S., Kenyon, K., Rimoldi, D. and Friedman, R.M. Expression of gene *rrg* is associated with reversion of NIH 3T3 transformed by *LTR-c-H-ras*. Science 1990; 249: 796-798.

Counts, D.F., Evans, J.N., Dipetrillo, T.A., Sterling, K.M. Jr and Kelley, J. Collagen lysyl oxidase activity in the lung increases during bleomycin-induced lung fibrosis. Journal of Pharmacology and Experimental Therapeutics 1981; 219: 675-678.

Cronshaw, A.D., Fothergill-Gilmore, L.A. and Hulmes, D.J. The proteolytic processing site of the precursor of lysyl oxidase. Biochemical Journal 1995; 306: 279-284.

Csiszar, K., Fong, S.F.T., Ujfalusi, A., Krawetz, S.A., Salvati, E.P., Mackenzie, J.W. and Boyd, C.D. Somatic mutations of the lysyl oxidase gene on chromosome 5q23.1 in colorectal tumors. International Journal of Cancer 2002; 97: 636-642.

Csiszar, K. Lysyl oxidases: a novel multifunctional amine oxidase family. In: Moldave, K. (ed). Progress in Nuclear Acid Research and Molecular Biology, Volume 70, pp 1-32, Academic Press, San Diego, CA, 2001.

Csiszar, K., Jourdan-Le Saux, C., Fong, S.F.T., Fong, K.S.K. and Boyd, C.D. Lysyl oxidase: a family of multifunctional proteins. In: Iriarte, A., Kagan, H.M. and Martinez-

Carrion, M. (eds). Biochemistry and Molecular Biology of Vitamin B6 and PQQ-dependent Proteins, pp 91-96, Birkhauser Verlag, Basel, Switzerland, 2000.

Csiszar, K., Entersz, I., Trackman, P.C., Samid, D. and Boyd, C.D. Functional analysis of the promoter and first intron of the human lysyl oxidase gene. Molecular Biology Reports 1996; 23: 97-108.

Csiszar, K., Mariani, T.J., Gosin J.S., Deak S.B. and Boyd, C.D. A restriction fragment length polymorphism results in a nonconservative amino acid substitution encoded within the first exon of the human lysyl oxidase gene. Genomics 1993; 16: 401-406.

Cunningham, C., Dunlop, M.G., Wyllis, A.H. and Bird, C.C. Deletion mapping in colorectal cancer of a putative tumor suppressor gene in 8p22-p21.3. Oncogene 1993: 8: 1391-1396.

Curtis, L.J., Bubb, V.J., Gledhill, S., Morris, R.G., Bird, C.C. and Wyllie, A.H. Loss of heterozygosity of MCC is not associated with mutation of the retained allele in sporadic colorectal cancer. Human Molecular Genetics 1994; 3: 443-446.

Debeer, P., Schoenmakers, E.F., Twal, W.O., Argraves, W.S., De Smet, L., Fryns, J.P. and Van De Ven, W.J. The fibulin-1 gene (FBLN1) is disrupted in a t(12;22) associated with a complex type of synpolydactyly. Journal of Medical Genetics 2002; 39: 98-104.

193

Decitre M, Gleyzal C, Raccurt M, Peyrol S, Aubert-Foucher E, Csiszar K, Sommer P. Lysyl oxidase-like protein localizes to sites of de novo fibrinogenesis in fibrosis and in the early stromal reaction of ductal breast carcinoma. Laboratory Investigation 1998; 78: 143-151.

de la Chapelle, A. and Peltomaki, P. Genetics of hereditary colon cancer. Annual Review in Genetics 1995; 29: 329-348.

Diaz, R., Ahn, D., Lopez-Barcons, L., Malumbres, M., Perez de Castro, I., Lue, J., Ferrer-Miralles, N., Mangues, R., Tsong, J., Garcia, R., Perez-Soler, R. and Pellicer, A. The N-*ras* proto-oncogene can suppress the malignant phenotype in the presence or absence of its oncogene. Cancer Research 2002; 62: 4514-4518.

Di Donato, A., Ghiggeri, G.M., Di Duca, M., Jivotenko, E., Acinni, R., Campolo, J., Ginevri, F. and Gusmano, R. Lysyl oxidase expression and collagen cross-linking during chronic adriamycin nephropathy. Nephron 1997a; 76: 192-200.

Di Donato, A., Lacal, J.C., Di Duca, M., Giampuzzi, M., Ghiggeri, G. and Gusmano, R. Micro-injection of recombinant lysyl oxidase blocks oncogenic p21-Ha-Ras and progesterone effects on *Xenopus laevis* oocyte maturation. Federation of European Biochemical Societies (FEBS) Letters 1997b; 419: 63-68.

Dimaculangan, D.D., Chawla, A., Boak, A., Kagan, H.M. and Lazar, M.A. Retinoic acid prevents downregulation of *RAS* recision gene/lysyl oxidase early in adipocyte differentiation. *Differentiation* 1994; 58: 47-52.

Dove, J.E. and Klinman, J.P. Trihydroxyphenylalanine quinone (TPQ) from copper amine oxidases and lysyl tyrosyl quinone (LTQ) from lysyl oxidase. In: Klinman, J.P., Dove, J.E. (eds). Advances in Protein Chemistry, Volume 58, pp 141-174. Academic Press, San Diego, CA, 2001.

Dove, J.E., Smith, A.J., Kuchar, J., Brown, D.E., Dooley, D.M. and Klinman, J.P. Identification of the quinone cofactor in a lysyl oxidase from *Pichia pastoris*. Federation of European Biochemical Societies (FEBS) Letters 1996; 398: 231-234.

Du, W., Lebowitz, P.F. and Prendergast, G.C. Elevation of α2(I) collagen, a suppressor of Ras transformation, is required for stable phenotypic reversion by farnesyltransferase inhibitors. Cancer Research 1999; 59: 2059-2063.

Eyre, D.R., Paz, M.A. and Gallop, P.M. Cross-linking in collagen and elastin. Annual Reviews in Biochemistry 1984; 53: 717-748.

Fearon, E.R. and Gruber, S.B. Molecular abnormalities in colon and rectal cancer. In: Mendelsohn, J., Howley, P.M., Israel, M.A. and Liotta, L.A. (eds): The Molecular Basis of Cancer, 2nd edition. W.B. Saunders Company, Philadelphia, PA, 2001. pp. 289-312.

Fearon, E.R. and Vogelstein, B. A genetic model for colorectal tumorigenesis. Cell 1990; 61: 759-767.

Fearon, E.R., Cho, K.R., Nigro, J.M., Kern, S.E., Simons, J.W., Ruppert, J.M., Hamilton, S.R., Preisinger, A.C., Thomas, G., Kinzler K.W. and Vogelstein, B. Identification of a chromosome 18q gene that is altered in colorectal cancers. Science 1990; 247: 49-56.

Feres-Filho, E.J., Menassa, G.B. and Trackman, P.C. Regulation of lysyl oxidase by basic fibroblast growth factor in osteoblastic MC3T3-E1 cells. Journal of Biological Chemistry 1996; 271: 6411-6416.

Feres-Filho, E.J., Choi, Y.J., Han, X., Takala, T.E. and Trackman, P.C. Pre- and post-translational regulation of lysyl oxidase by transforming growth factor-β1 in osteoblastic MC3T3-E1 cells. Journal of Biological Chemistry 1995; 270: 30797-30803.

Friedman, R.M., Yeh, A., Gutman, P., Contente, S. and Kenyon, K. Reversion by deletion of transforming oncogene following interferon-β and retinoic acid treatment. Journal of Interferon and Cytokine Research 1997; 17: 647-651.

Friedman, R.M., Yeh, A., Gutman, P., Contente, S. and Kenyon, K. Reversion by deletion of transforming oncogene following interferon-β and retinoic acid treatment. Journal of Interferon and Cytokine Research 1997; 17: 647-651.

Fukushima, M., Fukuda, Y., Kawamoto, M. and Yamanaka, N. Elastosis in lung carcinoma: Immunohistochemical, ultrastructural and clinical studies. Pathology International 2000; 50: 1004-1013.

Gacheru, S.N., Thomas, K.M., Murray, S.A., Csiszar, K., Smith-Mungo, L.I. and Kagan, H.M. Transcriptional and post-transcriptional control of lysyl oxidase expression in vascular smooth muscle cells: effects of TGF-β1 and serum deprivation. Journal of Cellular Biochemistry 1997; 65: 395-407.

Gacheru, S., McGee, C., Uriu-Hare, J.Y., Kosonen, T., Packman, S., Tinker, D., Krawetz, S.A., Reiser, K., Keen, C.L. and Rucker, R.B. Expression and accumulation of lysyl oxidase, elastin, and type I procollagen in human Menkes and mottled mouse fibroblasts. Archives of Biochemistry and Biophysics 1993; 301: 325-329.

Gacheru, S.N., Trackman, P.C., Shah, M.A., O'Gara, C.Y., Spacciapoli, P., Greenaway, F.T. and Kagan, H.M. Structural and catalytic properties of copper in lysyl oxidase. Journal of Biological Chemistry 1990; 265: 19022-19027.

Gardiner-Garden, M. and Frommer, M. CpG islands in vertebrate genomes. Journal of Molecular Biology 1987; 196: 261-282.

Garinis, G.A., Patrinos, G.P., Spanakis, N.E. and Menounos, P.G. DNA hypermethylation: When tumor suppressor genes go silent. Human Genetics 2002; 111: 115-127.

Giampuzzi, M., Oleggini, R. and Di Donato, A. Demonstration of in vitro interaction between tumor suppressor lysyl oxidase and histones H1 and H2: definition of the regions involved. Biochimica et Biophysica Acta 2003; 1647: 245-251.

Giampuzzi, M., Botti, G., Cilli, M., Gusmano, R., Borel, A., Sommer, P. and Di Donato, A. Down regulation of lysyl oxidase induced tumorigenic transformation in NRK-49F cells characterized by constitutive activation of Ras proto-oncogene. Journal of Biological Chemistry 2001; 276: 29226-29232.

Giampuzzi, M., Botti, G., Di Duca, M., Arata, L., Ghiggeri, G., Gusmano, R., Ravazzolo, R. and Di Donato, A. Lysyl oxidase activates the transcription activity of human collagene III promoter. Possible involvement of Ku antigen. Journal of Biological Chemistry 2000; 275: 36341-39349.

Gohla, A., Exkert, K. and Maurer, H.R. A rapid and sensitive fluorometric screening assay using YO-PRO-1 to quantify tumour cell invasion through Matrigel. Clinical and Experimental Metastasis 1996; 14: 451-458.

Goy, A., Gilles, F., Remache, Y. and Zelenetz, A.D. Physical linkage of the lysyl oxidase-like (LOXL1) gene to the PML gene on human chromosome 15q22. Cytogenetics and Cell Genetics 2000; 88: 22-24.

Gozzetti, A., Davis, E.M., Espinosa, R. 3rd, Fernald, A.A., Anastasi, J. and Le Beau, M.M. Identification of novel cryptic translocations involving IGH in B-cell non-Hodgkin's lymphomas. Cancer Research 2002; 62: 5523-5527.

Graversen, J.H., Madsen, M. and Moestrup, S.K. CD163: a signal receptor scavenging haptoglobin-hemoglobin complexes from plasma. International Journal of Biochemistry and Cell Biology 2002; 34: 309-314.

Green, R.S., Lieb, M.E., Weintraub, A.S., Gacheru, S.N., Rosenfield, C.L., Shah, S., Kagan, H.M. and Taubman, M.B. Identification of lysyl oxidase and other platelet-derived growth factor-inducible genes in vascular smooth muscle cells by differential screening. Laboratory Investigation 1995; 73: 476-482.

Grunert, S., Jechlinger, M. and Beug, H. Diverse cellular and molecular mechanisms contribute to epithelial plasticity and metastasis. Nature Reviews Molecular Cell Biology 2003; 4: 657-665.

Hajnal, A., Klemenz, R. and Schafer, R. Up-regulation of lysyl oxidase in spontaneous revertants of H-*ras*-transformed rat fibroblasts. Cancer Research 1993; 53: 4670-4675.

Hamalainen, E.R., Kemppainen, R., Kuivaniemi, H., Tromp, G., Veheri, A., Pihlajaniemi, T. and Kivirikko, K.I. Quantitative polymerase chain reaction of lysyl oxidase mRNA in malignantly transformed human cell lines demonstrates that their low lysyl oxidase activity is due to low quantities of its mRNA and low levels of transcription of the respective gene. Journal of Biological Chemistry 1995; 270: 21590-21593.

Hamalainen, E.R., Kemppainen, R., Pihlajaniemi, T. and Kivirikko. K.I. Structure of the human lysyl oxidase gene. Genomics 1993; 17: 544-548.

Hamalainen, E.R., Jones, T.A., Sheer, D., Taskinen, K., Pihlajaniemi, T. and Kivirikko, K.I. Molecular cloning of human lysyl oxidase and assignment of the gene to chromosome 5q23.3-31.2. Genomics 1991; 11: 508-516.

Harlow, C.R., Rae, M., Davidson, L., Trackman, P.C. and Hillier, S.G. Lysyl oxidase gene expression and enzyme activity in the rat ovary: regulation by follicle-stimulating

hormone, androgen, and transforming growth factor-β superfamily members *in vitro*. Endocrinology 2003; 144: 154-162.

Harlow, E. and Lane, D. (eds) *Using Antibody: a Laboratory Manual.* Cold Spring Harbor Laboratory Press, Cold Spring Harbor, NY, 1999.

Hein, S., Yamamoto, S.Y., Okazaki, K., Jourdan-Le Saux, C., Csiszar, K. and Bryant-Greenwood, G.D. Lysyl oxidases: Expression in the fetal membranes and placenta. Placenta 2001; 22: 49-57.

Hendrix, M.J.C., Seftor, E.A., Hess, A.R. and Seftor, R.E.B. Vasculogenic mimicry and tumor cell plasticity: lessons from melanoma. Nature Reviews Cancer 2003; 3: 411-421.

Hendrix, M.J.C., Seftor, E.A., Seftor, R.E.B. and Trevor, K.T. Experimental co-expression of vimentin and keratin intermediate filaments in human breast cancer cells results in phenotypic interconversion and increased invasive behavior. American Journal of Pathology 1997; 150: 483-495.

Hendrix, M.J.C., Seftor, E.A. and Fidler, I.J. A simple quantitative assay for studying the invasive potential of high and low human metastatic variants. Cancer Letters 1987; 38: 137-147.

Hohenester, E. and Engel, J. Domain structure and organisation in extracellular matrix proteins. Matrix Biology 2002; 21: 115-128.

Hohenester, E., Sasaki, T. and Timpl, R. Crystal structure of a scavenger receptor cysteine-rich domain sheds light on an ancient superfamily. Nature Structural Biology 1999; 6: 228-232.

Holtmeier, C., Gorogh, T., Beier, U., Meyer, J., Hoffman, M., Gottschlich, S., Heidorn, K., Anbrosch, P. and Maune, S. Overexpression of a novel lysyl oxidase-like gene in human head and neck squamous cell carcinoma. Anticancer Research 2003; 23: 2585-2591.

Hong, H.H. and Trackman, P.C. Cytokine regulation of gingival fibroblast lysyl oxidase, collagen, and elastin. Journal of Periodontology 2002; 73: 145-52.

Hong, H.H., Uzel, M.I., Duan, C., Sheff, M.C. and Trackman, P.C. Regulation of lysyl oxidase, collagen, and connective tissue growth factor by TGF-β1 and detection in human gingiva. Laboratory Investigation 1999; 79: 1655-1667.

Hough, C.D., Sherman-Baust, C.A., Pizer, E.S., Montz, F.J., Im, D.D., Rosenshein, N.B., Cho, K.R., Riggins, G.J. and Morin, P.J. Large-scale serial analysis of gene expression

reveals genes differentially expressed in ovarian cancer. Cancer Research 2000; 60: 6281-6287.

Hu, N., Roth, M.J., Polymeropolous, M., Tang, Z.Z., Emmert-Buck, M.R., Wang, Q.H., Goldstein, A.M., Feng, S.S., Dawsey, S.M., Ding, T., Zhuang, Z.P., Han, X.Y., Ried, T., Giffen, C. and Taylor, P.R. Identification of novel regions of allelic loss from a genomewide scan of esophageal squamous-cell carcinoma in a high-risk Chinese population. *Genes, Chromosomes and Cancer* 2000; 27: 217-228.

Huang, Y., Dai, J., Tang, R., Zhao, W., Zhou, Z., Wang, W., Ying, K., Xie, Y. and Mao, Y. Cloning and characterization of a human lysyl oxidase-like 3 gene (hLOXL3). *Matrix Biology* 2001; 20: 153-157.

Hughes, S.A., Carothers, A.M., Hunt, D.H., Moran, A.E., Mueller, J.D. and Bertagnolli, M.M. Adenomatous polyposis coli truncation alters cytoskeletal structure and microtubule stability in early intestinal tumorigenesis. *Journal of Gastrointestinal Surgery* 2002; 6: 868-875.

Iacopetta, B., DiGrandi, S., Dix, B., Haig, C., Soong, R. and House, A. Loss of heterozygosity of tumor suppressor gene loci in colorectal carcinoma. *European Journal of Cancer* 1994; 30A: 664-670.

International Agency for Research on Cancer, Unit of Descriptive Epidemiology, GLOBOCAN 2000. http://www-dep.iarc.fr/

Ishii, H., Baffa, R., Numata, S.I., Murakumo, Y., Rattan, S., Inoue, H., Mori, M., Fidanza, V., Alder, H. and Croce, C.M. The FEZ1 gene at chromosome 8p22 encodes a leucine-zipper protein, and its expression is altered in multiple human tumors. Proceedings of the National Academy of Sciences U.S.A. 1999; 96: 3928-3933.

Ito, H., Akiyama, H., Iguchi, H., Iyama, K.I., Miyamoto, M., Ohsawa, K. and Nakamura, T. Molecular cloning and biological activity of a novel lysyl oxidase-related gene expressed in cartilage. Journal of Biological Chemistry 2001; 276: 24023-24029.

Itoh, S., Harada, H., Nakamura, Y., White, R. and Taniguchi, T. Assignment of the human interferon regulatory factor-1 (IRF1) gene to chromosome 5q23-q31. Genomics 1991; 10: 1097-1099.

Jalkanen, S. and Salmi, M. Cell surface monoamine oxidases: enzymes in search of function. The European Molecular Biology Organization (EMBO) Journal 2001; 20: 3893-3901.

Jang, W., Hua, A., Spilson, S.V., Miller, W., Roe, B.A., Meisler, M.H. Comparative sequence of human and mouse BAC clones from the mnd2 region of chromosome 2p13. Genome Research 1999; 9: 53-61.

Jeay, S., Pianetti, S., Kagan, H.M. and Sonenshein, G.E. Lysyl oxidase inhibits ras-mediated transformation by preventing activation of NF-κB. Molecular and Cellular Biology 2003; 23: 2251-2263.

Jemal, A., Murray, T., Samuels, A., Ghafoor, A., Ward, E. and Thun, M..J. Cancer statistics, 2003. A Cancer Journal for Clinicians 2003; 53: 5-26.

Jenuwein, T., and Allis, C.D. Translating the histone code. Science 2001; 293: 1074-1080.

Jiang, Y., Zhang, W., Kondo, K., Klco, J.M., St Martin, T.B., Dufault, M.R., Madden, S.L., Kaelin, W.G. Jr. and Nacht, M. Gene Expression Profiling in a Renal Cell Carcinoma Cell Line: Dissecting VHL and Hypoxia-Dependent Pathways. Molecular Cancer Research 2003; 1: 453-462.

Joslyn, G., Carlson, M., Thliveris, A., Albertsen, H., Gelbert, L., Samowitz, W., Groden, J., Stevens, J., Spirio, L., Robertson, M., Sargeant, L., Krapcho, K., Wolff, E., Burt, R., Hughes, J.P., Warrington, J., McPherson, J., Wasmuth, J., LePaslier, D., Abderrahim, H.,

Cohen, D., Leppert, M. and White, R. Identification of deletion mutations and three new genes at the familial polyposis locus. Cell 1991; 66: 601-613.

Jourdan-Le Saux, C., Tomsche, A., Ujfalusi, A., Jia, L. and Csiszar, K. Central nervous system, uterus, heart, and leukocyte expression of the loxl3 gene, encoding a novel lysyl oxidase-like protein. Genomics 2001; 74: 211-218.

Jourdan-Le Saux, C., Tronecker, H., Bogic, L., Bryant-Greenwood, G.D., Boyd, C.D. and Csiszar, K. The LOXL2 gene encodes a new lysyl oxidase-like protein and is expressed at high levels in reproductive tissues. Journal of Biological Chemistry 1999; 274: 12939-12944.

Jourdan-Le Saux, C., Le Saux, O., Donlon, T., Boyd, C. and Csiszar, K. The human lysyl oxidase related gene (LOXL2) maps between markers D8S280 and D8S278 on chromosome 8p 21.2-21.3. Genomics 1998: 51: 301-307.

Kagan, H.M. and Li, W. Lysyl oxidase: Properties, specificity, and biological roles inside and outside of the cell. Journal of Cellular Biochemistry 2003; 88: 660-672.

Kagan, H.M., Reddy, V.B., Narasimhan, N. and Csiszar, K. Catalytic properties and structural components of lysyl oxidase. In: Mecham, R.P. and Roberts, D.D. (eds)

Molecular Biology and Pathology of Elastic Tissue, Ciba Foundation Symposium Series 1995;192:100-115.

Kagan, H.M. Characterization and regulation of LO. In: Mecham, R.P. (ed) Biology of the Extracellular Matrix, Academic Press, Orlando, FL, 1986, pp. 321-398.

Kagan, H.M., Williams, M.A., Calaman, S.D. and Berkowitz, E.M. Histone H1 is a substrate for lysyl oxidase and contains endogenous sodium borotritide-reducible residues. Biochemical and Biophyscal Research Communications 1983; 115: 186-192.

Kanazawa, T., Watanabe, T., Kazama, S., Tada, T., Koketsu, S. and Nagawa, H. Poorly differentiated adenocarcinoma and mucinous carcinoma of the colon and rectum show higher rates of loss of heterozygosity and loss of E-cadherin expression due to methylation of promoter region. International Journal of Cancer 2002; 102: 225-229.

Kaneda, A., Kaminishi, M., Yanagihara, K., Sugimura, T. and Ushijima, T. Identification of silencing of nine genes in human gastric cancers. Cancer Research 2002; 62: 6645-6650.

Kato, K., Cox, A.D., Hisaka, M.M., Graham, S.M., Buss, J.E. and Der, C.J. Isoprenoid addition to Ras protein is the critical modification for its membrane association and

transforming activity. Proceedings of the National Academy of Science U.S.A. 1992; 89: 6403-6407.

Kauppila, S., Stenback, F., Risteli, J., Jukkola, A. and Risteli, L. Aberrant type I and type III collagen gene expression in human breast cancer *in vivo*. Journal of Pathology 1998; 186: 262-268.

Kemppainen, R., Hamalainen, E.R., Kuivaniemi, H., Tromp, G., Pihlajaniemi, T. and Kivirikko, K.I. Expression of mRNAs for lysyl oxidase and type III procollagen in cultured fibroblasts from patients with the Menkes and occipital horn syndromes as determined by quantitative polymerase chain reaction. Archives of Biochemistry and Biophysics 1996; 328: 101-106.

Kenyon, K., Contente, S., Trackman, P.C., Tang, J., Kagan, H.M. and Friendman, R.M. Lysyl oxidase and *rrg* messenger RNA. Science 1991; 253: 802.

Kern, S.E. Progressive genetic abnormalities in human neoplasia. In: Mendelsohn, J., Howley, P.M., Israel, M.A. and Liotta, L.A. (eds) The Molecular Basis of Cancer, 2nd edition. W.B. Saunders Company, Philadelphia, PA, 2001. pp. 41-69.

Kiemer, A.K., Takeuchi, K. and Quinlan, M.P. Identification of genes involved in epithelial-mesenchymal transition and tumor progression. Oncogene 2001; 20: 6679-6688.

Kierszenbaum, A.L. Histology and Cell Biology. Mosby, St. Louis, MO. 2002.

Kim, G.J., Park, S.Y., Kim, H., Chun, Y.H. and Park, S.H. Chromosomal aberrations in neuroblastoma cell lines identified by cross species color banding and chromosome painting. Cancer Genetics and Cytogenetics 2001; 129: 10-16.

Kim, Y., Peyrol, S., So, C.K., Boyd, C.D. and Csiszar, K. Coexpression of the lysyl oxidase-like gene (LOXL) and the gene encoding type III procollagen in induced liver fibrosis. Journal of Cellular Biochemistry 1999; 72: 181-188.

Kim, S.K., Ro, J.Y., Kemp, B.L., Lee, J.S., Kwon, T.J., Hong, W.K. and Mao, L. Identification of two distinct tumor-suppressor loci on the long arm of chromosome 10 in small cell lung cancer. Oncogene 1998; 17: 1749-1753.

Kim, Y., Boyd, C.D. and Csiszar, K. A highly polymorphic (CA) repeat sequence in the human lysyl oxidase-like gene. Clinical Genetics 1997; 51: 131-132.

Kim, Y., Boyd, C.D. and Csiszar, K. A new gene with sequence and structural similarity to the gene encoding human lysyl oxidase. *Journal of Biological Chemistry* 1995; 270: 7176-7182.

Kimmelman, A., Bafico, A. and Aaronson, S.A. Oncogenes and signal transduction. In: Mendelsohn, J., Howley, P.M., Israel, M.A. and Liotta, L.A. (eds) The Molecular Basis of Cancer, 2nd edition. W.B. Saunders Company, Philadelphia, PA, 2001. pp. 115-133.

King, B.L., Carcangiu, M.L., Carter, D., Kiechle, M., Pfisterer, J., Pfleiderer, A. and Kacinski, B.M. Microsatellite instability in ovarian neoplasms. *British Journal of Cancer* 1995; 72: 376-382.

Kinzler, K. and Vogelstein, B. Lessons from hereditary colorectal cancer. *Cell* 1996; 87: 159-170.

Kinzler, K.W., Nilbert, M.C., Su, L.K., Vogelstein, B., Bryan, T.M., Levy, D.B., Smith, K.J., Preisinger, A.C., Hedge, P., McKechnie, D., Finniear, R., Markham, A., Groffen, J., Boguski, M.S., Altschul, S.F., Horii, A., Ando, H., Miyoshi, Y., Miki, Y., Nishisho, I. and Nakamura, Y. Identification of FAP locus genes from chromosome 5q21. *Science* 1991a; 253: 661-665.

Kinzler, K.W., Nilbert, M.C., Vogelstein, B., Bryan, T.M., Levy, D.B., Smith, K.J., Preisinger, A.C., Hamilton, S.R., Hedge, P., Markham, A., Carlson, M., Joslyn, G., Groden, J., White, R., Miki, Y., Miyoshi, Y., Nishisho, I. and Nakamura, Y. Identification of a gene located at chromosome 5q21 that is mutated in colorectal cancers. Science 1991b; 251: 1366-1370.

Kirschmann, D.A., Seftor, E.A., Fong, S.F.T., Nieva, D.R.C., Sullivan, C.M., Edwards, E.M., Sommer, P., Csiszar, K. and Hendrix, M.J.C. A molecular role for lysyl oxidase in breast cancer invasion. Cancer Research 2002; 62: 4478-83.

Kirschmann, D.A., Seftor, E.A., Nieva, D.R.C., Mariano, E.A. and Hendrix, M.J.C. Differentially expressed genes associated with the metastatic phenotype in breast cancer. Breast Cancer Research and Treatment 1999; 55: 127-136.

Knudson, A.G. Jr. Mutation and cancer: Statistical study of retinoblastoma. Proceedings of the National Academy of Sciences U.S.A. 1971; 68: 820-823.

Kolligs, F.T., Bommer, G. and Goke, B. Wnt/Beta-catenin/tcf signaling: a critical pathway in gastrointestinal tumorigenesis. Digestion 2002; 66: 131-144.

Kosonen, T., Uriu-Hare, J.Y., Clegg, M.S., Keen, C.L. and Rucker, R.B. Incorporation of copper into lysyl oxidase. Biochemical Journal 1997; 327: 283-289.

Krebs, C.J. and Krawetz, S.A. Lysyl oxidase copper-talon complex: a model. Biochimica et Biophysica Acta 1993; 1202: 7-12.

Krismann, M., Muller, K.M., Jaworska, M. and Johnen, G. Molecular cytogenetic differences between histological subtypes of malignant mesotheliomas: DNA cytometry and comparative genomic hybridization of 90 cases. Journal of Pathology 2002; 197: 363-371.

Krzyzosiak, W.J., Shindo-Okada, N., Teshima, H., Nakajima, K. and Nishimura, S. Isolation of genes specifically expressed in flat revertant cells derived from activated ras-transformed NIH 3T3 cells by treatment with azatyrosine. Proceedings of the National Academy of Science U.S.A. 1992; 89: 4879-4883.

Kuivaniemi, H., Korhonen, R.M., Vaheri A. and Kivirikko, K.I. Deficient production of lysyl oxidase in cultures of malignantly transformed human cells. Federation of European Biochemical Societies (FEBS) Letters 1986; 195: 261-264.

Kuivaniemi, H., Peltonen, L. and Kivirikko, K.I. Type IX Ehlers-Danlos syndrome and Menkes syndrome: the decrease in lysyl oxidase activity is associated with a corresponding deficiency in the enzyme protein. American Journal of Human Genetics 1985; 370: 798-808.

Lasko, D., Cavenee, W. and Nordenskjold, M. Loss of constitutional heterozygosity in human cancer. Annual Review of Genetics 1991; 25: 281-314.

Lazarus, H.M., Cruikshank, W.W., Narasimhan, N., Kagan, H.M. and Center, D.M. Induction of human monocyte motility by lysyl oxidase. Matrix Biology 1995; 14: 727-731.

Lengauer, C., Kinzler, K.W. and Vogelstein, B. Genetic instabilities in human cancers. Nature 1998; 396: 643-649.

Leonard, D.M. Ras farnesyltransferase: a new therapeutic target. Journal of Medical Chemistry 1997; 40: 2971-2990.

Leppert, M., Dobbs, M., Scambler, P., O'Connell, P., Nakamura, Y., Stauffer, D., Woodward, S., Burt, R., Hughes, J., Gardner, E. and White, R. The gene for familial polyposis maps to the long arm of chromosome 5. Science 1987; 238: 1411-1443.

Lerebours, F., Olschwang, S., Thuille, B., Schmitz, A., Fouchet, P., Laurent-Puig, P., Boman, F., Flejou, J.F., Monges, G., Paraf, F., Bedossa, P., Sabourin, J.C., Salmon, R.J., Parc, R. and Thomas, G. Deletion mapping of the tumor suppressor locus involved in colorectal cancer on chromosome band 8p21. Genes Chromosomes Cancer 1999; 25: 147-153.

Leube, B., Drechsler, M., Muhlmann, K., Schafer, R., Schulz, W.A., Santourlidis, S., Anastasiadis, A., Ackermann, R., Visakorpi, T., Muller, W. and Royer-Pokora, B. Refined mapping of allele loss at chromosome 10q23-26 in prostate cancer. Prostate 2002; 50: 135-144.

Li, W., Nugent, M.A., Zhao, Y., Chau, A.N., Li, S.J., Chou, I.N., Liu, G. and Kagan, H.M. Lysyl oxidase oxidizes basic fibroblast growth factor and inactivates its mitogenic potential. Journal of Cellular Biochemistry 2003; 88: 152-164.

Li, W., Liu, G., Chou, I.N. and Kagan, H.M. Hydrogen peroxide-mediated, lysyl oxidase-dependent chemotaxis of vascular smooth muscle cells. Journal of Cellular Biochemistry 2000; 78: 550-557.

Li, W., Nellaiappan, K., Strassmaier, T., Graham, L., Thomas, K.M. and Kagan, H.M. Localization and activity of lysyl oxidase within nuclei of fibrogenic cells. Proceedings of the National Academy of Sciences U.S.A. 1997; 94: 12817-12822.

Li, W., Chou, I.N., Boak, A. and Kagan, H.M. Downregulation of lysyl oxidase in cadmium-resistant fibroblasts. American Journal of Respiratory Cell and Molecular Biology 1995; 13: 418-425.

Liehr, J.G. Is estradiol a genotoxic mutagenic carcinogen? Endocrine Reviews 2000; 21: 40-54.

Liu, B., Nicolaides, N.C., Markowitz, S., Willson, J.K., Parsons, R.E., Jen, J., Papadopolous, N., Peltomaki, P., de la Chapelle, A., Hamilton, S.R., Kinzler, K.W. and Vogelstein, B. Mismatch repair gene defects in sporadic colorectal cancers with microsatellite instability. Nature Genetics 1995; 9: 48-55.

Loeb, L.A. A mutator phenotype may be required for multi-stage carcinogenesis. Cancer Research 1991; 51: 3075-3079.

Lu, N., Hu, N., Li, W.J., Roth, M.J., Wang, C., Su, H., Wang, Q.H., Taylor, P.R. and Dawsey, S.M. Microsatellite alterations in esophageal dysplasia and squamous cell carcinoma from laser capture microdissected endoscopic biopsies. Cancer Letters 2003; 189:137-145.

Maki, J.M., Rasanen, J., Tikkanen, H., Sormunen, R., Makikallio, K., Kivirikko, K.I. and Soininen, R. Inactivation of the lysyl oxidase gene Lox leads to aortic aneurysms, cardiovascular dysfunction, and perinatal death in mice. Circulation 2002; 106: 2503-2509.

Maki, J.M. and Kivirikko, K.I. Cloning and characterization of a fourth human lysyl oxidase isoenzyme. Biochemical Journal 2001; 355: 381-387.

Maki, J.M., Tikkanen, H. and Kivirikko, K.I. Cloning and characterization of a fifth human lysyl oxidase isoenzyme: the third member of the lysyl oxidase-related subfamily with four scavenger receptor cysteine-rich domains. Matrix Bioogy 2001; 20: 493-496.

Maniotis, A.J., Folberg, R., Hess, A., Seftor, E.A., Gardner, L.M., Pe'er, J., Trent, J.M., Meltzer, P.S. and Hendrix, M.J. Vascular channel formation by human melanoma cells *in vivo* and *in vitro*: vasculogenic mimicry. American Journal of Pathology 1999; 155: 739-752.

Mariani, T.J., Trackman, P.C., Kagan H.M., Eddy, R.L., Shows, T.B., Boyd, C.D. and Deak, S.B. The complete derived amino acid sequence of human lysyl oxidase and assignment of the gene to chromosome 5. Matrix 1992; 12: 242-248.

Martinez-Hernandez, A. and Catalano, E. Stromal reaction to neoplasia: colonic carcinomas. Ultrastructural Pathology 1980; 1: 403-410.

Martins, R.P., Ujfalusi, A.A., Csiszar, K., Krawetz, S.A. Characterization of the region encompassing the human lysyl oxidase locus. DNA Sequence 2001; 12: 215-227.

Matsumine, A., Senda, T., Baeg, G.H., Roy, B.C., Nakamura, Y., Noda, M., Toyoshima, K. and Akiyama, T. MCC, a cytoplasmic protein that blocks cell cycle progression from the G0/G1 to S phase. Journal of Biological Chemistry 1996; 271: 10341-10346.

McManus, M.T. and Sharp, P.A. Gene silencing in mammals by small interfering RNAs. Nature Reviews Genetics 2002; 3: 737-747.

Mello, M.L., Contente, S., Vidal, B.C., Planding, W. and Schenck, U. Modulation of *ras* transformation affecting chromatin supraorganization as assessed by image analysis. Experimental Cell Research 1995; 220: 374-382.

Melnick, A., Fruchtman, S., Zelent, A., Liu, M., Huang, Q., Boczkowska, B., Calasanz, M., Fernandez, A., Licht, J.D. and Najfeld, V. Identification of novel chromosomal rearrangements in acute myelogenous leukemia involving loci on chromosome 2p23, 15q22 and 17q21. Leukemia 1999; 13: 1534-1538.

Mendelsohn, J., Baird, A., Fan, Z. and Markowitz, S.D. Growth factors and their receptors in epithelial malignancies. In: Mendelsohn, J., Howley, P.M., Israel, M.A. and Liotta, L.A. (eds) The Molecular Basis of Cancer, 2nd edition. W.B. Saunders Company, Philadelphia, PA, 2001. pp. 137-161.

Mertens, F., Johanson, B., Hoglund, M. and Mitelman, F. Chromosomal imbalance maps of malignant solid tumors: a cytogenetic survey of 3185 neoplasms. Cancer Research 1997; 57: 2765-2780.

Miyoshi, Y., Nagase, H., Ando, H., Horii, A., Ichii, S., Nakatsuru, S., Aoki, T., Miki, Y., Mori, T. and Nakamura, Y. Somatic mutations of the APC gene in colorectal tumors: mutation cluster region in the APC gene. Human Molecular Genetics 1992; 1: 229-233.

Molnar, J., Fong, K.S.K., He, Q.P., Hayashi, K., Kim, Y., Fong, S.F.T., Fogelgren, B., Szauter, K.M., Mink, M. and Csiszar, K. Structural and functional diversity of lysyl oxidase and the LOX-like proteins. Biochimica et Biophysica Acta 2003; 1647: 220-224.

Montesano, R., Hollstein, M. and Hainaut, P. Genetic alterations in esophageal cancer and their relevance to etiology and pathogenesis: a review. International Journal of Cancer 1996; 69: 225-235.

Morin, P.J., Sparks, A.B., Korinek, V., Barker, N., Clevers, H., Vogelstein, B. and Kinzler, K.W. Activation of β-catenin-Tcf signaling in colon cancer by mutations in β-catenin or APC. Science 1997; 275: 1787-1790.

218

Murawaki, Y., Kusakabe, Y. and Hirayama, C. Serum lysyl oxidase activity in chronic liver disease in comparison with serum levels of prolyl hydroxylase and laminin. Hepatology 1991; 14: 1167-1173.

Murphy, M. and Levine, A.J. Tumor suppresor genes. In: Mendelsohn, J., Howley, P.M., Israel, M.A. and Liotta, L.A. (eds) The Molecular Basis of Cancer, 2nd edition. W.B. Saunders Company, Philadelphia, PA, 2001. pp. 95-114.

Oberhuber, H., Seliger, B. and Schafer, R. Partial restoration of pre-transformation levels of lysyl oxidase and transin mRNAs in phenotypic ras revertants. Molecular Carcinogenesis 1995; 12: 198-204.

Olumi, A.R., Grossfeld, G.D., Hayward, S.W., Carroll, P.R., Tisty, T.D. and Cunha, G.R. Carcinoma-associated fibroblasts direct tumor progression of initiated human prostatic epithelium, Cancer Research 1999; 59: 5002-5011.

Omori, K., Fujiseki, Y., Omori, K., Suzukawa, J. and Inagaki C. Regulation of the expression of lysyl oxidase mRNA in cultured rabbit retinal pigment epithelium cells. Matrix Biology 2002; 21: 337-348.

Ono, K., Tanaka, T., Tsunoda, T., Kitahara, O., Kihara, C., Okamoto, A., Ochiai, K.,

Takagi, T. and Nakamura, Y. Identification by cDNA microarray of genes involved in

ovarian carcinogenesis. Cancer Research 2000; 60: 5007-5011.

Palamakumbura, A.H. and Trackman, P.C. A fluorometric assay for detection of lysyl

oxidase enzyme activity in biological samples. Analytical Biochemistry 2002; 300: 245-

251.

Palanisamy, N., Abou-Elella, A.A., Chaganti, S.R., Houldsworth, J., Offit, K., Louie,

D.C., Terayu-Feldstein, J., Cigudosa, J.C., Rao, P.H., Sanger, W.G., Weisenburger, D.D.

and Chaganti, R.S. Similar patterns of genomic alterations characterize primary

mediastinal large-B-cell lymphoma and diffuse large-B-cell lymphoma. Genes,

Chromosomes and Cancer 2002; 33: 114-122.

Pamment, J., Ramsay, E., Kelleher, M., Dornan, D. and Ball, K.L. Regulation of the IRF-

1 tumour modifier during the response to genotoxic stress involves an ATM-dependent

signalling pathway. Oncogene 2002; 21: 7776-7785.

Park, S.Y., Choi, H.C., Chun, Y.H., Kim, H. and Park, S.H. Characterization of

chromosomal aberrations in lung cancer cell lines by cross-species color banding.

Cancer Genetics and Cytogenetics 2001; 124: 62-70.

Peralta, R.C., Casson, A.G., Wang, R.N., Keshavjee, S., Redston, M. and Bapat, B. Distinct regions of frequent loss of heterozygosity of chromosome 5p and 5q in human esophageal cancer. International Journal of Cancer 1998; 78: 600-605.

Peterson, B. Anatomy of the 5q- deletion: different sex ratios and deleted 5q bands in MDS and in AML. Leukemia 1996; 10: 1883-1890.

Peyrol, S., Raccurt, M., Ferard, F., Gleyzal, C., Grimaud, J.A. and Sommer, P. Lysyl oxidase gene expression in the stronal reaction to *in situ* and invasive ductal breast carcinoma. American Journal of Pathology 1997; 150: 497-507.

Plass, C. Cancer epigenomics. Human Molecular Genetics 2002; 11: 2479-2488.

Powell, S.M., Papadopoulos, N., Kinzler, K.W., Smolinski, K.N. and Meltzer, S.J. APC *gene mutations in the mutation cluster region are rare in esophageal cancers.* Gastroenterology 1994; 107: 1759-1763.

Powell, S.M., Zilz, N., Beazer-Barclay, Y., Bryan, T.M., Hamilton, S.R., Thibodeau, S.N., Vogelstein, B. and Kinzler, K.W. APC mutations occur early in colorectal tumorigenesis. Nature 1992; 359: 235-237.

Prockop, D.J. and Kivirikko, K.I. Collagens: molecular biology, diseases, and potentials for therapy. Annual Reviews in Biochemistry 1995; 64: 403-434.

Ravid, K., Smith-Mungo, L.I., Zhao, Z., Thomas, K.M. and Kagan, H.M. Upregulation of lysyl oxidase in vascular smooth muscle cells by cAMP: role for adenosine receptor activation. Journal of Cellular Biochemistry 1999; 75: 177-185.

Ren, C., Yang, G., Timme, T.L., Wheeler, T.M. and Thompson, T.C. Reduced lysyl oxidase messenger RNA levels in experimental and human prostate cancer. Cancer Research 1998; 58: 1285-1290.

Resnick, D., Pearson, A. and Krieger, M. The SRCR superfamily: a family reminiscent of the IG superfamily. Trends in Biochemical Sciences 1994; 19: 5-8.

Reuter, G. and Spierer, P. Position effect variegation and chromatin proteins. BioEssays 1992; 14: 605-612.

Riegman, P.H., Vissers, K.J., Alers, J.C., Geelen, E., Hop, W.C., Tilanus, H.W. and van Dekken, H. Genomic alterations in malignant transformation of Barrett's esophagus. Cancer Research 2001; 61: 3164-3170.

Riggs, A.D. and Jones, P.A. 5-methylcytosine, gene regulation and cancer. Advances in Cancer Research 1983; 40: 1-30.

Rodriguez, C., Raposo, B., Martinez-Gonzalez, J., Casani, L. and Badimon, L. Low density lipoproteins downregulate lysyl oxidase in vascular endothelial cells and the arterial wall. Arterioscleosis, Thrombosis and Vascular Biology 2002; 22: 1409-1414.

Roy, R., Polgar, P., Wang, Y., Goldstein, R.H., Taylor, L. and Kagan, H.M. Regulation of lysyl oxidase and cyclooxygenase expression in human lung fibroblasts: Interactions among TGF-β, IL-1β, and prostaglandin E. Journal of Cellular Biochemistry 1996; 62: 411-417.

Royce, P.M. and Steinmann, B. Markedly reduced activity of lysyl oxidase in skin and aorta from a patient with Menkes' disease showing unusually severe connective tissue manifestations. Pediatric Research 1990; 28: 137-141.

Royce, P.M., Camakaris, J. and Danks, D.M. Reduced lysyl oxidase activity in skin fibroblasts from patients with Menkes' syndrome. Biochemical Journal 1980; 192: 579-586.

Rubinfeld, B., Albert, I., Porfiri, E., Fiol, C., Munemitsu, S. and Polakis, P. Binding of GSK-3β to the APC-β-catenin complex and regulation of complex assembly. Science 1996; 272: 1023-1025.

Ryberg, D., Lindstedt, B.A., Zienolddiny, S. and Haugen, A. A hereditary genetic marker closely associated with microsatellite instability in lung cancer. Cancer Research 1995; 55: 3996-3999.

Sage, E.H. and Gray, W.R. Evolution of elastic structure.In: Sandberg, L.B., Gray, W.R., Franzblau, C. (eds) Elastin and Elastic Tissues. Plenum Press, city, NY, 1977. pp. 291-312.

Saito, H., Papaconstantinou, J. Sato, H. and Goldstein, S. Regulation of a novel gene encoding a lysyl oxidase-related protein in cellular adhesion and senescence. Journal of Biological Chemistry 1997; 272: 8157-8160.

Sambrook, J. and Russell, D.W. (ed.) Molecular Cloning: A Laboratory Manual, 3rd ed. Cold Spring Harbor Laboratory Press, Cold Spring Harbor, NY, 2001.

Sanger, F., Nicklen, S. and Coulson, A.R. DNA sequencing with chain-terminating inhibitors. Proceedings of the National Academy of Sciences USA 1977; 74: 5463-5467.

Sasaki, T., Brakebusch, C., Engel, J. and Timpl, R. Mac-2 binding protein is a cell adhesive protein of the extracellular matrix which self-assembles into ring-like structures and binds $\beta 1$ integrins, collagens and fibronectin. The European Molecular Biology Organization (EMBO) Journal 1998; 17: 1606-1613.

Sebti, S.M. and Hamilton, A.D. Inhibition of Ras prenylation: a novel approach to cancer chemotherapy. Pharmacological Therapy 1997; 74: 103-114.

Shanley, C.J., Gharaee-Kermani, M., Sarkar, R., Welling, T.H., Kriegel, A., Ford, J.W., Stanley, J.C. and Phan, S.H. Transforming growth factor- β_1 increases lysyl oxidase enzyme activity and mRNA in rat aortic smooth muscle cells. Journal of Vascular Surgery 1997; 25: 446-452.

Shibagaki, I., Shimada, Y., Wagata, T., Ikenaga, M., Imamura, M. and Ishizaki, K. Allelotype analysis of esophageal squamous cell carcinoma. Cancer Research 1994; 54: 2996-3000.

Shibanuma, M., Mashimo, J., Mita, A., Kuroki, T. and Nose, K. Cloning from a mouse osteoblastic cell line of a set of transforming-growth-factor-$\beta 1$-regulated genes, one of which seems to encode a follistatin-related polypeptide. European Journal of Biochemistry 1993; 217: 13-19.

225

Shibata, D., Peinado, M.A., Ionov, Y., Malkhosyan S. and Perusho, M. Genomic instability in repeated sequences in an early somatic event in colorectal tumorigenesis that persists after transformation. Nature Genetics 1994; 6: 273-281.

Siegel, R.C., Chen, K.H., Greenspan, J.S. and Aguiar, J.M. Biochemical and immunochemical study of lysyl oxidase in experimental hepatic fibrosis in the rat. Proceedings of the National Academy of Sciences U.S.A. 1978; 75: 2945-2949.

Siegel, R.C. Biosynthesis of collagen crosslinks: increased activity of purified lysyl oxidase with reconstituted collagen fibrils. Proceedings of the National Academy of Sciences U.S.A. 1974; 71:4826-4830.

Slee, R.B., Hillier, S.G., Largue, P., Harlow, C.R., Miele, G. and Clinton, M. Differentiation-dependent expression of connective tissue growth factor and lysyl oxidase messenger ribonucleic acids in rat granulosa cells. Endocrinology 2001; 142: 1082-1089.

Smith, K.J., Johnson, K.A., Bryan, T.M., Hill, D.E., Markowitz, S., Willson, J.K., Paraskeva, C., Peterson, G.M., Hamilton, S.R., Vogelstein, B. and Kinzler, K.W. The APC gene product in normal and tumor cells. Proceedings of the National Academy of Sciences U.S.A. 1993; 90: 2846-2850.

Smith-Mungo, L. and Kagan, H.M. PKC-MEK-MAPK-dependent signal transduction pathway mediates the stimulation of lysyl oxidase expression by serum and PDGF in rat aortic smooth muscle cells. Journal of Cellular Biochemistry 2002; 85: 775-784.

Smith-Mungo, L.I. and Kagan, H.M. Lysyl oxidase: properties, regulation and multiple functions in biology. Matrix Biology 1998; 16: 387-398.

Song, Y.L., Ford, J.W., Gordon, D. and Shanley, C.J. Regulation of lysyl oxidase by interferon-γ in rat aortic smooth muscle cells. Arteriosclerosis, Thrombosis and Vascular Biology 2000; 20: 982-988.

Streichenberger, N., Peyrol, S., Philit, F., Loire, R., Sommer ,P. and Cordier, J.F. Constrictive bronchiolitis obliterans. Characterisation of fibrogenesis and lysyl oxidase expression patterns. Virchows Archiv 2001; 439: 78-84.

Szpirer, C., Szpirer, J., Riviere, M., Hajnal, A., Kiess, M., Scharm, B. and Schafer R. Chromosomal assignment of three rat and human H-rev genes, putative tumor suppressors, down-regulated in malignantly HRAS-transformed cells. Mammalian Genome 1996; 7: 701-703.

Takagi, Y., Kohmura, H., Futamura, M., Kida, H., Tanemura, H., Shimokawa, K. and Saji, S. Somatic alterations of the DPC4 gene in human colorectal cancers *in vivo*. Gastroenterology 1996; 111: 1369-1372.

Takahara, K., Lyons, G.E. and Greenspan, D.S. Bone morphogenetic protein-1 and a mammalian tolloid homologue (mTld) are encoded by alternatively spliced transcripts which are differentially expressed in some tissues. Journal of Biological Chemistry 1994; 269: 32572-32578.

Takai, D. and Jones, P.A. Comprehensive analysis of CpG islands in human chromosomes 21 and 22. Proceedings of the National Academy of Sciences U.S.A. 2002; 99: 3740-3745.

Tan, R.S.P., Taniguchi, T. and Harada, H. Identification of the lysyl oxidase gene as a target of the antioncogenic transcription factor, IRF-1, and its possible role in tumor suppression. Cancer Research 1996; 56: 2417-2421.

Tanaka, K., Kikuchi-Yanoshita, R., Muraoka, M., Konishi, M., Oshimura, M. and Miyaki, M. Suppression of tumorigenicity and invasiveness of colon carcinoma cells by introduction of chromosome 8p12-pter. Oncogene 1996; 12: 405-410.

Tanaka, N., Ishihara, M., Kitagawa, M., Harada, H., Kimura, T., Matsuyama, T., Lamphier, M.S., Aizawa, S., Mak, T.W. and Taniguchi, T. Cellular commitment to oncogene-induced transformation or apoptosis is dependent on the transcription factor IRF-1. Cell 1994a; 77: 829-839.

Tanaka, N., Ishihara, M. and Taniguchi, T. Suppression of *c-myc* or *fos*B-induced cell transformation by the transcription factor IRF-1. Cancer Letters 1994b; 83:191-196.

Tanaka, N. and Taniguchi, T. Cytokine gene regulation: regulatory *cis*-elements and DNA binding factors involved in the IFN system. Advances in Immunology 1992; 52: 263-281.

Tang, S.S., Trackman, P.C. and Kagan, H.M. Reaction of aortic lysyl oxidase with β -aminopropionitrile. Journal of Biological Chemistry 1983; 258:4331-4338.

Thiery, J.P. Epithelial-mesenchymal transitions in tumor progression. Nature Reviews Cancer 2002; 2: 442-454.

Timar, J., Diczhazi, C., Ladanyi, A., Raso, E., Hornebeck, W., Robert, L. and Lapis, K. Interaction of tumour cells with elastin and the metastatic phenotype. Ciba Foundation Symposium 1995; 192: 321-335.

Timar, J., Lapis, K., Fulop, T., Varga, Z.S., Tixier, J.M., Robert, L. and Hornebeck, W. Interaction between elastin and tumor cell lines with different metastatic potential; *in vitro* and *in vivo* studies. Journal of Cancer Research and Clinical Oncology 1991; 117: 232-238.

Tomlinson, I., Ilyas, M., Johnson, V., Davies, A., Clark, G., Talbot, I. and Bodmer, W. A comparison of the genetic pathways involved in the pathogenesis of three types of colorectal cancer. Journal of Pathology 1998; 184: 148-152.

Trackman, P.C., Graham, R.J., Bittner, H.K., Carnes, D.L., Gilles, J.A. and Graves, D.T. Inflammation-associated lysyl oxidase protein expression *in vivo*, and modulation by FGF-2 plus IGF-1. Histochemistry and Cell Biology 1998; 110: 9-14.

Trackman, P.C., Bedell-Hogan, D., Tang, J. and Kagan, H.M. Post-translational glycosylation and proteolytic processing of a lysyl oxidase precursor. Journal of Biological Chemistry 1992; 267: 8666-8671.

Travers, H., French, N.S. and Norton, J.D. Suppression of tumorigenicity in Ras-transformed fibroblasts by $\alpha2(I)$ collagen. Cell Growth and Differentiation 1996; 7: 1353-1360.

Trivedy, C., Warnakulasuriya, K.A., Hazarey, V.K., Tavassoli, M., Sommer, P. and Johnson, N.W. The upregulation of lysyl oxidase in oral submucous fibrosis and squamous cell carcinoma. Journal of Oral Pathology and Medicine 1999; 28: 246-251.

Tur, S.S. and Lerch. K. Unprecedented lysyl oxidase activity of *Pichia pastoris* benzylamine oxidase. Federation of European Biochemical Societies (FEBS) Letters 1988; 238: 74-76.

Uzel, M.I., Scott, I.C., Babakhanlou-Chase, H., Palamakumbura, A.H., Pappano, W.N., Hong, H.H., Greenspan, D.S. and Trackman, P.C. Multiple bone morphogenetic protein 1-related mammalian metalloproteinases process pro-lysyl oxidase at the correct physiological site and control lysyl oxidase activation in mouse embryo fibroblast cultures. Journal of Biological Chemistry 2001; 276: 22537-22543.

Vaiphei, K., Joshi, K., Ayyagari, S. and Banerjee, C. Histomorphological criteria for prognosis in breast cancer. Indian Journal of Pathology and Microbiology 1990; 33: 328-333.

Vermeulen, S.J., Bruyneel, E.A., Bracke, M.E., De Bruyne, G.K., Vennekens, K.M., Vleminckx, K.L., Berx, G.J., van Roy, F.M. and Mareel, M.M. Transition from the noninvasive to the invasive phenotype and loss of α-catenin in human colon cancer cells. Cancer Research 1995; 55: 4722-4278.

Virmani, A.K., Fong, K.M., Kodagoda, D., McIntire, D., Hung, J., Tonk, V., Minna, J.D. and Gazdar, A.F. Allelotyping demonstrates common and distinct patterns of chromosomal loss in human lung cancer types. Genes, Chromosomes and Cancer 1998; 21: 308-319.

Vogelstein, B., Fearon, E.R., Kern, S.E., Hamilton, S.R., Preisinger, A.C., Nakamura, Y. and White, R. Allelotype of colorectal carcinomas. Science 1989; 244: 207-211.

Wakasaki, H. and Ooshima, A. Immunohistochemical localization of lysyl oxidase with monoclonal antibodies. Laboratory Investigation 1990; 63: 377-384.

Wang, S.X., Mure, M., Medzihradszky, K.F., Burlingame, A.L., Brown, D.E., Dooley, D.M., Smith A.J., Kagan H.M. and Klinman, J.P. A crosslinked co-factor in lysyl oxidase: redox function for amino acid side chains. Science 1996; 273: 1078-1084.

Watanabe, T., Ichihara, M., Hashimoto, M., Shimono, K., Shimoyama, Y., Nagasaki, T., Murakumo, Y., Murakami, H., Sugiora, H., Iwata, H., Ishiguro, N. and Takahashi, M. Characterization of gene expression induced by RET with MEN2A or MEN2B mutation. American Journal of Pathology 2002; 161: 249-256.

Wessendorf, S., Schwaenen, C., Kohlhammer, H., Kienle, D., Wrobel, G., Barth, T.F., Nessling, M., Moller, P., Dohner, H., Lichter, P. and Bentz, M. Hidden gene

amplifications in aggressive B-cell non-Hodgkin lymphomas detected by microarray-based comparative genomic hybridization. Oncogene 2003; 22: 1425-1429.

Williamson, M.P. The structure and function of proline-rich regions in proteins. Biochemical Journal 1994; 297: 249-260.

Yeowell, H.N., Marshall, M.K., Walker, L.C., Ha, V. and Pinnell, S.R. Regulation of lysyl oxidase mRNA in dermal fibroblasts from normal donors and patients with inherited connective tissue disorders. Archives of Biochemitry and Biophysics 1994; 308: 299-305.

Young, B. and Heath, J.W. Wheater's Functional Histology, fourth edition. Harcourt Publishers Limited, Edinburgh, United Kingdom, 2000.

Zhang, Z., Wang, Y., Vikis, H.G., Johnson, L., Liu, G., Li, J., Anderson, M.W., Sills, R.C., Hong, H.L., Devereux, T.R., Jacks, T., Guan, K.L. and You, M. Wildtype K*ras*2 *can inhibit lung carcinogenesis in mice*. Nature Genetics 2001; 29: 25-33.

Zuber, J., Tchernitsa, O.I., Hinzmann, B., Schmitz, A.C., Grips, M., Hellriegel, M., Sers, C., Rosenthal, A. and Schafer R. A genome-wide survey of RAS transformation targets. Nature Genetics 2000; 24: 144-152.